DEVELOPMENT OF A CELL-BASED STREAM FLOW ROUTING MODEL

A Thesis

by

RAJEEV RAINA

Submitted to the Office of Graduate Studies of
Texas A&M University
in partial fulfillment of the requirements for the degree of

MASTER OF SCIENCE

May 2004

Major Subject: Civil Engineering

DEVELOPMENT OF A CELL-BASED STREAM FLOW ROUTING MODEL

A Thesis

by

RAJEEV RAINA

Submitted to Texas A&M University
in partial fulfillment of the requirements
for the degree of

MASTER OF SCIENCE

Approved as to style and content by:

Francisco Olivera (Chair of committee)	Ralph Wurbs (Member)
Clyde Munster (Member)	Paul N. Roschke (Head of Department)

May 2004

Major Subject: Civil Engineering

ABSTRACT

Development of a Cell-Based Stream Flow Routing Model. (May 2004)

Rajeev Raina, B.E., Veermata Jijabai Technological Institute (VJTI), Mumbai University, Mumbai, India

Chair of Advisory Committee: Dr. Francisco Olivera

This study presents the development of a cell-based routing model. The model developed is a two parameter hydrological routing model that uses a coarse resolution stream network to route runoff from each cell in the watershed to the outlet. The watershed is divided into a number of equal cells, which are approximated as cascade of linear reservoirs or tanks. Water is routed from a cell downstream, depending on the flow direction of the cell, using the cascade of tanks. The routing model consists of two phases, first is the overland flow routing, which is followed by the channel flow routing. In this study, the cell-to-cell stream flow routing model is applied to the Brazos River Basin to demonstrate the impact of the cascade of tanks on the flow over a simple linear reservoir method. This watershed was tested with a uniform runoff depth in absence of observed runoff data. A case study on Waller Creek in Austin, Texas with observed runoff depths and stream flow is used to demonstrate the calibration and validation of model parameters.

DEDICATION

To God, my parents, sister and fiancé

ACKNOWLEDGMENTS

This research was conducted at Texas A&M University and was supported by the Department of Civil Engineering through the Texas Engineering Experiment Station (TEEX).

I would like to thank my advisory committee members: Dr. Francisco Olivera, Dr. Ralph Wurbs and Dr. Clyde Munster for their trust, guidance and contributions throughout this research project.

I also wish to thank my fellow classmates and friends for their active help and contribution: Zubin Sukheswalla, Srikanth Koka, Milver Valenzuela, and Ashish Agarwal.

Special thanks to my parents, sister and fiancé for their constant support and motivation without which, I would have never come this far.

TABLE OF CONTENTS

Page

Page

LIST OF FIGURES

Figure Page

Figure Page

LIST OF TABLES

1. INTRODUCTION

Water is the most widespread substance found in the natural environment. The hydrological cycle, which is responsible for the transport of water throughout the earth's environment, is an important factor in the earth's climate and for supply of water to mankind. Studying the water cycle especially the terrestrial cycle thus, is an extremely important topic in the ongoing research across the world. Stream flow is the closing link to the hydrological cycle, which transports the water back to oceans from where it has originated. Since stream flow is routinely measured throughout the world, this data can be used to test the accuracy of the climatological and hydrological models by comparing the simulated flow to the observed flow. Stream flow prediction models can be coupled to atmospheric models to test their performance on a climatological basis (Lucas-Pitcher et al., 2003) and these studies can be used to determine the impact of climatic changes on flow patterns in a watershed (Arora and Boer, 2001). Flow routing algorithms that track the water from any point on the surface to the outlet can be divided into three major groups (Olivera et al. 2000). The cell-to-cell or cell based stream flow routing (Vörösmarty et al., 1989; Vörösmarty and Moore, 1991; Liston et al., 1994; Miller et al., 1994; Sausen et al., 1994; Coe, 1997; Hagemann et al., 1998; Coe, 2000) simulate the transport of runoff generated within the modeling units (e.g. grid cells), through river networks across continents into the oceans. The source-to-sink stream flow routing models (Naden et al., 1999; Olivera et al., 2000) defines specific sources or areas, where excess runoff enters the

---

This thesis follows the style and format of the Journal of the American Water Resources Association.

hydrologic system, and sinks or areas, where excess runoff leaves the hydrologic system. A hydrograph is calculated at the sinks as a summation of the contribution of all the sources. The element-to-element stream flow routing method (USDA, 2004; USCOE, 2004) represents a watershed as a collection of elements like basins, reaches, reservoirs, sources and sinks. Flow is routed to the outlet element-to-element. Hydrographs are calculated at each element as well as at the outlet.

Most previous routing schemes are based on the cell-to-cell stream routing technique, as they are simple to implement over a variety of scales, and they give simulated flow with a reasonable degree of accuracy (Olivera et al., 2000). As a result, these algorithms are utilized in numerous hydrologic and meteorological applications on both local and global scales (e.g. Liston et al., 1994; Miller et al., 1994; Marengo et al., 1994; Sausen et al., 1994; Coe, 1997; Hagemann and Dumenil, 1998). Models developed in the past aim at routing the water in each cell downstream depending on the flow direction of the cell and predicting the flow across the network to the outlet. Both kinematic wave (Vörösmarty et al., 1989; Vörösmarty and Moore, 1991; Liston et al., 1994; Miller et al., 1994; Sausen et al., 1994, Lohmann et al., 1996; Coe, 1997; Hagemann, 1998) and diffusion wave (Julien et al., 1995; Downer et al., 2002; Odgen, 2004) approximations of the Saint Venant equations have been used to develop these cell-based routing algorithms.

The kinematic wave model assumes that inertia and pressure terms are negligible as compared to the frictional and gravity terms. Depending on how the parameters (e.g. velocity, retention coefficient) in the cell-to-cell flow routing models

are calculated, kinematic models can be grouped into four categories (Arora and Boer, 1999; Arora, 2001; Arora et al., 2001). According to Arora and Boer (1999), one method is physically based, where the continuously evolving stream velocities and flows are calculated using the Manning's equation (Arora and Boer, 1999; Arora et al., 1999; Lucas-Picher et at. 2003). In the second method, a uniform constant flow velocity (e.g. Vörösmarty and Moore, 1991; Miller et al., 1994; Oki et al., 1996; Oki, 1997; Coe, 1998; Coe et al., 1998; Oki et al., 1999) is assumed. The third category is in which, the time-independent flow velocities (velocities are constant over time) are calculated as a function of the topographic gradient and the grid size (e.g. Miller et al., 1994; Marengo et al., 1994; Sausen et al., 1994; Coe, 1997; Costa and Foley, 1997; Hagemann and Dumenil, 1998; Coe, 2000). The fourth approach is the one in which an empirical formulae is used to estimate time-independent flow velocities as a function of mean annual discharge (Vörösmarty et al., 1989), or as a function of mean annual discharge and slope (Liston et al., 1994).

The diffusive wave approximation neglects the only the inertia terms and takes into account the pressure term in the St. Venant equations (Singh, 2002). The diffusive wave form of the equation is superior to the kinematic wave form as it accounts for backwater effects, and allows flow on adverse slopes. The ability to simulate backwater effects is essential for unsteady simulations over irregular topography because adverse flow is common in flatter regions (Julien et al., 1995; Ogden, 2004). The diffusive wave solution to the St. Venant equations also account for attenuation, which kinematic waves do not (Ponce et al., 1978). However, in

regions where backwater is not a significant phenomenon, kinematic wave models give similar results to the diffusive wave models. This is because the numerical solution of the kinematic wave is similar to the analytic solution of the diffusive wave (Ponce et al., 1978). Also, Singh (2002) notes that kinematic wave approximation gives sufficiently accurate values for overland flow as well as channel flow. He notes that in channel flow, all waves – kinematic, diffusion and dynamic as well as their variants – exist. At any given time and position the relative significance of these waves changes with change in flow. For most of the river flow without artificial structures kinematic waves are dominant and hence kinematic wave theory can be used for modeling channel flow (Singh, 2002).

The cell-based models are implemented by dividing a given area into equal cells, which are connected to each other in a dendritic network, where each cell represents a unit in which energy and water balance calculations are done by any of the above given methods. As a system of cells all together, they represent the flow pattern of the study area. However, the lack of efficient and accurate methods to generate digital data sets for cell-to-cell routing at large scales has limited improvements in hydrologic modeling. As a result, in the past, spatial data was developed for a specific hydrologic study (e.g. Vörösmarty et al., 1989 and Miller et al., 1994). The development of the Network Tracing Method (NTM) (Olivera and Raina, 2003) is an important step for delineating coarse resolution gridded stream networks for river transport modeling at local, regional, and global scales. The NTM calculates coarse resolution river networks based on fine-resolution stream network

data in vector format. The NTM identifies the downstream cell of each cell of the system, and estimates the flow distance between them. Flow direction in a cell follows the convention of an eight direction-pour point algorithm. This algorithm dictates that flow occurs in only one of the eight allowed directions (north, south, east, west, northeast, northwest, southeast and the southwest).

The cell-to-cell stream flow routing models can be implemented at various scales, either at large spatial scale (~200-500km) or at small spatial scale (~25km or less), depending on the requirements of the study or the applications. Cell-to-cell stream flow routing models at large spatial scales are generally integrated with general circulation models (GCMs). They are used to study the effectiveness of the GCMs to simulate accurate runoff (e.g. Liston et al., 1994; Sausen et al., 1994; Miller et al., 1994; Marengo et al., 1994; Coe, 1997; Hagemann and Dumenil, 1998; Arora et al., 2001). Since the main objective of flow routing schemes in GCMs is to compute the runoff at the outlet, the runoff is routed via the land grid cells into the cells at the ocean-land boundaries to produce realistic stream flow on a monthly or an annual basis. This is compared to the observed stream flow to test the effectiveness of the GCMs. Models that are used for flood prediction, water management or any other typical hydrological applications (e.g. Nijssen, 1997) are operated at smaller resolutions (~1-25km). The predicted flow is compared with the observed values and this is used to assess the accuracy of the model and hence, this model can be used in the future for numerous practical applications like flood warning systems. The time step in such models is daily or sub-daily and they need to predict the flow at numerous

points over the watershed and not only at the mouth of the river or the continental edges. However, a model that operates at both a large resolution and a small resolution depending on the demands of the application is missing.

The purpose of this study was to develop a simple yet accurate cell based stream flow routing model. This cell-based stream flow routing model, cell-to-cell stream flow routing model, divides a watershed into a set of interconnected cells which are represented as a cascade of n equal linear reservoirs. This model operates at a variety of cell resolutions with the same operating parameters namely, stream velocity and coefficient of dispersion. Thus, it can be effectively used for typical hydrological applications and climate or atmospheric models used for climate prediction. A tool has been developed in visual basic for the implementation of the algorithm. This model has been implemented on the Brazos River basin to test the routing algorithm with a given uniform input at four spatial scales (8,045 m, 16,090 m, 32,180 m, and 64,360 m). As a case study, Waller Creek in Austin has been used to demonstrate the calibration and validation of model parameters at three spatial scales (250m, 500m and 1000m). The model predicted accurately flow measurements for Waller Creek at 38th and 23rd Street in all the three resolutions; however the effect of the cascade was not clear due small size of the cells used in this case. Modeling of Brazos river basin has been done with uniform runoff depths due to unavailable runoff data, which even thought is an unrealistic assumption validates the model algorithm and the parameters used. The effect of the cascade was clearly evident at cell resolutions with which the Brazos River was modeled. In future, this model can be

coupled to a climatological model (GCM) for runoff data and the algorithm can be improved to handle reservoirs, lakes and regulated rivers, an aspect that has been neglected in this study.

2. BACKGROUND AND LITERATURE REVIEW

The cell-to-cell stream flow routing has been studied extensively in the past (Vörösmarty et al., 1989; Vörösmarty and Moore, 1991; Liston et al., 1994; Marengo et al., 1994; Miller et al., 1994; Sausen et al., 1994; Oki et al., 1996; Oki, 1997; Coe, 1997; Hagemann et al., 1998; Arora and Boer, 1999; Oki et al., 1999; Coe, 2000; Arora et al, 2001; Coe et al., 2002). This algorithm routes the water from one cell to another, depending on the cell connectivity to the outlet of the watershed. Using the cell-to-cell model, a watershed can be represented as a single cell, a cascade of n equal cells, or a network of n equal cells (Singh, 1988). The storage in the cells is calculated as given below:

$$\frac{dS_t}{dt} = I_t - O_t \quad \text{.....(2.1)}$$

where, S_t = the time-variant storage in a grid cell, I_t in the summation of input coming into the cell from upstream cells and the runoff generated in the cell, and O_t is the outflow from the cell which is calculated by various methods, e.g. the linear reservoir method.

This section will discuss in detail the work done by researchers towards the development of cell-to-cell flow routing models followed by a critical discussion about these models.

Vörösmarty et al. (1989) developed a drainage basin model (DBM) for both water and constituent flux. This DBM consisted of a water balance model (WBM) and the water transport model (WTM). They modeled the watershed at a geographically

referenced 0.5^{o}x0.5^{o} (latitude x longitude) resolution. The WBM operates independently on each grid cell and uses biogeophysical information to predict monthly soil moisture, evaporation and runoff. The WTM is a multigrid dynamic model, where each cell is connected to the other, thus forming the stream network. Each grid cell is assumed to be a linear reservoir. In a linear reservoir, discharge is linearly varied to the storage. A transfer coefficient, which is the retention time in each cell, was dependent of the geometrics of the influent and effluent cells. So for cells exiting from the corners, the transfer coefficient was given a higher value to accommodate for a longer residence time. The value of the transfer coefficient was computed using physically meaningful quantities like the velocity, width of the channel and a dimensionless expansion factor. The velocity is predicted from the mean annual downstream discharge. They concluded that for the transfer coefficient 15-75/month was a reasonable range and a value of 20/month (~1.5 days) produced the best model performance. They applied this DBM to the Amazon/ Tocantins river system. Liston et al. (1994) used a 2^{0}x2.5^{0} (latitude x longitude) grid cell resolution, to test the performance of the GCM for the Mississippi river basin. They separated the runoff generated by the GCM into fast (surface flow), and slow runoff or (subsurface flow) each routed via two separate linear reservoirs with different retention coefficients. Subsurface transfer coefficient was assumed to be higher than the surface flow coefficient. The transfer coefficient was calculated using an empirical relationship, which was dependent on stream length, the overland slope and the mean discharge. The values used for the surface reservoir transfer coefficient range between

3-7 days in all directions of flow and for the subsurface reservoir it was fixed at 30 days. Later, Jayawardena and Mahanama (2002) proposed a High Resolution Runoff Routing Method (HR-RRM) at a resolution of 5'x5' (~9km), which is basically similar to the model proposed by Liston et al. (1994), except for inclusion of floodplain inundation as presented by Vörösmarty et al. (1989). They used the same empirical equations used by Liston et al. (1994) to calculate the surface reservoir transfer coefficient; however, for the subsurface linear reservoir they used a value of 10 days as compared to 30 days used by Liston et al. (1994). This input to the HR-RRM was derived from the Variable Infiltration Capacity (VIC) model (Liang et al., 1994) and the two-layer Variable Infiltration Capacity (VIC-2L) (Liang et al, 1999) model. The VIC model was operated at resolution of 1^0x1^0 and the routing model was operated at a resolution of 5'x5', and was applied to the Mekong river basin in China and Chao Pharaya river basin in Thailand.

Miller et al. (1994) developed a 2.0^0x2.5^0 resolution river routing model for a number of World Rivers, coupled with an atmospheric-ocean model. The GCM of NASA/Goddard Institute for Space Studies (GISS) (Hansen et al., 1983) was used to calculate the runoff for each grid cell which was then routed to the outlet of the watershed using the linear reservoir method. The velocity of flow was calculated either empirically using a topography gradient or given a constant value over time and space. Marengo et al. (1994) and Costa and Foley (1997) have developed models similar to Miller et al. (1994). Marengo et al. (1994) applied the linear reservoir river routing method proposed by Miller et al. (1994) to the Amazon and Tocantins River

basins at a resolution of 2.0^0 X 2.5^0 using the coarse river network developed by Miller et al. (1994). Input to each of the grid cell was derived from the improved GISS GCM (Hansen et al., 1983), which improved the model prediction of discharge. Costa and Foley (1997) used the model presented by Miller et al. (1994) and Marengo et al. (1994) and coupled it with the LSX land surface model to predict the water balance and transport in the Amazon River basin at a cell resolution of 0.5^0 x 0.5^0. The river network was developed by digitizing a 1:6,930,000 river direction map onto a 0.5^0x0.5^0 map. The stream velocities are calculated using the method suggested by Miller et al. (1994) and Marengo et al. (1994).

Oki et al. (1996) used the runoff routing model of Miller et al. (1994) and the runoff generated by the bucket model given by Kondo (1993) embedded in the atmospheric GCM of the Center for Climate System Research (CCSR), University of Tokyo and the National Institute for Environmental Studies (NIES) to model the Amazon, Ob and Amur River basins. River channel networks were delineated manually at a cell resolution of 5.6^0x5.6^0 for these rivers from digital elevation maps and a world atlas, of rivers. The flow velocity in the river channel was fixed at 0.3 m/s, thus giving a good seasonal prediction of river discharge for the Amazon, Ob and Amur River basins. Oki (1997) developed a global river channel network (GRCN) at a cell resolution of 1^0x1^0 using the method developed by Oki and Sud (1998) for implementing the linear reservoir routing method developed by Oki et al. (1996). The velocity chosen was 2.0m/s as compared to 0.3m/s used earlier by Oki et al. (1996) as

it truly represented the channel velocity and not average of overland flow and channel flow in larger cells.

Ma et al. (2000) also have used the concept of linear reservoir in their macroscale hydrological model used for the analysis of the Lena River Basin at a cell resolution of 0.1^0x0.1^0. This model is similar in description to the model proposed by Liston et al. (1994), Miller et al. (1994), Oki et al. (1996) and Oki et al. (1999). The runoff is calculated at a cell resolution of 1^0x1^0, which was later distributed to the routing model resolution of 0.1^0x0.1^0. They use a constant channel flow velocity of 0.4 m/s.

Coe (1997) developed a terrain based Surface Water Area Model (SWAM) for simulating surface water area and river transport at the continental scale and it was applied to northern Africa. Coe (1998) improved SWAM by integrating rivers, lakes and wetlands in the model, thus improving the discharge characteristics of the rivers. SWAM operates at a cell resolution of 5'x5', which is approximately 10 km by 10 km at the equator. SWAM consists of two main components, the first one being the land surface component, which is derived from a digital terrain model (DTM). This module determines the potential surface water areas, the maximum water volume within these areas and the wetlands and the direction in which the cell will flow. The second component is the linear reservoir method. It predicts the discharge based on the runoff, precipitation and the evaporation in the grid cell. The water transport direction define the path water follows to the ocean, which is calculated dynamically by SWAM rather than being calculated manually (Coe, 1998). The continuity equation used in this

model for simulating the storage in each grid cell is similar to the other models except that, in this study the net transport by ground water was considered to be zero. The transfer coefficient used to determine flux out of the grid cell was taken to be proportional to the ratio of distance between the grid cell centers and the effective velocity, which in this case was chosen to be $0.003ms^{-1}$. A time step of 10 days is used in the model. Based on SWAM, Coe (2000) developed a global hydrological routing algorithm (HYDRA) that simulates seasonal river discharge and changes in the surface water levels on a spatial resolution of 5'x5'. HYDRA contains all the features of SWAM but differs from it in some aspects. HYDRA can simulate seasonal variation in the rivers as compared to annual simulations in SWAM and stream velocities in the grid cell are computed using the method suggested by Miller et al. (1994) and are not taken as constant as in SWAM. HYDRA is operated at a time step of 1 hour as compared to 10 days in SWAM. Coe (2000) forced HYDRA with the mean monthly estimates of the National centers for environmental prediction (NCEP) reanalyzed dataset (Kalnay et al., 1996) for the whole globe. 70% of the NCEP runoff was taken as subsurface runoff and the rest 30% was taken as the surface runoff. Coe et al. (2002) coupled HYDRA with Integrated Biosphere simulator (IBIS) (Kucharik et al., 2000) to model the Amazon/ Tocantins River basin at a 5' resolution. The IBIS simulated runoff was used as the input to the HYDRA model and the flow directions of the cells were used as defined by Costa et al. (2002).

Ducharne et al. (2003) have developed a high-resolution (25km x 25km) river routing model RiTHM or the River-Transfer Hydrological Model based on the

hydrological model MODCOU (Ledeux, 1980). RiTHM consists of a riverflow production module and a river routing module. Runoff fed to the model from a GCM was transformed into riverflow at the outlet of the cell. The runoff was separated into subsurface flow and surface flow. The entry of the subsurface flow was delayed using a set of two linear reservoirs into the grid cell. This delayed runoff was added to the surface runoff and transformed into riverflow, which is routed to the outlet of the watershed at a daily time step under the assumption of pure translation (Ducharne et al., 2003). Transfer from one cell to another is independent of any other cell and the transfer coefficient is calculated as a function of the distance and the slope between the two cells and a scaling factor. The scaling factor is dependent upon the time of concentration, which is the only parameter of calibration in the river routing algorithm. The time of concentration in the watershed and the retention coefficients in the riverflow production module were found using calibration. Results of flow for 11 large rivers across the globe were more realistic as compared to Oki et al. (1999) who used a single constant cell velocity for the whole of the watershed, clearly demonstrating the need and importance of accounting for the spatial variability of velocities.

Nijssen et al. (1997) used a linear reservoir model coupled to the 2-layer variable infiltration capacity (VIC-2L) to predict the flow in the Columbia River with a cell resolution of 1^0x1^0 and the Delaware River with a cell resolution of 0.5^0 x 0.5^0. The VIC-2L model produces one time series for each grid cell. This time series is then distributed non-uniformly over the grid cell depending on the varying soil moisture

capacity across the grid cell. A triangular unit hydrograph is used to simulate the routing within the grid cell. This accounts for the different travel times of the runoff produced in different parts of the grid. The hydrographs produced for each cell are then routed to the outlet of the basin using a linear reservoir model with a small retention coefficient. The river network was derived for the two basins manually by defining the flow direction of the grid cell using the actual flow paths in maps.

Sausen et al. (1994) used linear reservoir model in their river runoff model for the general circulation model ECHAM (ECMWF forecast models, modified and extended in Hamburg) with the resolution of 5.6^0x2.8^0. They used the concept of two retention coefficients, acknowledging the fact that cells flowing through the short sides (north-south) take less time to travel that the cells flowing though the longer sides (east-west). This model had two retention coefficients, one for each direction of flow namely, north-south and east west direction.

Hagemann and Dumenil (1998) noted that most of the cell to cell runoff routing models are single parameter models (e.g. Vörösmarty et al., 1989 Vörösmarty and Moore, 1991; Liston et al., 1994; Miller et al., 1994; Marengo et al., 1994; Sausen et al., 1994; Oki et al., 1996; Oki, 1997; Coe, 1997; Costa and Foley, 1997; Coe, 1998; Coe et al., 1998). Single parameter models can satisfactorily simulate either the retention or the translation of flow processes, but not both. Hagemann and Dümenil (1998) proposed a two-parameter hydrological discharge (HD) model at a resolution of 0.5^0x0.5^0 to replace the model presented by Sausen et al. (1994) in the ECHAM. The hydrology in the grid cell was represented by three reservoirs, one each for

overland flow, subsurface flow and channel flow. Overland flow was fed by the runoff and base flow and river flow were fed from the overland flow and the inputs from the upstream cells. This model modified the routing model presented by Sausen et al. (1994) by representing the surface and overland flow reservoirs in the cell as a cascade of n equal linear reservoirs. The cascade of n equal linear reservoirs describes the serial arrangement of n equal linear reservoirs, which have the same retention coefficient. The outflow from a reservoir i equals the inflow into the reservoir i + 1. This model is a two-parameter model with the number of linear reservoirs in the cascade (n) and the retention coefficient (k) being the two variables. The HD model was applied to the Baltic Sea catchments Bothnian Bay and Bothnian Sea (Hagemann and Dümenil, 1999) coupled with two atmospheric circulation models, ECHAM4 (Roeckner et al., 1992). In this study, the river flow was routed through a cascade of n equal reservoirs but for overland flow the cascade of linear reservoirs was replaced by a single linear reservoir. Hagemann and Dümenil (2001) used the HD model to validate the runoff produced by the Europoean Center for Medium-Range Weather Forecasts (ECMWF) and the National Centers for Environmental Prediction (NCEP) reanalysis data (Kalnay et al., 1996). The study area for this study was the Mississippi River basin, the Baltic Sea and the Artic Ocean represented by six large rivers draining into it, namely, Yenisey, Kolyma, Lena, Mackenzie, Northern Dvina and the Ob river basins.

Lohmann et al. (1996) employ a response function for within cell routing and the linearized St. Venant equation to route the stream flow across the cells in the

watershed to the outlet. This model calculates the effective runoff from observed precipitation using a non-linear inverse calculation. Starting from the assumption that all precipitation becomes runoff, the model iteratively calculates the effective precipitation using the minimum least squares solution. This runoff, which is divided into to slow (subsurface) and fast (surface) flows, is transported to the outlet of the grid using an impulse response function. This division of runoff into surface and base flow gives a timescale separation between the flows. The runoff at the outlet of grid is routed to the outlet of the watershed via other cells in the stream network with the linearized Saint Venant equation. The parameters in this model are cell velocity and diffusivity. These can be found for each cell iteratively or by estimation from graphical data of the riverbed. This model was applied to the 37500 km^2 Weser River in Germany.

Lohmann et al (1998 a, b) coupled large-scale river routing model (Lohmann et al., 1996) to the Variable Infiltration Capacity (VIC-2L) model (Liang et al., 1994; Liang et al., 1999). This model consists of two components a runoff producing model (VIC-2L) and a river routing model that transports grid cell surface runoff and the baseflow produced within each grid cell to the outlet a grid cell and then into the river system without any feedback to the VIC-2L model. There is no interaction between the soil water of neighboring grid cells. Both parts of the large-scale routing model (within grid and river routing) are built as simple linear transfer functions. This model was implemented for the Weser River in Germany at a grid resolution of 10'x10'. Later, Nijssen et al. (2001) used the large-scale river routing model (Lohmann et al.,

1996) to predict the discharge of various global rivers. The VIC-2L model (Liang et al., 1994; Liang et al., 1999) generated the runoff for the routing model.

Recently, physically based approaches (Julien et al., 1995, Arora and Boer, 1999; Arora et al., 1999; Arora, 2001; Arora and Boer, 2001; Arora et al., 2001; Downer et al., 2002; Lucas-Pichar et al., 2003) that relate time independent flow velocities to slope, mean annual discharge and river cross-section simultaneously, with the help of Manning's equation have been used in flow routing algorithms to predict flow (Arora et al., 1999). Arora and Boer (1999) used Manning's equation to determine time-evolving flow velocities as a function of river cross-section, channel slope, and amount of runoff generated in the GCM grid cell. This cell-based model has two reservoirs one for surface flow and one for ground water. In this algorithm, the storage for each cell is calculated using the continuity equation and the Manning's equation is used to determine time evolving channel flow velocities, which depend on the amount of stream flow in the river channel, the slope of the channel and the river cross-section. The cross-section of the river was assumed to be rectangular. The width of the riverbed was related to the mean annual discharge. The slope is calculated using the mean elevations of the upstream and the downstream cells. Arora (2001) coupled the variable velocity flow routing algorithm (Arora and Boer, 1999) to the General Circulation Model of the Canadian Climate Modeling and Analysis (CCCma) to compute stream flow simulation for 23 of the world's largest rivers at a GCM resolution of 3.75^0. Precipitation and runoff data was calculated using the Atmospheric Model Intercomparison Project II. Lucas-Picher et al. (2003) coupled the variable

velocity flow routing algorithm (Arora and Boer, 1999) to the Canadian Regional Climate Model (CRCM). They applied this algorithm to the Mackenzie, Frazer Mississippi and the St. Lawrence rivers with a cell resolution of 45km, as this is the resolution at which the CRCM operates. The stream network used was delineated by Graham et al. (1999) and a methodology developed by Lucas-Picher et al. (2003). Variable Infiltration capacity (VIC) model (Liang et al., 1994) was used to generate the input runoff in each cell. They show the importance of taking into account the effect of reservoirs, lakes and dams within the routing algorithm in the calculation of discharge at the outlet. Lakes and reservoirs reduce the annual variablility of the observed discharge to nearly zero due to large reservoir capacity and correspondingly, large retention times (Hagemann and Dumenil, 1998). Using the variable velocity flow routing algorithm without any changes they showed that for the St Lawrence River, the discharge was poorly predicted. However, with modifications to the algorithm, in which a linear reservoir is used, the flow prediction to the ocean from the St Lawrence River was simulated with greater accuracy.

Gutowski et al. (2002) have developed a physically based stream flow routing model CLASP (Coupled Land Atmospheric Simulation Program) to study the coupled land atmospheric hydrologic cycle. This model consists of 3 modules: the atmospheric column model (ATMOS), a soil vegetation-atmospheric transfer (SVAT) model, and a groundwater/surface water (GW/SW) model. The SVAT simulates the behavior of the soil and computes the exchange of water and energy between the atmosphere, groundwater and surface water. The GW/SW simulates the flow of

surplus water or the runoff from the SVAT through a subsurface and river drainage network. The surface water flow is computed using a set of differential equations representing each cell. The channel flow velocities are calculated using the Manning's equation, where the river depth in each cell was assumed to be constant for each time step. First ISLSCP (International Satellite Land Surface Climatology Project) Field Experiment (FIFE) observation data set from the Konza Prairie Research Natural Area (KPRNA) were used for calibration and validation of the model on the Kansas River basin in central United States.

Zhang et al. (2003) used RIEMS-BATS (Regional integrated environmental model system coupled with biosphere –atmosphere transfer scheme) to generate input to a large-scale river routing model (Lohmann et al., 1996). The parameters, C (wave velocity) and D (diffusivity), in this case were determined by graphical data of the riverbed as compared to method of iteration used and suggested by Lohmann et al. (1996), Lohmann et al. (1998b) and Nijssen et al. (2001). The model was implemented for the Yellow river basin in China and the river network was derived from digital data at a cell resolution of 1^0x1^0.

All the models discussed above are kinematic wave approximations of the Saint Venant equations. The kinematic wave model has been successfully been applied in a variety of applications over the past few years. However, diffusion wave models are applicable for a wider range of river beds and slopes as compared to kinematic wave models (Ponce et al., 1978). Diffusive wave models have the capacity to model backwaters, which the kinematic wave models lack. CASC2D (Julien et al.,

1995; Downer et al., 2002; Ogden, 2004) is a physically based, distributed, raster (gridded), two-dimensional and an infiltration-excess (Hortonian) hydrological model for simulating the hydrological response of a watershed subject to an input rainfall. CASC2D uses an explicit two-dimensional, finite difference, diffusive-wave scheme to route overland flow and a one-dimensional diffusive wave formulation for channel flow. The overland flow velocity and hence, the discharge is calculated using the Manning's equation, which gives accurate values for discharge as it accounts for dynamic flow depths and velocities. Channel routing is done using either a explicit, one dimensional, finite volume, diffusive wave formulation or using the one dimensional equations of motion using the Preissmann 4–point implicit scheme (Downer et al., 2002; Odgen, 2001) The latest version of CASC2D has variety of ways to enter the cross-section data (Ogden, 2004). CASC2D can simulate backwater effects, which is a good feature in areas where the slope is low, or in regulated or dammed rivers. In other cases, the effects of backwaters are negligible and can be overlooked as suggested by Lohmann et al. (1998a).

Coarse resolution river transport models are based on tracking water across the landscape through a network of interconnected cells (Vörösmarty et al., 1989; Liston et al., 1994; Miller et al., 1994; Sausen et al., 1994; Coe, 1997; Hagemann and Dümenil, 1998). As discussed earlier, development of large-scale river transport models has been limited due to the lack of accurate and widely available coarse resolution stream networks. Researchers in the past have depended on custom made coarse resolution river networks for each application. Initial methods to determine the

cell connectivity were manual (Vörösmarty et al., 1989; Miller et al., 1994). The networks were determined by the flow direction of the fine resolution stream network. Vörösmarty et al. (1989) delineated a 0.5^0 cell stream network manually from a series of 1:1,000,000 Operational Navigation Charts by examining the predominant stream in the grid cell. Miller et al. (1994) also delineated a 2^0x2.5^0 resolution river network for the whole world by manually determining the flow direction of each grid cell. Other examples of manual determination of coarse resolution networks include Marengo et al. (1994) for the Amazon River and Liston et al. (1994) for the Mississippi River. Vörösmarty et al. (1989) noted that the manual method was accurate as long as a major stream crosses the grid cell. Absence of a major stream in a cell induces errors in the network. Thus, this is an accurate method to calculate flow direction in a very coarse network (cell size greater that 2^0). It results in inaccurate networks when cell size decreases. Moreover, each time the cell resolution changes the network needs to be redrawn when manual delineation is used (O'Donnell et al., 1999).

Recently, methods based on DEMs and vector data have been developed that are no longer manual and depend on more than just the flow direction of the fine resolution streams. DEM based methods present a more accurate method to derive coarse resolution networks. High resolution DEMs are resampled to lower resolutions and these are used to delineate coarse resolution river networks. Oki and Sud (1998) constructed a coarse resolution river networks on a global scale with a 1^o resolution. Arora and Boer (1999) upscaled the network developed by Oki and Sud (1998) from a

resolution of 1^0 to 2.8125^0 for use in global circulation models (GCMs). Graham et al. (1999) resampled a 1-km DEM into 5-minute, 0.5-degree, and 1-degree DEMs, burned-in a fine-resolution river network into the DEM, and finally created river networks from each of the resulting DEMs. Renssen and Knoop (2000) used a similar approach to resample a 5-minute DEM to generate a 0.5-degree global river network.

Fekete et al. (2001) used the concept of upstream drainage area to derive flow direction of the grid cells at 10, 15 and 30-minute resolution river networks from a 5-minute DEM for the Danube River basin in Europe. O'Donnell et al. (1999) proposed a similar method based on the contributing area, which tracks the river network beyond the boundary of the grid cells. Olivera et al. (2002) generalized O'Donnell et al.'s (1999) approach by making it applicable to coarse resolution grids that are not aligned with the DEMs.

Even though DEM based methods are simple to implement, the delineated coarse resolution river network does not always compare well with the fine resolution network unless the streams are burnt into the DEM (Graham et al., 1999; Renssen and Knoop, 2000). Burning reduces the chances of error as the stream network is forced onto the DEM. Even though, the stream network delineated using DEM methods is very accurate, the flow distances calculated between the cells cannot be ascertained accurately. Researchers in past have used a fixed meandering factor to define the relationship between actual flow distances and the distances between the centers of the cells. This method improves the prediction of reach lengths but is not accurate. A vector based approach presents a more accurate method as the vector stream network

captures the topology much better than the DEMs, especially in areas of low relief where minor inaccuracies in the topographic data may lead to major errors in the delineation of streams. Additionally, vector fine-resolution stream data are easier to trace downstream after they leave the cell for which the flow direction is being determined.

The network tracing method (Olivera and Raina, 2003) uses vector fine resolution stream network as input to compute coarse resolution stream networks. The use of vector stream data in NTM to calculate the stream lengths results in a nearly error free calculation of the river lengths. This is essential in flow routing as errors in length can generate errors in flow time towards the outlet from a point. Most of the coarse resolution stream networks developed neglect the meandering in a river and they represent the length of the stream equal to the distance between the centers or multiply this distance to a fixed value. Thus, in principle the complexity of the river system is overlooked. This results in unde rprediction of the river lengths. The NTM assigns a meandering factor to each line of the grid-ded network, which is defined as the flow distance from a cell to its downstream cell along the fine-resolution flow-path divided by the flow distance along the coarse-resolution flow-path (i.e. the length of the cell side or cell diagonal, depending on the flow direction in the cell).

Cell to cell flow routing models present a simplistic approach to calculate the discharge of rivers with a reasonable degree of accuracy (Olivera et al., 2002). The cell-to-cell stream flow routing models enable computation of hydrographs at any cell and not only at the outlet. These are some of the reasons why over the last few years

numerous models of varying degree of complexity of parameters and accuracy of the prediction of flow have been developed. They range from a network of simple linear reservoirs to highly complex physically based models. Both models have their own advantages and disadvantages, the simple models are computationally less challenging but they lack ability to take into account the parameters within the cells, which have implication on the discharge, like slope of the channel and the channel width. The physically based models give accurate simulated flow values as they take into account within grid variability, the slope characteristics of the channel and the flow in the channels. These models are ideal for smaller cell sizes, where data is available for all the desired model parameters. However, as the cell size increases, these physically based models tend to lump parameter values over a large area, giving them an equal degree of uncertainty as the simple models. Moreover, data sets with observed data about these most of the parameters are available for limited areas, thus limiting the application of the physically based models. CASC2D (Julien et al., 1995) is implemented at a smaller resolution (30-300m), which gives it an edge over other physically based models. However, unlike other hydrologic models CASC2D requires a very carefully prepared input data set, which is a prerequisite for a good model performance. The input data includes information about saturated. Application of CASC2D is thus limited to watersheds where a sufficient quantity of high-quality input data is available. CASC2D can be numerically unstable if the data set contains errors (Downer et al., 2002).

Most cell-based models developed in the past, except for CASC2D (Julien et al., 1995) are operated at one single resolution that is be between $1/2^0$ to 4^0. This presents a serious limitation of these models as any change in cell resolution leads to changes in parameter and input values. Even though CASC2D operates at a number of resolutions, effect of change of grid size on the hydrographs has not been rigorously studied to date (Downer et al., 2002). The cell-to-cell stream flow routing model presented in this study is independent of the grid size of the cells in the watershed. The input parameters do no change as the cell size changes. The number of reservoirs in the cascade, which is dependent on the velocity and the dispersion within the cell, changes accordingly as the cell size changes. Thus, once for a watershed these values are found they are fixed for that case and need not be changed.

Fueled by the desire to develop a simple and easy to implement cell-based model with few model parameters, which can be derived through calibrated to fit the observed flow measurement over a range of cell resolutions, the cell-to-cell stream flow routing model was developed. The cell-to-cell stream flow routing model is a two-parameter model that divides a watershed into equal grid cells, which are approximated as a cascade of linear reservoirs with the same retention time. Velocity and dispersion coefficient are the two parameters used for model calibration. Since the approach presented here is not dependent on the topography of the region, there is certainty involved in the determination of various parameters like width and flow depth of the river. Not only that, unlike the number of unknowns are few which make this model much simpler to operate as compared to CASC2D. The input data consists

of data about the cell connectivity, reach lengths, velocity and dispersion values and a time series of runoff values for each cell in the watershed. The number of reservoirs in the cascade is variable and is dependent on the stream velocity and the coefficient of dispersion and not constant as proposed by Hagemann and Dumneil (1998). The model parameters are found using calibration. This is important, as these values are effective values are not actual values. With cell sizes of 25km or greater, it is impossible to find out actual velocities and dispersion coefficients. At those resolutions, they are lumped values of channel flow and overland flow. Thus, instead of taking constant velocities in all cells we calibrate the model by tuning these parameters for each cell. The cell-to-cell stream flow routing model presented in this study is capable of being operated at a number of cell sizes to adjust to the requirements of the application. At higher resolutions it can be coupled to a GCM to access the accuracy of the runoff generation of the GCM and at smaller resolutions it can be used for hydrologic studies like flood prediction.

3. METHODOLOGY

In this section, a cell-based two-parameter runoff routing model, the Cell-to-Cell stream flow routing model, used to calculate flow hydrographs at any point in the watershed using a network of connected identical square cells is developed. Flow is predicted by routing the runoff in each cell, cell-to-cell to the outlet of the watershed. The first part of this section, the theory behind the development of the model is discussed and the second part discusses the spatial analysis to derive a connected set of cells from raw data like a stream network and a mesh. The third part will discuss the development of the tool for implementing the cell-to-cell stream flow routing model.

With a given set of cells connected to each other in a dendritic network, this model routes the water downstream to the outlet of the watershed depending on the flow direction of the cells and calculates the flow and storage of all cells for the period of simulation.

3.1 Model Development

The cell-to-cell stream flow routing model is a two-parameter model in which a watershed is divided into identical square cells. Each of these cells can be approximated as a cascade of linear reservoirs. Routing in this model is done with the help of two cascades of linear reservoirs. The first cascade of reservoirs routes the runoff within each cell is to the outlet of each cell through a cascade of reservoirs and the second cascade routes this water to the outlet of the watershed over a network of

cells. Figure 3.1 shows a model watershed with a nine cells acting as the drainage area. The arrows in the figure show how the cells are connected to each other. The numbers in each cell is the BoxID. The cell-to-cell stream flow routing model will route the water from each cell to the outlet. The dashed lines are the fine resolution stream network.

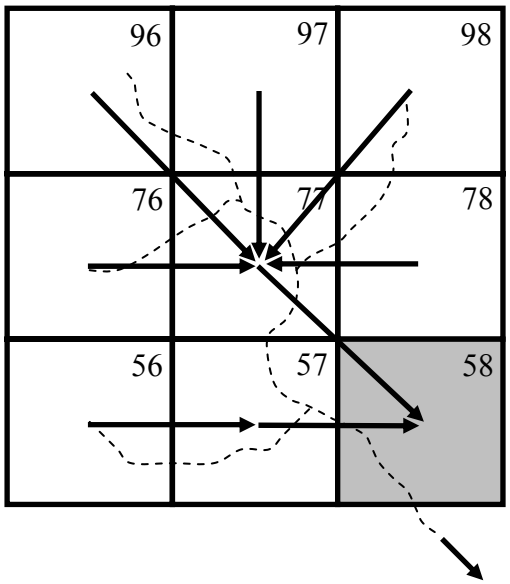

Figure 3.1. A model watershed depicting a dendritic network.

3.1.1 Inflow determination

The inflow for each cell is the excess runoff generated within it and the water coming from all the upstream cells. This water is routed to the outlet of the cell (from A to B as shown in Figure 3.2) and then from outlet of the cell, cell-to-cell to the watershed outlet (from C to D in Figure 3.2) assuming that A is the center of the circle, B is the edge of the cell to where the runoff is routed, C is the exit node of the cell and D is outlet of the watershed. The runoff for each cell is applied to the first

reservoir in the cascade along with the summation of fluxes from upstream cells. For the rest of the reservoirs in the cascade the inflow is the outflow of the upstream reservoir.

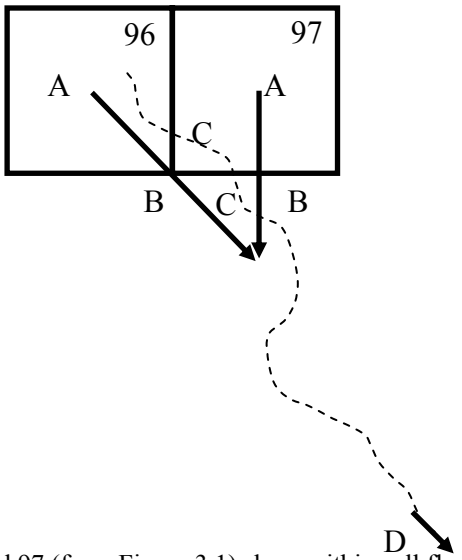

Figure 3.2. Cells 96 and 97 (from Figure 3.1) show within cell flow and channel flow.

3.1.2 Within-Cell flow routing

The Network Tracing Method (NTM) (Olivera and Raina, 2003), calculates the reach of a cell as the distance between the exit point (which is located at the edge or the corner) of the given cell (point C in Figure 3.2) and the exit point of the immediate downstream cell. The available runoff data however, is applied at the center of a cell and not at the exit point. During the routing phase, the routing algorithm transports the water from the exit point to the outlet of the watershed. This in effect means that algorithm is routing the runoff from the edge of the cell even before it reaches the edge of the cell. This leads to significant errors if the cell size is

big, e.g. in case of a 100 km cell this error equals to approximately 6 days if we consider that the water moves from the center of the cell to the edge at a velocity of 0.1m/s. To prevent this error, the runoff was delayed to the exit point of each cell via a cascade of linear reservoirs (from A to B in Figure 3.2). The flow from the center to the exit point is assumed to be overland flow. The number of reservoirs in the cascade is a function of the overland flow velocity and the overland flow coefficient of dispersion. The number of reservoirs or tanks in the cascade is calculated using the following relationship(Olivera et al., 1999) :

$$N_i = \frac{L_i \times Vo_i}{2 \times Do_i} \qquad (3.1)$$

Where, N_i is the number of tanks in a cell i, Vo_i is the overland flow velocity in the cell i, and Do_i is the overland flow coefficient of dispersion in the cell i, L_i is the length calculated between the center of the cell to the exit or the outlet of the cell. This length is equal to Cell Side/2 if the flow direction of the cell is 1, 4, 16 and 64 and is equal to Cell Side*1.414/2 is the flow direction is 2, 8, 32 and 128. These flow directions are determined by the Network Tracing Method (Olivera and Raina, 2003, see section 3.4.1).

3.1.3 Channel flow routing

The cell-to-cell flow routing model divides a watershed as a network of grid cells (Figure 3.1). Each of the grid cell is approximated as a cascade of equal linear reservoirs. The number of reservoirs or tanks (N) in a cell is a function of two parameters namely; channel flow velocity (V) and the channel flow coefficient of

dispersion (D). N varies from cell to cell. N for each cell is calculated using the following relationship (Olivera et al., 1999):

$$N_i = \frac{L_i \times Vc_i}{2 \times Dc_i} \quad \text{.....(3.2)}$$

Where, N_i is the number of tanks in the cell i, L_i is the reach of the cell i, defined as the stream length between the exit point of the cell and the exit point of the immediate downstream cell. This distance is the actual stream length calculated from the fine-resolution stream network and not the distance between the centers of the cells. Vc_i is the stream velocity in the cell i, and Dc_i is the coefficient of dispersion in the cell i.

The delayed runoff is routed using the cell-to-cell stream routing algorithm to the outlet of the watershed (from C to D in Figure 3.2). The Cell-to-Cell flow routing model is based on the kinematic wave approximation of the St. Venant equation to route the water in the channel, in which the momentum equation is not taken into account.

The storage in each of the reservoirs in the cascade is given by the following continuity equation,

$$\frac{dS}{dt} = I - O \quad \text{.....(3.3)}$$

The above differential equation is numerically solved using the explicit scheme in two different ways depending on the location of the tank in the cascade (see Figure 3.3). For the first tank in the cascade the solution to the above equation is,

$$S_{t+1} = S_t + R_t \times A \times \Delta T + \sum (I_t) \times \Delta T - O_t \times \Delta T \quad \text{.....(3.4)}$$

Where, S_{t+1} is the storage of the tank at time any time step t+1, S_t is the storage of the tank at the time any time step t, R_t is the excess rainfall coming into the tank at time any time step t, I_t is the inflow coming into the tank at time any time step t from upstream cells, O_t is the outflow from the tank at time any time step t, ΔT is the model time step and A is the area of a given cell.

For any other tank in the cascade the solution to the continuity equation is,

$$S_{t+1} = S_t + I_t \times \Delta T - O_t \times \Delta T \quad \text{.....(3.5)}$$

Where, S_{t+1} is the storage of the tank at time any time step t+1, S_t is the storage of the tank at the time any time step t, I_t is the inflow coming into the tank at time any time step t from upstream tank, O_t is the outflow from the tank at time any time step t, ΔT is the model time step.

The kinematic wave approximation uses a modified version of the momentum equation in which the inertial and pressure forces are neglected, in effect assuming a balance between the frictional forces and the gravitational forces. This relationship can be depicted as

$$S_f = S_o \quad \text{.....(3.6)}$$

This relationship can be interpreted as either as a depth-discharge relationship, which is given by

$$Q = \acute{\alpha} h^n \quad \text{.....(3.7)}$$

Where, Q is the discharge per unit width, h is flow depth, ά and n are empirical parameters.

For as a storage-discharge relationship given by

$$S = kO^m \quad \text{.....(3.8)}$$

Where, S is the storage, Q is the discharge and k and m are empirical parameters. If m is assumed to be equal to one, K becomes the lag time. This assumption implies that the watershed is linear and this forms the basis for the linear reservoir theory as well as the unit hydrograph theory.

Assuming m equal to one we have that the discharge from a linear reservoir O_t varies linearly to the storage and is equal to,

$$O_t = \frac{S_t}{k} \quad \text{.....(3.9)}$$

Where, S_t is the storage of the tank at the time any time step t, k is the retention time in the linear reservoir, which is calculated as,

$$k_i = \frac{L_i}{V_i \times N_i} \quad \text{.....(3.10)}$$

Where, L_i is the reach of the cell, V_i is the stream flow velocity and N_i is the number of linear reservoirs in the cascade in a given cell i.

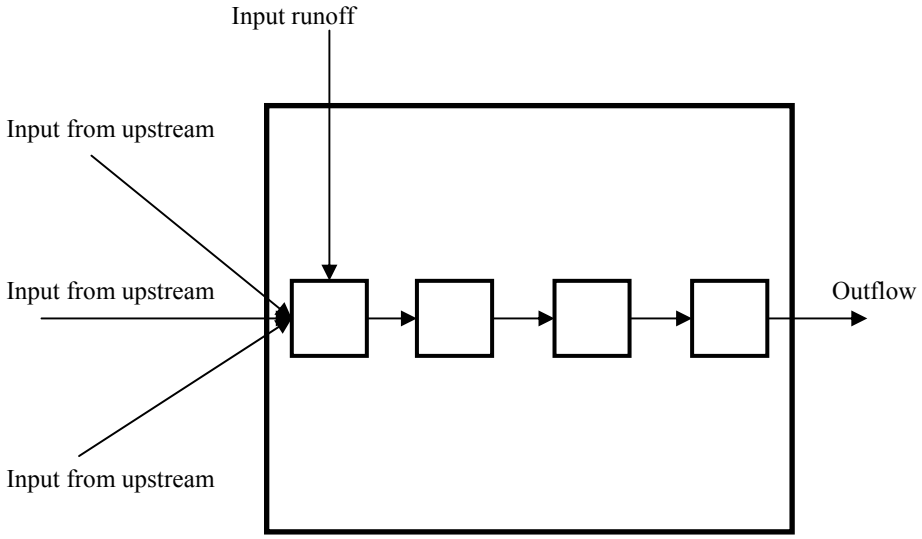

Figure 3.3. Cross section of a cell in a watershed.

The tanks are connected to each other in a series arrangement (Figure 3.3) such that the discharge of the *i*th reservoir will be equal to the inflow into the *i*+1th reservoir. The retention time of all the linear reservoirs in a cascade is same, but it varies cell to cell. The discharge of the last reservoir in the cascade of the n^{th} cell will be the inflow to the first reservoir of the cascade of the $n+1^{th}$ cell.

This continuity equation is applied to all the cells in the watershed and the time step that will be used for modeling of the storage and flow is governed by the courant condition (Chow, 1998). The courant condition states that the model time step cannot be greater than the minimum ratio of the reach and the velocity. This is necessary to ensure that the model does not become numerically unstable.

3.2 Effect of the cascade of linear reservoirs

The continuity equation for a linear reservoir is given in equation 2.1 as:

$$\frac{dS_t}{dt} = I_t - O_t \quad \text{.....(3.11)}$$

Where, S is the storage, I_t is the inflow rate, and O_t is the outflow rate which is proportional to the storage given in equation 3.9 as:

$$O_t = \frac{S_t}{k} \quad \text{.....(3.12)}$$

Where, k is the coefficient of proportionality, also known as the residence time in a given cell or the retention coefficient. Replacing the value of S_t from equation 3.5 in equation 1 we have:

$$k\frac{dO_t}{dt} = I_t - O_t \quad \text{.....(3.13)}$$

Using D to denote d/dt we have,

$$O_t = \frac{1}{1+kD} I_t \quad \text{.....(3.14)}$$

Now equation 3.9 is what is known as a linear reservoir and the coefficient $1/(1+kD)$ signifies the effect of a linear reservoir on a given input. Let

$$H = \frac{1}{1+kD} \quad \text{.....(3.15)}$$

The operator H represents the effect of a linear reservoir with the proportionality coefficient k. This operator is cumulative. The instantaneous unit hydrograph (IUH) of a linear reservoir is given as,

$$h_t = \frac{e^{-t/k}}{k} \quad \text{.....(3.16)}$$

Now replacing this linear reservoir by a cascade of n linear reservoirs with the same k we get,

$$O = \frac{1}{(1+kD)^n} I_t \quad \text{.....(3.17)}$$

and the IUH as,

$$h_t = \frac{1}{(n-1)!}\left(\frac{t}{k}\right)^{n-1} \frac{e^{-t/k}}{k} \quad \text{.....(3.18)}$$

This equation is a gamma distribution (see Figure 3.4) with the parameters *n* and *k*. The two parameters *n* and *k* are calculated using the equations 3.2 and 3.10 respectively. Being a two-parameter model, the cell-to-cell stream flow routing model can effectively predict both translation and dispersion in the stream.

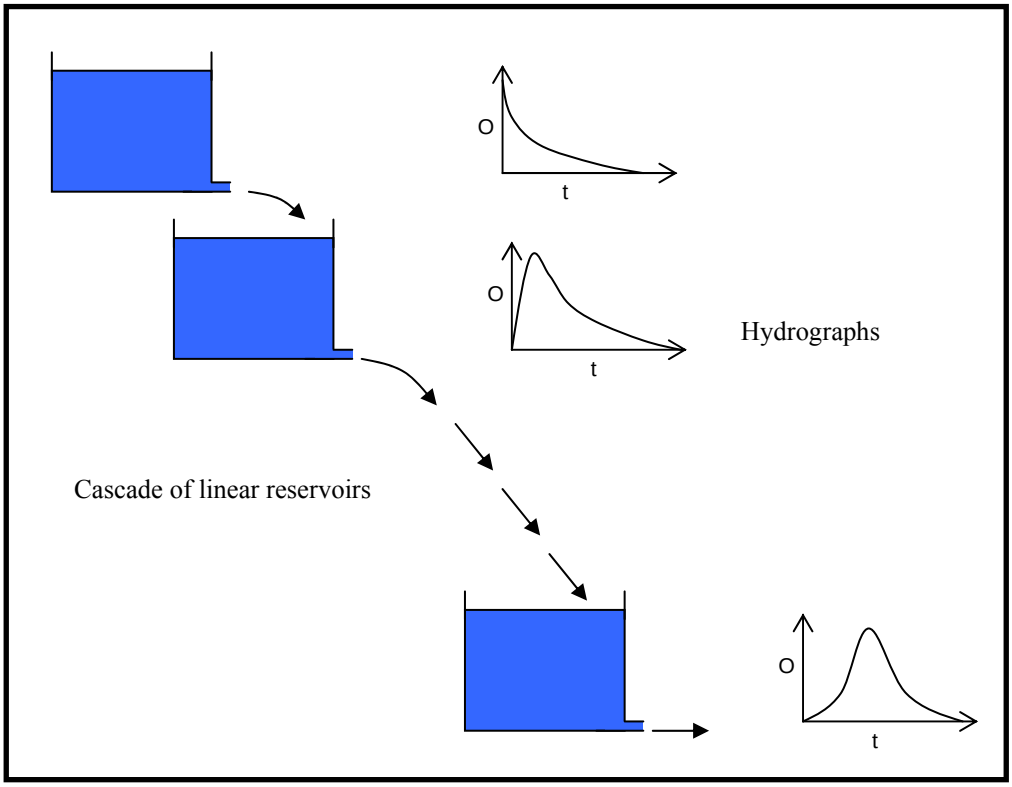

Figure 3.4. Effect of cascade of linear reservoirs (Singh, 1988).

3.3 Effect of change of resolution

Olivera et al. (1999) state that cell-to-cell runoff routing models (with one tank per cell) show different flow characteristics as resolution of the terrain changes. As resolution increases, the attenuation becomes less visible with larger flows increasing and lesser flows decreasing to a stage until pure translation occurs. Replacing a cell in the watershed with a cascade of linear reservoirs or tanks results in correct prediction of translation and attenuation even if the resolution changes. The parameters in the model are dependent on the reach, velocity and dispersion in the stream. When the resolution changes, the reach changes accordingly, leading to a change in number to tanks, such that from any given point in the watershed the

number of tanks to the outlet remains the same. The stream flow routing model presented in this paper is resolution independent for channel flow.

3.4 Spatial data analysis

The cell-to-cell stream flow routing model requires a set of inter connected cells with a dendritic network also known as a coarse resolution stream network to route the water from a given cell to the outlet. These coarse resolution networks are not readily available and need to be created for a specific application. The Network Tracing Method (NTM) (Olivera and Raina, 2003) is a method with which coarse resolution networks are created. This section outlines the steps that are used for the development the coarse resolution dendritic stream network from raw data, which generally is the DEM.

Most conventional rainfall-runoff modeling methods are tedious and time-consuming due to the enormous amount of data available for processing. With the advancements in GIS and the computer hardware, processing large amounts of spatial data and hence modeling, has become easy and less time consuming. A grid-based GIS offers an excellent approach to store land surface. Most commercially available software packages like ESRI ARCVIEW and ARCGIS have in-built functions that can be used on grids to achieve various goals like watershed delineation. Moreover, data in grid format is easily and readily available. A grid-based approach is used in this study to derive the stream network and the watershed.

A digital elevation model (DEM), which is a digital map of the elevation data was used for the delineation of the watershed and the fine resolution stream network

of a watershed. Now for the coarse resolution network we need a framework. This framework is provided by a polygon shapefile called as a mesh. Each mesh element is called a "cell" throughout this discussion. Intersection of a dendritic river network with the mesh results in a stream network in which, all lines are split at the cell boundaries, such that each line is within one and only one cell and new nodes at the intersection of the arcs and the mesh are created. This process ensures that to-node and from-node are correctly assigned to all nodes. From node is the upstream node of an arc and to node is the downstream node of an arc. All these functions are readily available in all major commercial GIS softwares. A table containing the information about the stream network e.g. (1) RECNO, (2) Length (3) FNODE, (4) TNODE was created and exported. Where, RECNO is the unique vaule given to each arc, FNODE is from node of the arc, TNODE is to node of the arc, and length is the distance measured between FNODE and the TNODE. For further information refer to section 3.4.1. This fine-resolution stream network is up scaled to a coarse resolution network using the Network Tracing Method (NTM) developed by Olivera and Raina (2003). Section 3.4.1 discusses the network tracing method in detail. The cell-to-cell stream flow routing algorithm is applied to the coarse resolution watershed delineated. Flows are calculated at the outlet of all the cells in the watershed.

3.4.1 NTM theory

Network Tracing Method (NTM) (Olivera and Raina, 2003) is a method developed to upscale fine-resolution stream networks into coarse resolution gridded stream networks. NTM requires a coarse-resolution mesh that subdivides a study area

into identical square cells and a fine-resolution dendritic river network of the same area. The NTM (1) identifies the downstream cell of each grid cell of the system in which a stream is found, and (2) estimates meandering factors for the coarse streams.

Even though NTM works best with square cells which have little or no distortion, meshes originally defined in geographic coordinates (i.e. longitude and latitude), which get distorted when projecting the curved surface of the earth onto the flat surface of a map can also be used even though the accuracy of the method is less (Olivera and Raina, 2003).

In the following sections, the NTM algorithm is discussed in brief and for the better understanding of the readers a sample grid and a sample stream network is used. For complete explanation about the NTM, the readers are suggested to refer Olivera and Raina (2003). Figure 3.5 presents a detail of a coarse-resolution grid (i.e., a nine-cell window) and of its corresponding fine-resolution dendritic river network. In the network, the lines are connected to each other only at their edges and point downstream, thus creating a dendritic stream network. In a dendritic network, a line can have more than one line upstream, but only one line downstream. Similarly, a node can be the downstream node of more than one line, but the upstream node of only one line.

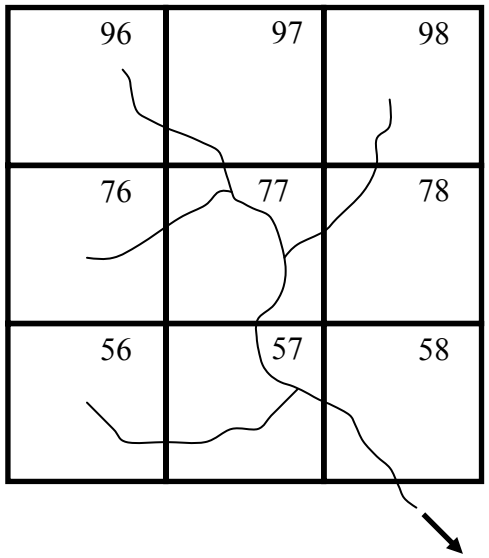

Figure 3.5. Sample grid with a fine resolution stream network.

Once the fine-resolution river network with the coarse-resolution grid are obtained, they are intersected with each other resulting in a new network, in which the lines are split at the grid cell boundaries, so that each line lies entirely within one cell (see Figure 3.6 and Table 3.1).

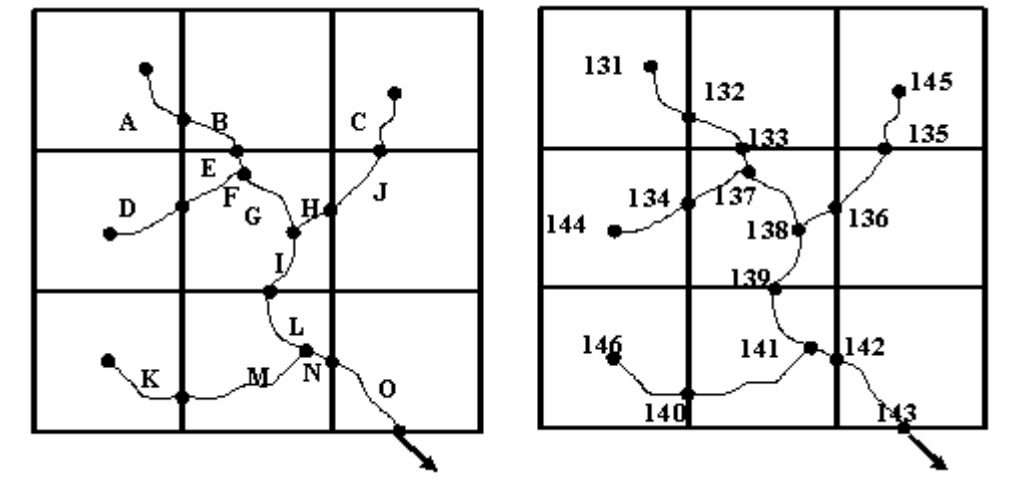

Figure 3.6. Stream network after intersection.

Table 3.1. Fine resolution streams after intersection with a coarser resolution mesh.

Line	Grid cell	Length *	Upstream node	Downstream node	Upstream Length *
A	96	51	131	132	51
B	97	48	132	133	99
C	98	46	145	135	46
D	76	62	144	134	62
E	77	14	133	137	113
F	77	44	134	137	106
G	77	58	137	138	171
H	77	32	136	138	133
I	77	48	138	139	219
J	78	55	135	136	101
K	56	66	146	140	66
L	57	52	139	141	271
M	57	98	140	141	164
N	57	12	141	142	283
O	58	71	142	143	354

The nodes on each line are randomly assigned a unique number (Figure 3.6), which are stored in the network table as the line upstream and downstream nodes (see fields “Upstream Node” and “Downstream Node” in Table 3.1).

The next step of the NTM is to identify the “exit-node” of each grid cell. Exit-nodes are the points through which the main stream flows out of the cells except, in case of continental margins and closed depressions. Cells at the continental margin and closed depressions are sink cells and do not have exit nodes. The exit-node of a cell is defined as the node with the greatest upstream flow length. The upstream flow length of a node is calculated as the greatest of the distances from the node itself to the most upstream node. Once the exit node of a cell is located, the NTM traces the stream network downstream to identify the “next-exit-node” of the cell, which is the exit node

of the cell immediately downstream. The flow distance between the exit-node and the next-exit-node of each cell, called here reach length, is then calculated. This reach length is compared to a user-defined threshold distance. The threshold value specified by the user is the minimum desired distance that a stream should stay in that cell so that that cell can be termed as the downstream box. A reach length greater than the threshold implies the cell is flowing to its immediate downstream cell, while a value less than the threshold implies that it is flowing further downstream. In this case (threshold greater than reach length), the network is further traced downstream and a new exit node is located and new reach is calculated. A correct threshold is determined using a trial and error technique until the ratio of the cells flowing through the sides to the corners equal to 59/41 (Olivera et al., 2002). Threshold values should be carefully chosen as a very high threshold value will mean more cells with flow through the corners and vice versa. In an extreme case, when using a very small threshold value, no flow through the corners is predicted; and, similarly, when using a very large one, the minimum number of cells with flow through the sides is predicted. Ideally, the threshold should be set such that the eight flow directions are equally likely to occur. Threshold values depend on the grid cell size and on the level of detail of the fine-resolution stream data. Finally, the downstream cell is defined as the cell that drains through the next-exit-node. Once the downstream cells are identified, a gridded river network can be obtained (Figure 3.7). The grid cells are assigned a flow direction code and a meandering factor. The flow direction code is a number associated with the direction in which the flow takes place. Code 1 corresponds to the East direction, 2 to

the Southeast, 4 to the South, and 8 to southwest 16 to west, 32 northwest, 64 to north and 128 northeast.

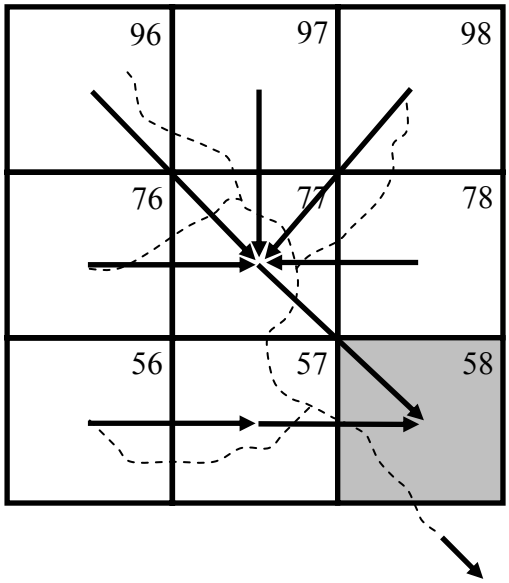

Figure 3.7. Determination of flow direction of the cells

An important contribution of the NTM is the concept of meandering factor. Most coarse resolution networks assume the length of the streams to be the distance between the cells centers. As a result, river lengths are underestimated because rivers tend to meander a lot and this is not captured by the coarse resolution network. A solution to this problem suggested in the literature earlier is to multiply the distance between the cell centers by a fixed number to improve the prediction of reach lengths. The meandering factor is equal to the reach length divided by the grid cell size if flow takes place through the side or 1.41 the grid cell size if flow takes place through the corner. Generally, this factor is greater than one because of the presence of meanders; however, factors lower than one are also possible if the exit nodes of consecutive cells

are located relatively close to each other. Sink cells are automatically assigned downstream cell, flow direction code and meandering factor values of 0 (zero).

Even though this method creates accurate flow direction for each cell there are two cases in which manual intervention and change of algorithm is needed to avoid errors in the network. The first case occurs when the threshold value is greater than the cell size, and the river network crosses the cell's downstream cell from side to the next cell along a flow path shorter than the threshold (see Figure 3.8a). According to the method, the downstream cell would be two cells down, in the direction of one of the sides. This is not an acceptable solution as a cell can flow only into one of its eight immediate neighbors. Consequently, this anomaly is corrected by redefining the downstream cell as the immediate downstream cell, without further tracing of the network even though the reach length would be less than the threshold.

The second case occurs when a pair of adjacent cells point to their downstream cells along diagonals that intersect each other. This situation results due to a stream that flows around the corner of four cells (see Figure 3.8b). This condition is corrected by redefining the downstream cells as the immediate downstream cells, even though the reach lengths would be less than the threshold. Note that the immediate downstream cells are always in the direction of the sides and that no intersection can occur when cells point to their downstream cells along their sides.

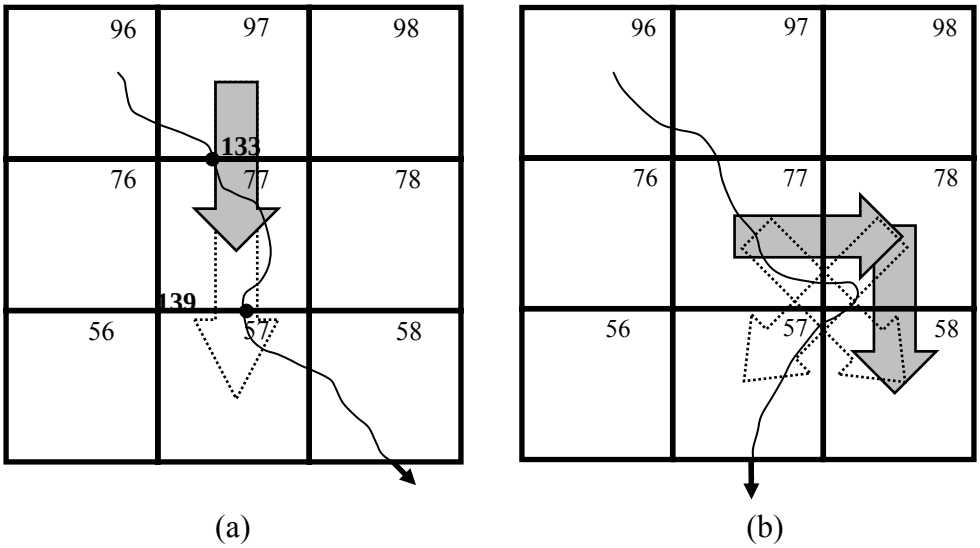

Figure 3.8. Two cases in which the NTM algorithm is changed to avoid errors in the network.

3.4.2 Errors in basin area and river length prediction

After developing coarse gridded river networks, major basins and rivers can be identified, and their areas and lengths can be evaluated.

Basin areas determined from coarse river networks tend to be overestimated in case of large basins, and underestimated in case of small basins. The reason for this over- and under-estimation is that coarse river networks assign a single downstream cell to each cell, regardless of the different directions in which each of the fine-resolution streams flow out of it. That is, whenever two fine-resolution streams coincide in a grid cell, the smaller stream and its corresponding drainage area become absorbed by the cell main stream. This process tends to make larger basins larger and smaller basins smaller. This problem, though, is intrinsic to the upscaling process itself and is not caused by the NTM. Additionally, a correction of half a grid cell is

recommended for all predicted basin areas to account for the fact that sink cells are only partially within the basin.

Likewise, river lengths tend to be underestimated because at the river mouth the meandering factor of the sink cell is assumed equal to zero, and meandering factor of the cell immediately upstream equal to the length of the stream segments in the sink cell divided by the cell size, which is most likely significantly less than one. In addition, the reach lengths stream segments of the most upstream cell are neglected in the algorithm. On an average, the river length is underestimated by one cell. The reach lengths and the meandering factors of a cell are also under predicted when a stream crossed back and forth from one cell to its adjacent cell (Figure 3.9a). The reach length and meandering factors were underestimated because the method tracked the network only in the immediate two downstream cells. The reach length in NTM is calculated as the flow distance between the exit-node and the next-exit-node of a cell; however, since the stream could be entering and leaving the downstream cell a number of times, the next-exit-node does not really represent the point at which the stream ultimately leaves it. Even thought this situation, affects only a limited number of cells, it can cause significant underestimation of overall river lengths. Now instead of tracing only up to the next two cells the method uses a TraceArc method, wherein it keep on tracing the network till the threshold is achieved, no matter how many times the network goes to and fro between the grid cells. This has improved the river length prediction by the NTM. A sample case (Figure 3.9b) illustrates this case. For cell 97 the exit node is 133. Now the next exit node is to be located. The network is traced to

node 136 then to 137. At this point, the reach length accumulated is compared to the user threshold. If the threshold is more than the reach the network is further traced to 138,139, 140, 141 and finally to 142. Similarly, for cell 77 the reach is calculated as the distance between 142 and 148.

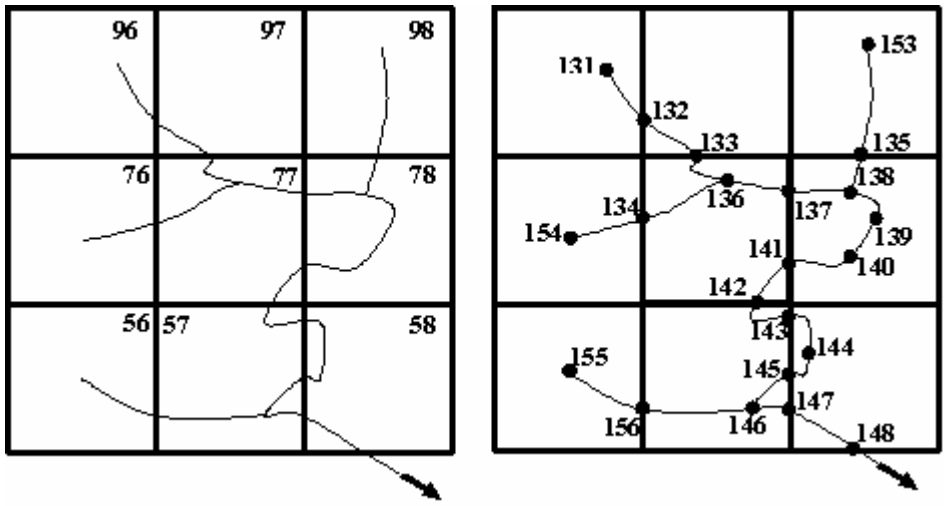

(a) (b)

Figure 3.9. Calculation of reach lengths with TraceArc.

A vector theme of the mesh with flow directions and a user-defined outlet is used to delineate a watershed of the study area. The attribute table of this watershed contains the data about each cell: (1) Identification number of each cell, BoxID (2) its immediate downstream cell, DSBoxID (3) area of the cell, Area and (4) reach of the cell. This table is edited to include the stream flow velocity, overland flow velocity, coefficient of dispersion and the overland coefficient of dispersion. The area of the watershed delineated is compared to the observed area of the study area. Difference in areas gives inaccurate results because with more area, runoff will be overestimated

leading to more flow and volume and vice versa. A runoff time series for each cell in the watershed, which contributes to the total flow to the outlet, is required. With the watershed information and the runoff time series the cell-to-cell stream flow routing model is applied to the study area.

3.5 Implementation of the model - the Visual Basic tool

The cell-to-cell stream flow routing is implemented in Visual Basic 6 (Figure 3.10). There are various reasons as to why Visual Basic 6 is chosen as the language to implement the algorithm. It is easy to understand and it is easy to write instructions to do any operation. The graphical user interface of the Visual Basic provides intuitively appealing views for the management of the program. Visual Basic provides a comprehensive interactive and context-sensitive online help system. The Visual Basic tool completes the following objectives: (1) takes as input, the file containing the data about watershed cell network and the runoff time-series file. (2) It asks the user to input the desired time-step and the total time of simulation. (3) It calculates the flow and storage in each cell at every user time-step.

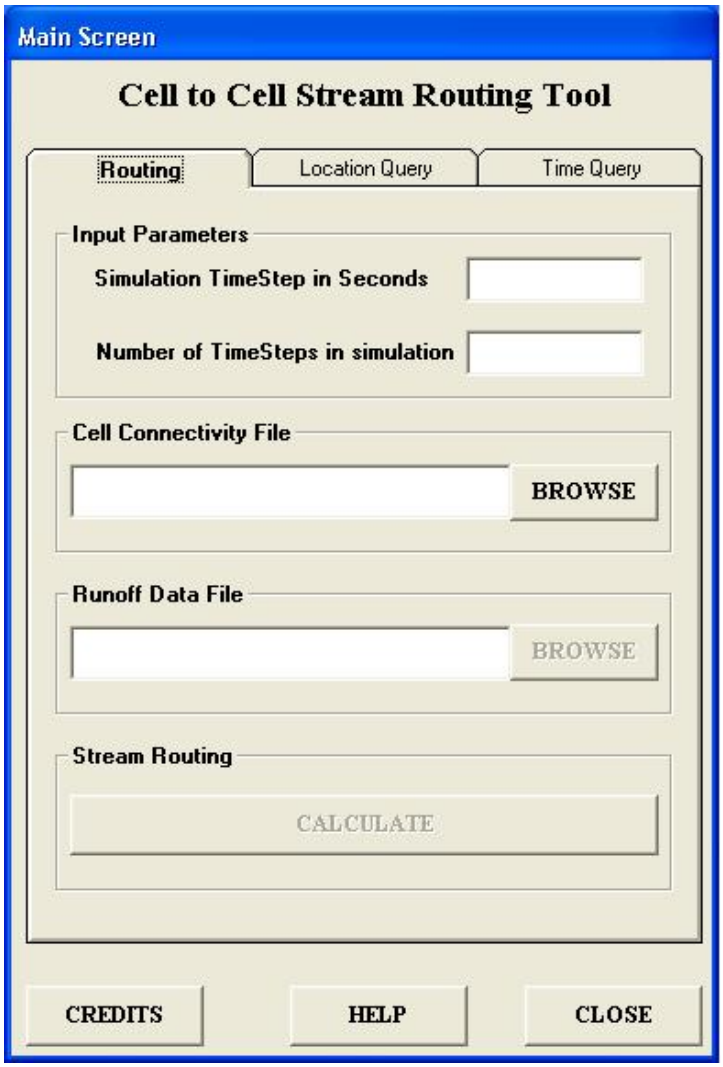

Figure 3.10. Main screen of the cell-to-cell stream flow routing tool.

The *Cell-to-Cell stream flow routing tool* consists of basically 3 tab windows.

a) The main window

b) The location query

c) The time query

3.5.1 The main window

This graphical user interface (Figure 3.10) is input and output screen for the stream flow routing program. It has been divided into four sections. In the first section *"Input Parameters",* the user is asked to input the simulation time step, and total number of simulations desired. The next section "*Cell Connectivity file*" prompts the user to input the coarse resolution river network file. This is a comma delimited file with the following fields:

a) BoxID - Identification number of a cell (Integer)

b) DSBoxID – Identification number of the downstream cell of the given cell (determined by the NTM) (Integer)

c) Area – Area of a given cell (square meters)

d) Reach – Reach of a given cell (in meters)

e) FDBoxID – Flow direction of a given cell (determined by NTM)

f) V_o – Overland flow velocity (m/s)

g) D_o – Overland coefficient of dispersion (m^2/s)

h) V_c – Channel flow velocity (m/s)

i) D_c – Channel coefficient of dispersion (m^2/s)

The third section "Runoff Data File", the user is prompted to input the runoff depth time series data file. The runoff time series data is a comma delimited file in the following format:

$BoxID_1$, $BoxID_2$, …….. $BoxID_n$

$RO_{1,1}$, $RO_{2,1}$,……$RO_{n,1}$

$RO_{1,2}$, $RO_{2,2}$,……$RO_{n,1}$

$RO_{1,m}$, $RO_{2,m}$,……$RO_{n,m}$

Where, RO is runoff depth in meters. The runoff data file should contain values for each cell at a user defined time step. This is form of a two dimensional matrix of size n by m where n are the total number of cells in the watershed and m is the total number of time steps. Once the runoff table is uploaded, the tool delays the runoff to the edge or the corner of the cell using the method explained in section 3.1.2.

The last section *"Stream Routing"*, computes the flow and storage values for all the cells in the watershed. The cell-to-cell stream flow routing model operates at a model time step, which is governed by the courant condition. According to this condition, the time step can not be greater than the smallest ratio of reach and the velocity. This value can be as smaller as few seconds to even hours. It is not desired to create an output file at intervals of few seconds as it leads to a huge file with a huge number of records. The user is thus, prompted to input a time step at which results are desired. This time step can range from a few minutes to days. The program however, supports the input only in the form of seconds. So the user has to input the time step in seconds and not in days, or in hours or in minutes. The program assigns the velocity of the downstream cell to the given cell. This is because the reach of a given cell is from its exit node to the exit node of the downstream cell, which means that the most of the reach is in the downstream cell. Thus, velocity of the downstream cell is applied to the stream flow routing. This velocity is used for the calculation of the retention coefficient. The program calculates the minimum value of the ratio of reach and

velocity and reduces this to ½ of the calculated value. This value is again lowered until the user time step is completely divisible by the model time step. This results in a whole number of model time steps within the user time step. The program calculates the flow and storage at each model time step but prints only the results at the user time step.

The program next calculates the number of tanks in each cell using the equations given in section 3.2. The program then creates a new table, where a single record of a cell is replaced by records equal to the number of tanks calculated earlier. The new table has records equal to the total number to tanks in the watershed. Only first tank in the cell is connected to the upstream cells and only the last tank is connected to the downstream cell. The runoff generated within a cell and input from the upstream cells is applied only to the first tank in the cell. The outflow to the downstream cells is the outflow from the last tank. All other tanks within the cascade are connected in a series to the first and last tank in the cell. The inflow to these cells is the outflow from the previous tank. Since the runoff is available at the user time step and the program runs at a smaller model time step, equal fractions of the runoff totaling the total runoff for a given user time step is applied within a user time step.

The program creates 4 comma delimited files output files. The first comma delimited file has the following fields:

a) BoxID - Identification number of a cell (Integer)
b) DSBoxID – Identification number of the downstream cell of the given cell (determined by the NTM) (Integer)

c) Area – Area of a given cell (square meters)

d) Reach – Reach of a given cell (in meters)

e) V_o – Overland flow velocity (m/s)

f) D_o – Overland coefficient of dispersion (m^2/s)

g) Velocity_ds – stream flow velocity of the downstream cell of a given cell(e.g. m/s)

h) Dispersion

i) Dispersion_ds –stream flow coefficient of dispersion of the downstream cell of a given cell (e.g. m^2/s)

j) K – transfer coefficient of the cell (e.g. Seconds)

k) N – total number of tanks

l) Ksmall – transfter coefficient of each tank in the cascade (e.g. Seconds)

The second comma delimited file one has the following fields:

a) BoxID - Identification number of a cell (Integer)

b) TankID – identification number of a given tank

c) TankID_Upstream – identification number the upstream tank of a given tank

d) TankID_DownStream – identification number of the downstream tank of a given tank

e) Area – In this only the first tank in the cell has the area, rest others have the value of zero.

f) Ksmall – Transfer coefficient of each tank in the cascade (e.g. Seconds)

The third comma delimited text file created by the program contains the values for storage in cubic meters for all cells at a user defined time interval. It is in the format of a two dimensional matrix of size n by m where n are the total cells in the watershed and m are the total time steps.

$BoxID_1$, $BoxID_2$, …….. $BoxID_n$

$S_{1,1}$, $S_{2,1}$,……$S_{n,1}$

$S_{1,2}$, $S_{2,2}$,……$S_{n,1}$

$S_{1,m}$, $S_{2,m}$,……..……$S_{n,m}$

Where, S is the storage in cubic meters.

The last comma delimited text file created by the program contains the values for flow in cubic meters per second for all cells at a user defined time interval. It is again in the format of a two dimensional matrix of size n by m where n are the total cells in the watershed and m are the total time steps.

$BoxID_1$, $BoxID_2$, …….. $BoxID_n$

$F_{1,1}$, $F_{2,1}$,……$F_{n,1}$

$F_{1,2}$, $F_{2,2}$,……$F_{n,1}$

$F_{1,m}$, $F_{2,m}$,……...……$F_{n,m}$

Where, F is the flow in cubic meters per second.

3.5.2 The location query

The location query has been created to given the user an option of querying the output files from the routing algorithm and displaying the results of only the desired BoxIDs. The input file required for this query is the flow result file or the

storage result file. The user can then specify the desired BoxIDs either as an input text file (Figure 3.11) or through the interface (Figure 3.12). Only five BoxIDs can be entered through the interface at a time.

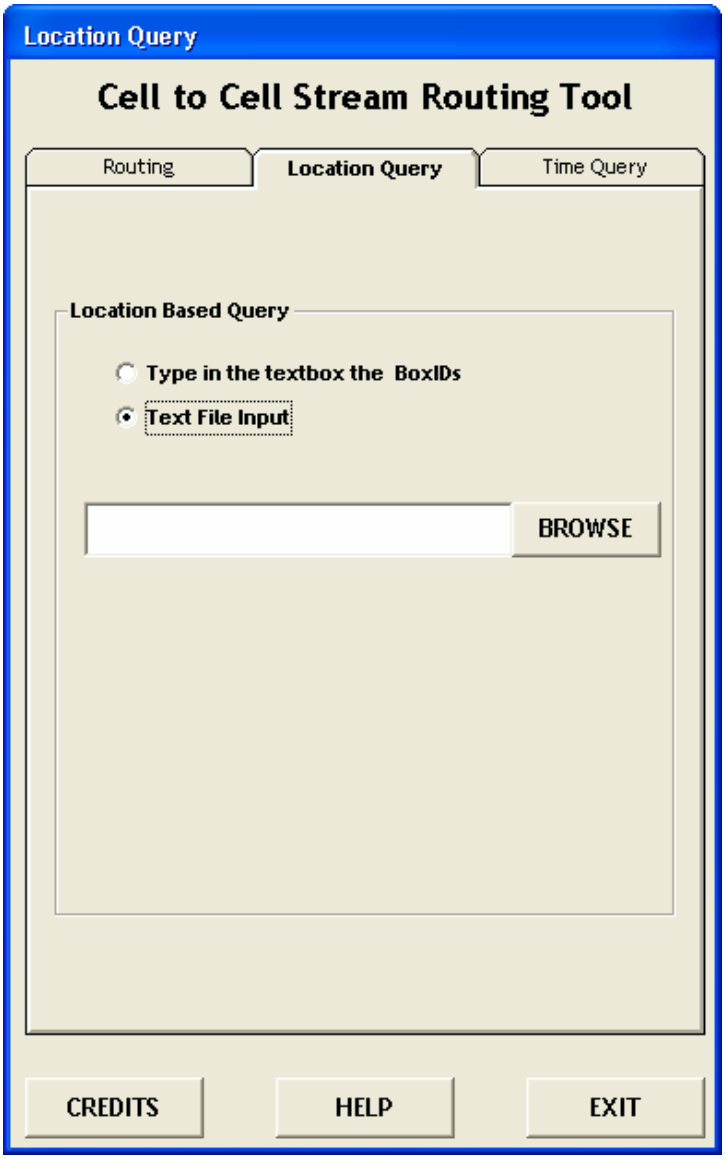

Figure 3.11. Location query screen (file input) of the cell-to-cell stream flow routing tool.

The format of the input text file specifying the BoxIDs is as follows:

$BoxID_1$

$BoxID_2$

$BoxID_3$

$BoxID_4$

$BoxID_5$

$BoxID_n$

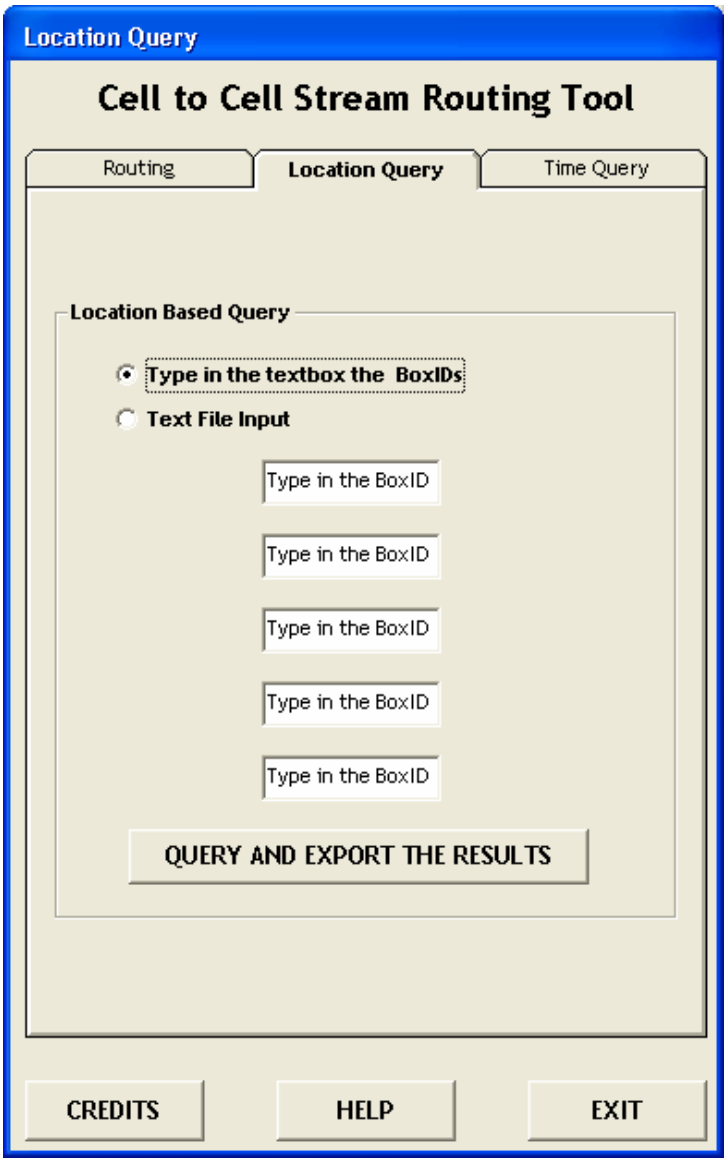

Figure 3.12. Location query screen (GUI input) of the cell-to-cell stream flow routing tool.

3.5.3 The time query

The time query has been created to given the user an option of querying the output files from the routing algorithm and displaying the results of only at the desired time steps. The input file required for this query is the flow result file or the storage result file. The user can then specify the desired time steps either as an input text file

(Figure 3.13) or through the interface (Figure 3.14). Only 5 time steps can be entered through the interface at a time.

The format of the input text file specifying the BoxIDs is as follows:

$TimeStep_1$

$TimeStep_2$

$TimeStep_3$

$TimeStep_4$

$TimeStep_5$

$TimeStep_n$

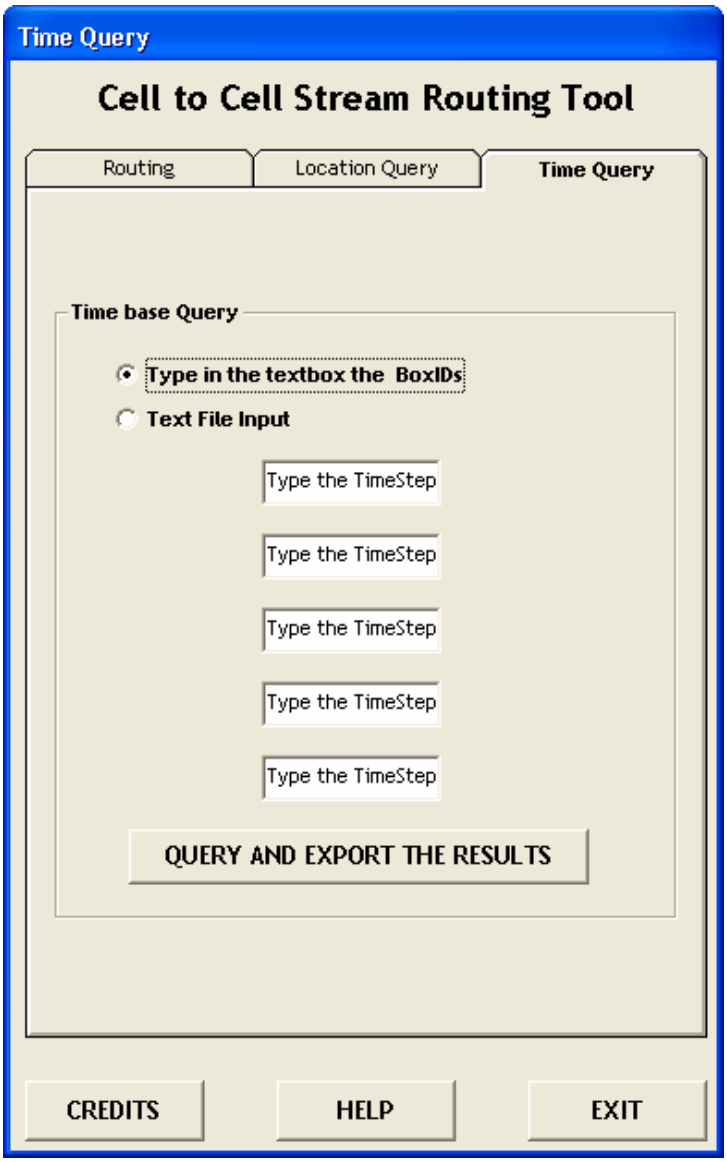

Figure 3.13. Time query screen (GUI input) of the cell-to-cell stream flow routing tool.

Figure 3.14. Time query screen (file input) of the cell-to-cell stream flow routing tool.

4. APPLICATION, DISCUSSION AND RESULTS

In this section, the procedure of application of the methodology is presented. Results and figures are presented as needed with a critical discussion, in order to help the reader follow the procedure of application.

Although, the procedure of application is explained with the help of an example data, it can be applied to any watershed. Data of the Brazos River basin (Figure 4.1) is used for the implementation of the cell-to-cell stream flow routing model. Following the application of the cell-to-cell stream flow routing algorithm to the Brazos River, a case study on Waller Creek, Austin was undertaken. Runoff and stream flow data is available and documented by Olivera et al. (1996) for Waller Creek from October 14th, 1994 at 7:45 p.m. to October 17th, 1994, at 6:45 p.m. The model parameters are calibrated with this data for Waller Creek.

4.1 Application to the Brazos River Basin

This section describes the application of the cell-to-cell stream flow routing model to the Brazos River basin in Texas and part of New Mexico (see Figure 4.1). The cell-to-cell stream flow routing model is used to determine the flow at any point in the watershed. This two-parameter routing model, routes the available excess precipitation depth (runoff) to the watershed outlet using a coarse resolution river network. The cells in the river network are approximated as a cascade of linear reservoirs with an equal retention coefficient.

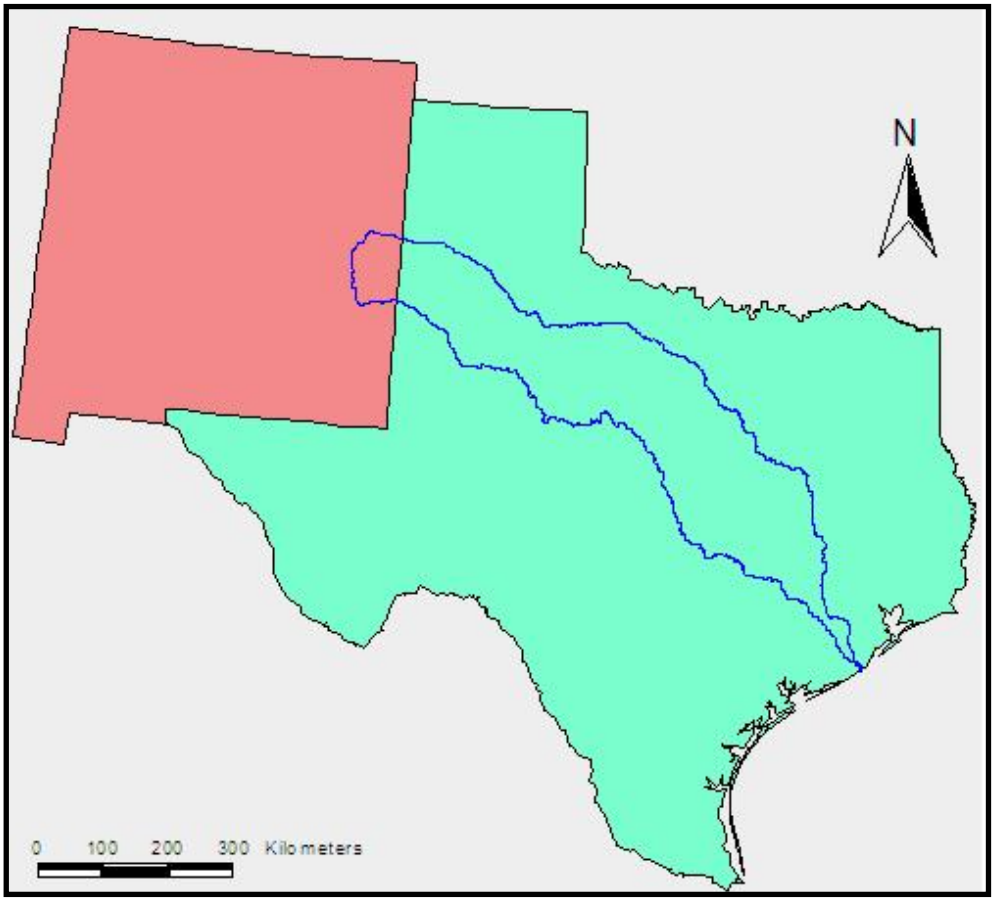

Figure 4.1. Brazos River Basin in Texas and New Mexico.

4.1.1 Data requirements

a) A coarse resolution river network (see Figure 4.2)

The coarse resolution mesh should have the following attributes:

i. Box ID – this is the identification number of each cell in the watershed

ii. DSBoxID – this is the identification number of the downstream cell for each cell. The DSBoxID is zero for the outlet.

iii. FDBoxID – This is the direction of flow for each cell. Values in this field are 1, 2, 4, 8, 16, 32, 64, 128

iv. Area – This is the area for each cell. Since all cells are squares all cell areas are equal unless cells are initially defined with latitude and a longitude and then projected. In this case, cells are no longer squares and cell areas vary. All cell areas are in sq. meters.

v. Reach – this is the reach length of each cell. It is defined in meters.

vi. Velocity – this is the stream flow velocity in the cell. This velocity is used to route the water from the outlet of the cell to the outlet of the watershed over the network of cells.

vii. Dispersion – This is the coefficient of dispersion in each cell, which is used for stream flow routing.

viii. Velocity_overland – This is the overland flow velocity in the cell. This velocity is used to route the runoff from the center of the cell to the outlet of the cell.

ix. Dispersion_overland – this is the coefficient of dispersion used in overland flow.

b) Excess precipitation depth (runoff) time series for each cell. Runoff depth is taken in meters for each cell.

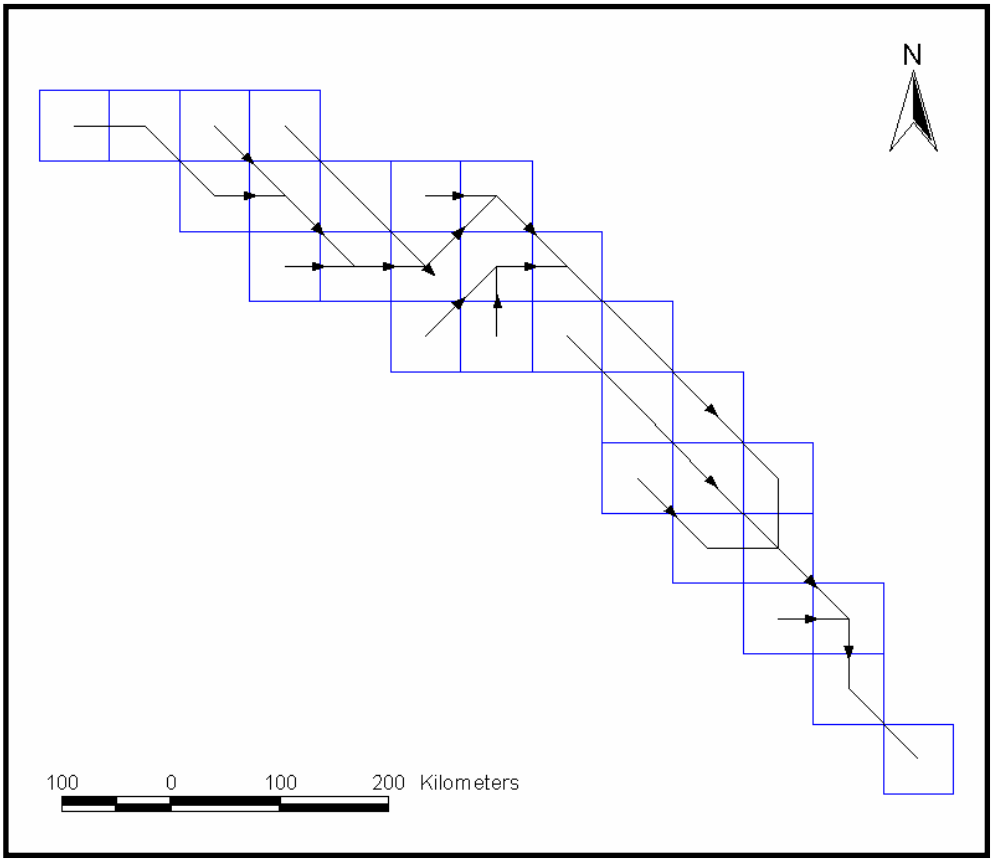

Figure 4.2. An example coarse resolution river network of the Brazos River.

4.1.2 Data available

a) DEM (90 m DEM for Texas and New Mexico, Source: USGS, 2004a)

b) Hydrologic Unit Code (HUC) for Brazos river basin (Source: USGS, 2004b)

A digital elevation model (DEM) is a digital file consisting of terrain elevations for ground positions at regularly spaced horizontal intervals. The 90 DEM of the Brazos River was downloaded from the USGS website http://edcsgs9.cr.usgs.gov/glis/hyper/guide/1_dgr_demfig/index1m.html. This DEM is available in tile format for the whole of the United States in Geographic Projection with datum WGS72 and spheroid WGS1972.

The following DEM tiles were downloaded from the USGS website: San Angelo, Brownwood, Waco, Sonora, Llano, Austin, Del Rio, San Antonio, Sequin, Eagle pass, Crystal city, Beeville, Pecos, Hobbs, Houston, Bay City, Carlsbad, Roswell, Brownfield, and Van horn. Each of these tiles contains two parts (east tile and west tile). All these DEM tiles were merged into single file using the "merge" command in the arcview 3.x extention "CRWR Raster". Since the DEM is in geographical projection, it was projected to "Albers Equal Area-Conic". The output projection file specified for projecting the grid was:

Output
Projection albers equal area-conic
Datum NAD 83
Spheroid GRS 80
Units meters
Parameters
-96 00 00
23 00 00
29 30 00
45 30 00
0
0
end

This projection was used for all the data in this study.

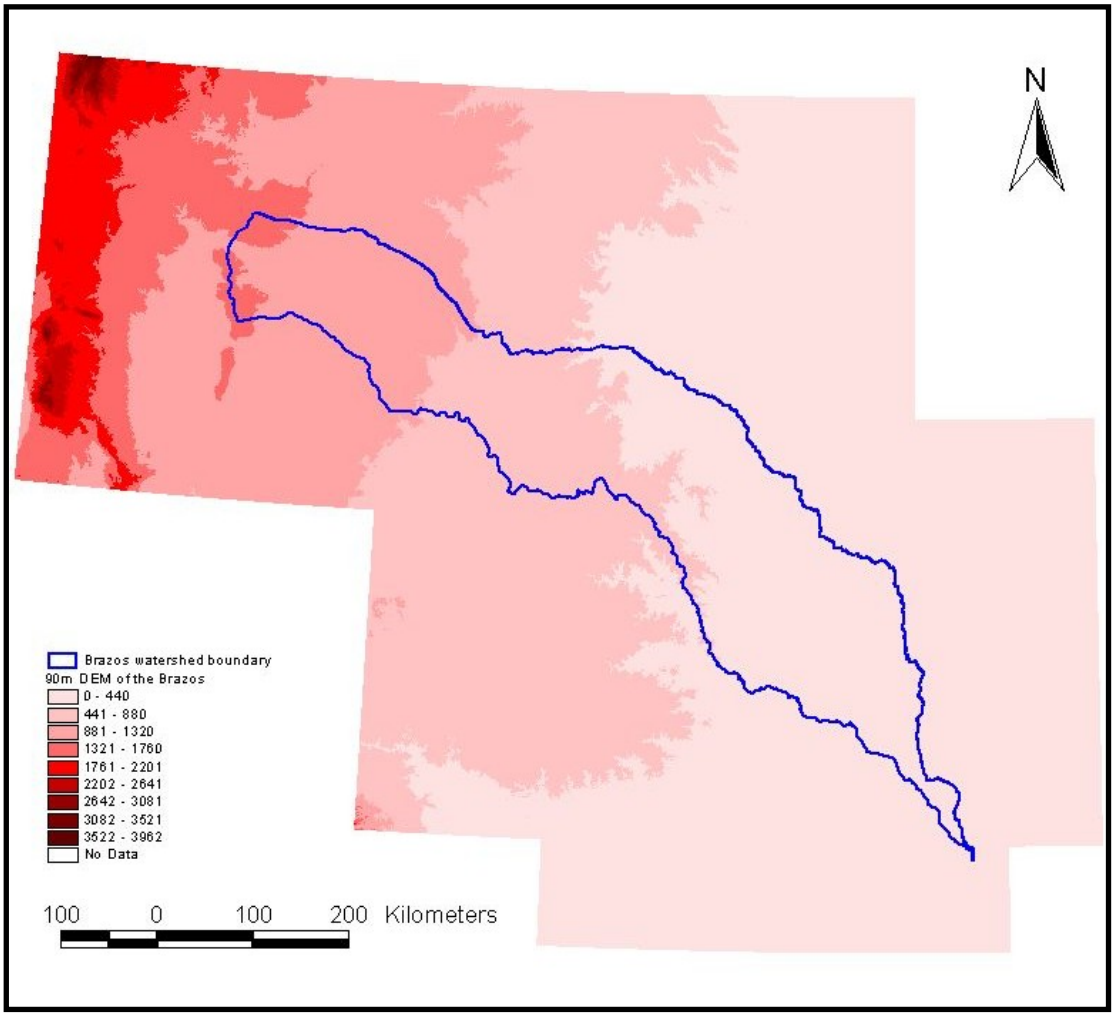

Figure 4.3. Merged tiles of the 3" DEM with the Brazos River Basin.

The DEM (Figure 4.3) was used as a foundation for building the stream network for the Brazos River. The following section enlists in detail the steps used to delineate a coarse resolution stream network from the available 90m DEM.

4.1.3 Spatial analysis of the data

4.1.3.1 Filling the DEM

Digital Elevation Models (DEMs) (Figure 4.3) contain errors called sinks, and they need to be filled before any other operation. Sinks are cells in the DEM with

a lower value than all other neighboring areas. This creates errors in the stream delineation as sinks appear like local minima and all streams drain into them, which is not the case in reality. Filling the sinks is done by first identifying such cells in the DEM that have a lower value than the surrounding cells and then assigning an average value of the neighboring cells. Most GIS softwares like ArcInfo and ArcGIS have inbuilt functions to fill DEMs. The DEM was filled using the ArcINFO command

FILDEM = fill (DEM)

Where, DEM is the merged DEM of the Brazos River basin, and FILDEM is the filled DEM.

4.1.3.2 Flow direction grid generation

The flow direction command calculates the direction in which the cell will flow. The direction of flow is determined by finding the direction of the steepest descent from each cell. This request uses an eight direction-point pour algorithm (ESRI, 1992) (Figure 4.4) to compute the downstream cell. This algorithm assigns a code to each cell depending on the direction of the steepest slope. The ArcINFO command used to compute flow direction of a DEM is

FDR = flowdirection (FILDEM)

Where, FDR is the flow direction grid of the filled DEM

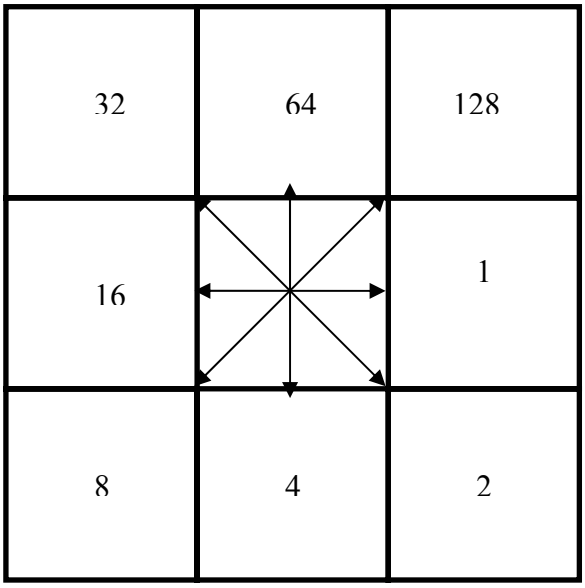

Figure 4.4. The eight direction-point pour algorithm (Source: ESRI, 1992).

4.1.3.3 Flow accumulation grid generation

The flow accumulation is an integer number representing the number of upstream DEM cells whose flow paths "pass through" the given cell. Figure 4.5 displays the flow accumulation grid for the Brazos.

This ArcINFO command used to compute the flow accumulation is

FAC = flowaccumulation (FDR)

Where, FAC is the flow accumulation grid of the filled DEM

Figure 4.5. Flow accumulation grid. Darker the color, higher is the flow accumulation of the cell.

4.1.3.4 Fine resolution stream network delineation

This function creates arcs from the cells in the DEM, whose flow accumulation values are above a user-defined threshold. An arc vertex is created for each DEM point that has a flow accumulation value greater than the user-defined threshold. For delineating the streams for the Brazos River, a threshold value of 1000 was chosen for the resolutions of cell sizes 64,360 m, 32,180 m and 16,090 m. However, for the cell size 8,045 m, a threshold of 500 was chosen, thus leading to

greater number of arcs. If the number of arcs is less, it can often lead to a situation in which after the intersection of the stream network with a coarse resolution mesh that there will be some cells in the resulting mesh with no arcs. This creates problems while delineating the coarse resolution stream network as some cells with no arcs in the middle of the watershed will have no flow direction and reach lengths.

This ArcINFO command used was

STR = con (FAC >1000, 1).

Where, STR is the fine resolution stream network. The value 1000 signifies the threshold value.

4.1.3.5 Streamlinks generation

Streamlinks are segments of a stream, which connect two consecutive junctions, one upstream of the stream and one downstream. This ArcINFO command used for obtaining stream links was

LNK = streamlink (STR, FDR).

Where, LNK is the stream link grid

Stream network in a coverage format is required for the intersection with a mesh. Thus, the streamlinks grid was converted from a grid format into a coverage format (Figure 4.6). The ArcINFO command used was

LNKCOV = streamline (LNK, FDR)

Where LNKCOV is the coverage of the stream link grid

Figure 4.6. Stream network of the Brazos River Basin.

4.1.4 Generation of the coarse resolution polygon mesh

For delineating, the coarse resolution stream network four cell sizes were chosen: 5 miles, 10 miles, 20 miles, and 40 miles. Accordingly, four polygon coarse resolution meshes with cell sizes 8,045 m (5 miles) 16,090 m (10 miles), 32,180 m (20 miles), and 64,360 m (40 miles) were generated in ArcINFO using the FISHNET function. All the coarse resolution meshes were then projected to the "Albers Equal Area-Conic" projection.

The following AML was used to generate the 16,090 m (10 mile) mesh. Coarse resolution meshes of 8,045 m, 32,180 m and 64,360 m were also generated using the same procedure. A avenue code file with the following information was created and run in Arc command mode.

```
' On-screen input
&sv mesh      = MESH16KM
&sv xmin      = -800,000
&sv ymin      = 500,000
&sv cellsize  = 16090
&sv nrows     = 56
&sv ncols     = 60
&sv prjfile   = meshprj
'Generating and projecting the grid
'Box numbering: left to right and bottom to top
generate %mesh%
fishnet
%xmin%, %ymin%
%xmin%, 90
%cellsize%, %cellsize%
%nrows%, %ncolumns%
quit
build %mesh%
project cover %mesh% %mesh%prj %prjfile%
build %mesh%prj
quit
&return
```

The projection file specified is as below:

Output
projection albers equal area-conic
datum NAD 83
Spheroid GRS 80
Units meters
Parameters
-96 00 00
23 00 00
29 30 00
45 30 00
0
0
end

4.1.5 Intersection of the coarse resolution mesh with the fine resolution stream network

Intersection is an inbuilt command in ArcINFO. It divides the existing streams in such a way that each stream is contained in only one cell (refer Figure 3.5 for explanation). Intersection of the 16,090 m coarse resolution mesh and the fine resolution Brazos River stream network was done in ArcINFO. Table 4.1 is the attribute table of the fine resolution stream network before the intersection with the 16,090 m resolution mesh and Table 4.2 is the table generated after the intersection. The number of arcs increased from 42,080 to 48, 241. Other meshes were also intersected in the similar fashion.

Table 4.1. Attribute table of the fine resolution stream network before intersection.

Shape	Fnode#	Tnode#	Lpoly#	Rpoly#	Length	Lnk1000cov#	Lnk1000cov-id
PolyLine	4	2	0	0	790.68980	1	39
PolyLine	1	7	0	0	4015.72128	2	37
PolyLine	3	7	0	0	3974.20641	3	42
PolyLine	7	13	0	0	1902.81432	4	61
PolyLine	6	13	0	0	9237.71313	5	56
PolyLine	13	14	0	0	1153.63939	6	69
PolyLine	5	14	0	0	3676.04742	7	50
PolyLine	15	18	0	0	120.98320	8	74
PolyLine	17	18	0	0	2124.02328	9	73
PolyLine	12	20	0	0	2200.97331	10	66
PolyLine	8	21	0	0	5242.74929	11	58
PolyLine	19	22	0	0	498.61052	12	76
PolyLine	16	22	0	0	2507.73031	13	75
PolyLine	20	21	0	0	4623.15557	14	78
PolyLine	14	26	0	0	1475.07412	15	71
PolyLine	10	26	0	0	6494.09614	16	82
PolyLine	27	25	0	0	85.54804	17	86
PolyLine	9	28	0	0	5140.00523	18	62
PolyLine	28	20	0	0	2593.27835	19	77
PolyLine	30	31	0	0	769.93236	20	92
PolyLine	21	32	0	0	1339.41319	21	79
PolyLine	23	34	0	0	1330.81518	22	81
PolyLine	35	28	0	0	1103.52651	23	91
PolyLine	31	35	0	0	3847.14350	24	87
PolyLine	36	35	0	0	292.07928	25	103
PolyLine	18	31	0	0	8119.50890	26	94
PolyLine	29	39	0	0	1303.97804	27	90
PolyLine	33	39	0	0	896.99527	28	97
PolyLine	11	43	0	0	7092.93242	29	70
PolyLine	40	43	0	0	1354.09092	30	112
PolyLine	22	44	0	0	2755.77642	31	80
PolyLine	39	46	0	0	740.57691	32	110
PolyLine	38	47	0	0	1310.05775	33	108
PolyLine	41	44	0	0	1274.62259	34	117
PolyLine	49	47	0	0	120.98320	35	123
PolyLine	50	32	0	0	3097.96858	36	93
PolyLine	53	50	0	0	1189.07455	37	120
PolyLine	24	54	0	0	3089.37056	38	85
PolyLine	34	54	0	0	6688.46796	39	98
PolyLine	52	55	0	0	890.91556	40	127
PolyLine	37	59	0	0	2398.90653	41	72
PolyLine	47	60	0	0	5307.53989	42	113
PolyLine	61	62	0	0	206.53124	43	139
PolyLine	59	62	0	0	755.25464	44	136
PolyLine	32	46	0	0	5903.85787	45	121
PolyLine	51	49	0	0	5564.18401	46	122
PolyLine	63	67	0	0	448.49764	47	144

An AML with the following commands was created and run in Arc command mode. The actual code is preceded by comments (lines starting with “ ' ”) to help the reader understand the code.

```
' Intersecting streams with boxes
' Topology is built as part of the interesection
' On-screen input
&sv mesh        = MESH16KMPRJ     'Projected Mesh
&sv streams     = LNKCOV          'Fine resolution stream network
intersect %streams% %mesh%prj %streams%%mesh% line 0.01    'Threshold value
' Creating output file and writing column headers
&setvar file_unit = [open %streams%%mesh%.txt openstatus -write]
&setvar record = "RecordNumber, Length, FromNode, ToNode, MeshboxId"
&if [write %file_unit% %record%] = 0 &then
   &type %streams%%mesh%.txt written successfully
&if [close %file_unit%] = 0 &then
   &type %streams%%mesh%.txt closed successfully
'Writing (exporting) table values
tables
sel %streams%%mesh%.aat
unload %streams%%mesh%.txt $recno length fnode# tnode# %mesh%prj-id
quit
&return
```

Table 4.2. Table generated after the intersection of the streams and the mesh.

Recno	Fnode#	Tnode#	Length	Mesh1-id
1	6	84	27.87315	3302
2	84	7	370.06531	3302
3	20	86	27.87315	3307
4	19	86	19.70929	3307
5	57	87	148.85634	3316
6	88	66	576.59654	3319
7	89	75	148.85634	3321
8	90	11	269.83954	3304
9	61	92	319.95242	3316
10	60	92	234.40438	3316
11	93	44	281.97510	3312
12	94	10	276.35341	3303
13	95	12	390.82274	3304
14	2	96	2898.98720	3302
15	97	73	2356.34352	3321
16	3	98	803.88522	3302
17	32	99	518.31981	3309
18	31	99	1246.30314	3309
19	59	100	482.88465	3316
20	101	77	482.88465	3322
21	58	102	568.43269	3316
22	103	98	241.96640	3302
23	96	103	413.06248	3302
24	26	104	768.45006	3308
25	102	100	3469.51618	3316
26	98	4	2612.55348	3302
27	87	102	2970.90567	3316
28	106	15	910.23009	3305
29	107	103	413.06248	3302
30	24	108	1317.17346	3307
31	23	108	1010.41646	3307
32	109	93	613.97202	3311
33	105	109	1581.37959	3311
34	110	5	1780.34882	3302
35	22	111	1016.93032	3307
36	21	111	1715.55821	3307
37	43	112	1052.36548	3311
38	42	112	1488.26954	3311
39	113	50	1173.34868	3313
40	114	51	1287.81801	3313
41	80	116	1379.87992	3325
42	117	107	362.94960	3302
43	16	106	2016.19610	3306

4.1.6 Application of the Network Tracing Method (NTM)

The NTM was applied to the intersected stream network of the Brazos River basin (LNKCOVMESH). The NTM computes for each cell the flow direction, the reach length, and the meandering factor. The NTM was applied with different thresholds till the corner to side ratio reached a value of 59/41. The NTM computes the stream rank and upstream flow length as intermediate steps before it calculates the flow direction for each cell.

4.1.6.1 Computing "stream rank"

This function calculates the "stream rank" for the lines of a dendritic network. The "stream rank" of a line is 1 for the headwater lines, and the "stream rank" of the upstream line plus 1 for all other lines. If a line has more than one line upstream, the greatest "stream rank" is considered.

4.1.6.2 Computing the upstream flow length

This function computes the upstream length of each line.

4.1.6.3 Flow direction for each of the cell

This is the final step in the application of the NTM. It calculates the flow direction and the reach length of each cell. Table 4.3 lists the threshold values used in achieving the ideal side to corner ratio of 59/41. The threshold values were changed until this ratio is achieved.

Table 4.3. Threshold values for the meshes to achieve the value of 59/41.

Cell size (km)	No. of columns	Threshold (Km)	Side/Corner ratio
8.045	120	8.95	$58.99/41.01$
16.090	60	18.33	$59.06/40.94$
32.180	30	42.70	$59/41$
64.360	15	86.40	$59.38/40.63$

4.1.7 Delineation of the Brazos watershed

The table (Table 4.4) obtained after the application of NTM to the Brazos River basin contains fields with the information about the identification of the cells (BoxID), flow direction of each cell (FDBoxID) and its reach length (Reach). This table was joined to the attribute table of the 16,090 m mesh using the MeshID attribute. The coarse resolution 16,090 m mesh was converted in into a grid format using the FDBox attribute (see FDBox attribute in Table 4.4). The grid cells have BoxID in the ID field and flow direction of the cell in the value field. In physical meaning, this is a flow direction grid (see Figure 4.7). Flow accumulation was obtained from this grid using the ArcInfo command "flowaccumulation", followed by the stream delineation and stream links generation. The stream links grid was converted to a coverage format (Figure 4.9) and it visually depicts a coarse resolution network of the Brazos.

Table 4.4. Table after application of NTM.

Bou	Dsbou	Fdbo	Reach	Meandering	Exitlineinde	Bou/slength	Exitbou	Exitbouinde	Shortreach	Nextexitbou
3302	0	0	0.000	0.000	36191	21448.410	0	0	0.000	0
3307	3308	1	21904.685	1.361	43817	104634.857	3308	10	21904.685	3309
3316	3317	1	22609.459	1.405	40614	46713.744	3317	17	22609.459	3318
3319	0	0	0.000	0.000	26068	20066.874	0	0	0.000	0
3321	0	0	0.000	0.000	36192	30943.634	0	0	0.000	0
3303	3304	1	21540.427	1.339	39647	38781.365	3304	7	21540.427	0
3304	0	0	0.000	0.000	41131	60321.792	0	0	0.000	0
3309	3310	1	23397.629	1.454	44801	148237.255	3310	16	23397.629	3311
3322	0	0	0.000	0.000	37035	22454.664	0	0	0.000	0
3308	3309	1	21697.713	1.349	44320	126539.542	3309	8	21697.713	3310
3311	3312	1	281.975	0.018	45442	200842.359	3312	22	281.975	0
3313	0	0	0.000	0.000	37729	38808.584	0	0	0.000	0
3325	3266	2	27754.868	1.220	269	19221.261	3265	47	9918.563	3266
3306	3307	1	23534.038	1.463	40886	68933.712	3307	2	23534.038	3308
3305	3306	1	26318.422	1.636	37037	42615.290	3306	14	26318.422	3307
3310	3311	1	29207.475	1.815	45237	171634.884	3311	11	29207.475	3312
3317	3318	1	14725.798	0.915	42458	69323.203	3318	19	14725.798	0
3301	3302	1	9425.948	0.586	29681	12022.462	3302	1	9425.948	0
3318	0	0	0.000	0.000	43313	84049.001	0	0	0.000	0
3327	3268	2	30096.085	1.323	42136	56480.368	3328	27	1632.513	3268
3314	0	0	0.000	0.000	38315	43749.616	0	0	0.000	0
3312	0	0	0.000	0.000	45468	201124.334	0	0	0.000	0
3324	3265	2	34069.516	1.497	41370	39743.760	3264	55	14815.346	3265
3315	0	0	0.000	0.000	32098	26821.175	0	0	0.000	0
3326	3327	1	19920.756	1.238	39998	36559.612	3327	20	19920.756	3328
3323	3264	2	21418.266	0.941	40321	33140.840	3263	36	2665.887	3264
3328	3268	4	28463.572	1.769	42302	58112.881	3268	57	28463.572	3208
3320	0	0	0.000	0.000	37038	35795.122	0	0	0.000	0
3257	3318	128	29492.299	1.296	37737	24456.815	3317	17	14766.501	3318
3266	3207	2	28779.188	1.265	45172	163482.408	3206	67	9421.598	3207
3251	3311	64	11364.934	0.706	42303	67115.309	3311	11	11364.934	3312
3252	3251	16	3217.338	0.200	29708	15556.828	3251	31	3217.338	3311
3243	3304	128	24803.917	1.090	37738	35517.875	3303	6	3263.490	3304
3245	3246	1	19922.414	1.238	41962	53153.421	3246	56	19922.414	3247
3253	3254	1	582.811	0.036	32124	19084.788	3254	48	582.811	3314
3263	3264	1	18752.379	1.165	40888	35806.727	3264	55	18752.379	3265
3248	3309	128	36566.993	1.607	42879	78097.296	3249	38	13196.846	3309
3249	3309	64	23370.147	1.452	43500	91294.142	3309	8	23370.147	3310
3255	3316	128	26339.180	1.158	32120	20374.564	3256	52	2421.403	3316
3260	3261	1	21774.378	1.353	39648	37908.799	3261	49	21774.378	3262
3241	3181	4	21332.190	1.326	40892	33325.352	3181	77	21332.190	3121
3250	3251	1	23914.170	1.486	40621	43201.139	3251	31	23914.170	3311
3262	3202	4	20729.793	1.288	42141	62844.944	3202	76	20729.793	3203
3259	3260	1	19175.376	1.192	35195	18733.423	3260	40	19175.376	3261
3247	3308	128	36711.875	1.613	43501	89827.667	3307	2	14807.190	3308
3267	3208	2	22335.183	0.982	45519	189156.030	3207	69	3105.566	3208
3265	3206	2	27257.903	1.198	44844	145646.103	3266	30	17836.305	3206

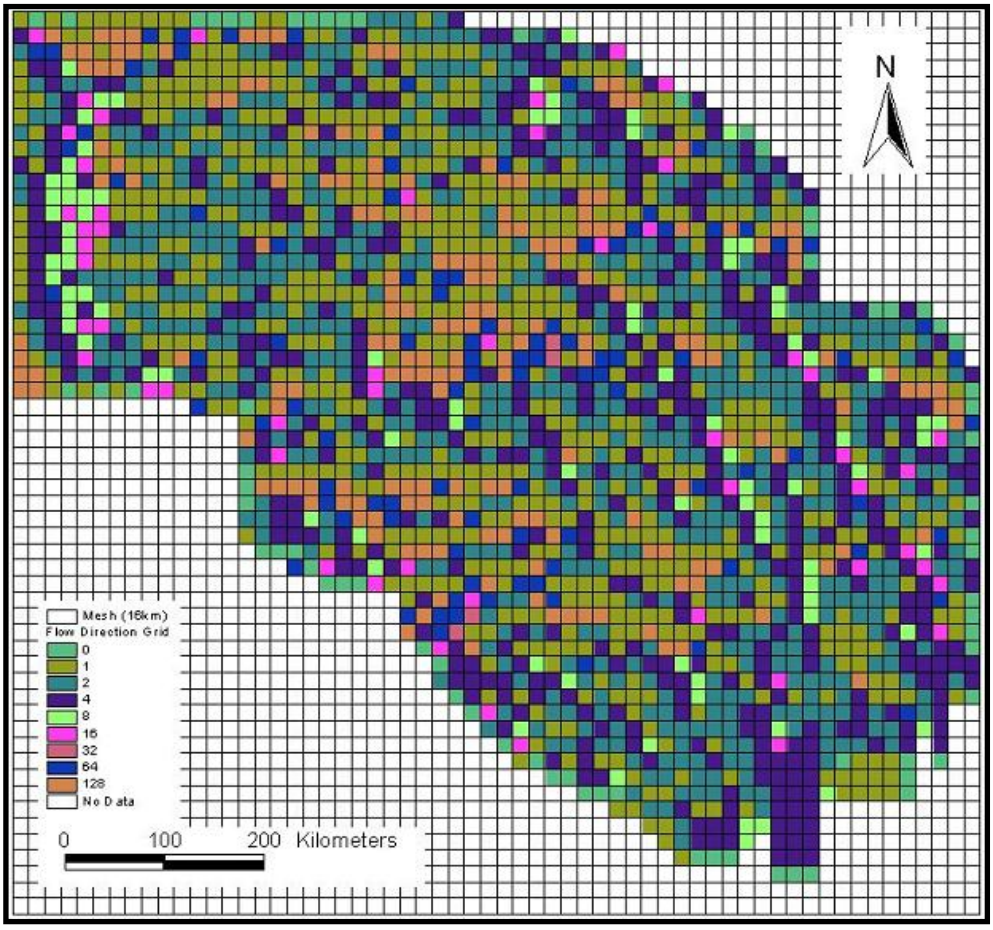

Figure 4.7. Coarse resolution flow direction grid at a cell resolution of 16km.

The coverage of the streamlinks is an important data set as it visually depicts the coarse resolution stream network and helps in the identification of errors in the computation of flow direction. The cell with the maximum flow accumulation was identified as the outlet. The watershed for the 16km mesh was delineated with the chosen outlet and the flow direction grid generated earlier. The command used for watershed delineation was

WSH = watershed (FDR, Outlet)

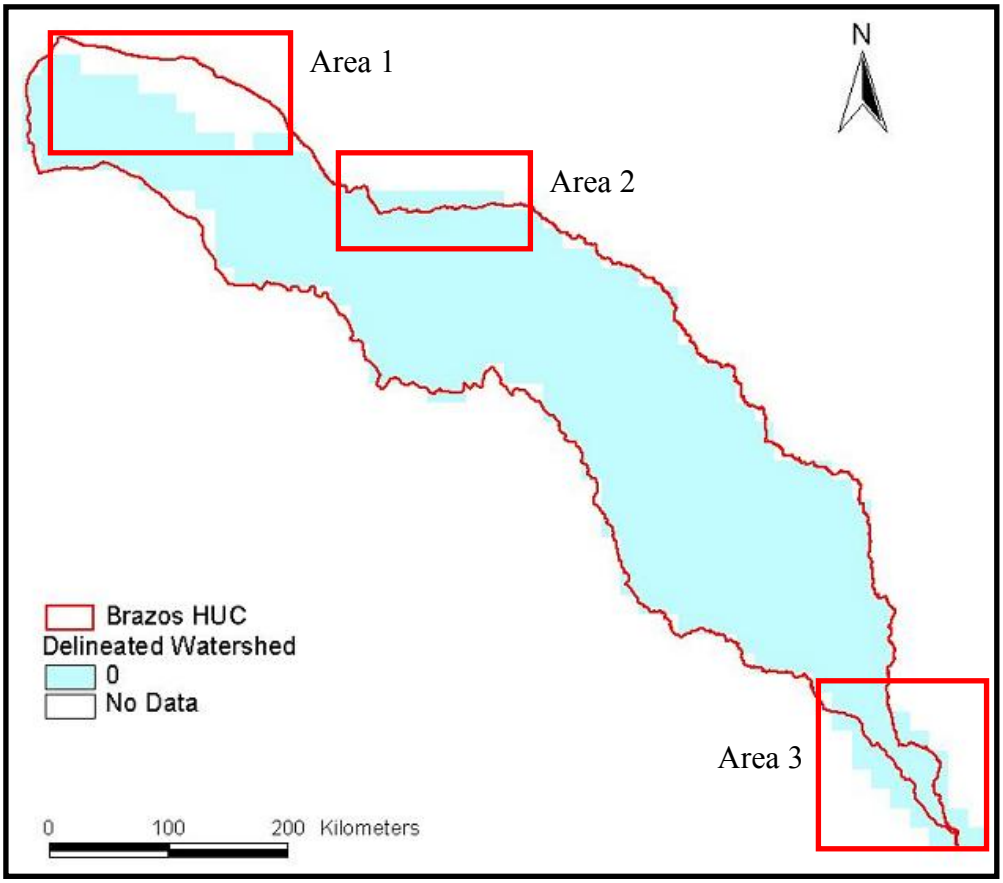

Figure 4.8. Delineated watershed of the Brazos River at a cell resolution of 16km with errors in red boxes.

The delineated watershed of the Brazos is compared to the observed watershed hydrologic unit code (HUC) boundary (see Figure 4.8 and Table 4.5). The delineated area does not match with the observed area at three places, shown as area 1, area 2 and area 3 in Figure 4.9. The error in area 1 is due to the incorrect stream delineation, the errors at areas 2 and 3 are due to wrong determination of flow direction in the coarse resolution stream network. These errors, along with solutions to improve the watershed delineation are explained in detail in section 4.1.8

Table 4.5. Attributes of the coarse resolution watershed delineated at a resolution of 16km.

Shape	Perimeter	Mesh1_id	Area2	Dsbowid	Fdbow	Reach	Meandering
Polygon	64360.000	2947	258888096	2887	4	24919.374	1.549
Polygon	64360.000	2948	258888096	2888	4	19793.691	1.230
Polygon	64360.000	2949	258888096	2950	1	18469.794	1.148
Polygon	64360.000	2950	258888096	2951	1	20485.568	1.273
Polygon	64360.000	2951	258888096	2892	2	18836.071	0.828
Polygon	64360.000	2952	258888096	2893	2	24711.821	1.086
Polygon	64360.000	2953	258888096	2893	4	21740.915	1.351
Polygon	64360.000	2954	258888096	2895	2	26156.799	1.150
Polygon	64360.000	2886	258888096	2887	1	20631.011	1.282
Polygon	64360.000	2887	258888096	2828	2	27203.417	1.196
Polygon	64360.000	2888	258888096	2829	2	21886.432	0.962
Polygon	64360.000	2889	258888096	2829	4	18018.176	1.120
Polygon	64360.000	2890	258888096	2831	2	24317.525	1.069
Polygon	64360.000	2891	258888096	2832	2	27907.725	1.226
Polygon	64360.000	2892	258888096	2893	1	23010.901	1.430
Polygon	64360.000	2893	258888096	2894	1	19855.106	1.234
Polygon	64360.000	2894	258888096	2835	2	25603.822	1.125
Polygon	64360.000	2895	258888096	2836	2	24287.390	1.067
Polygon	64360.000	2896	258888096	2837	2	25533.813	1.122
Polygon	64360.000	2897	258888096	2837	4	19853.603	1.234
Polygon	64360.000	2826	258888096	2887	128	29767.750	1.308
Polygon	64360.000	2827	258888096	2828	1	19248.017	1.196
Polygon	64360.000	2828	258888096	2769	2	23757.017	1.044
Polygon	64360.000	2829	258888096	2770	2	31776.304	1.396
Polygon	64360.000	2830	258888096	2771	2	22303.587	0.980
Polygon	64360.000	2831	258888096	2832	1	18501.568	1.150
Polygon	64360.000	2832	258888096	2773	2	19065.877	0.838
Polygon	64360.000	2833	258888096	2774	2	33221.402	1.460
Polygon	64360.000	2834	258888096	2835	1	24116.970	1.499
Polygon	64360.000	2835	258888096	2836	1	19230.895	1.195
Polygon	64360.000	2836	258888096	2777	2	23466.093	1.031
Polygon	64360.000	2837	258888096	2778	2	31076.367	1.366
Polygon	64360.000	2838	258888096	2780	2	19889.534	1.159
Polygon	64360.000	2766	258888096	2767	1	19731.301	1.226
Polygon	64360.000	2767	258888096	2828	128	18745.473	0.824
Polygon	64360.000	2768	258888096	2769	1	19936.710	1.239
Polygon	64360.000	2769	258888096	2770	1	16090.000	1.000
Polygon	64360.000	2770	258888096	2771	1	18301.658	1.137
Polygon	64360.000	2771	258888096	2712	2	33263.074	1.462
Polygon	64360.000	2772	258888096	2712	4	21884.603	1.360
Polygon	64360.000	2773	258888096	2774	1	30347.343	1.886
Polygon	64360.000	2774	258888096	2715	2	29921.210	1.315
Polygon	64360.000	2775	258888096	2776	1	18808.755	1.169
Polygon	64360.000	2776	258888096	2777	1	21925.440	1.363
Polygon	64360.000	2777	258888096	2778	1	19146.022	1.190
Polygon	64360.000	2778	258888096	2779	1	19537.284	1.214
Polygon	64360.000	2779	258888096	2721	2	29422.479	1.151

4.1.8 Errors in watershed delineation

Incorrect delineation of the fine resolution stream network in the upper Brazos River basin and errors due to the NTM result in the incorrect delineation of the coarse resolution Brazos River basin watershed. These errors are discussed in detail in this section, along with the corrections that were done manually to rectify the errors.

4.1.8.1 Error in the fine resolution stream network

Comparison of the stream network delineated from the DEM and the National Hydrologic Data (NHD) network shows that DEM delineation was wrong (Figure 4.9). This wrong delineation of the Brazos watershed might be due to errors in the DEM or due to a coarser resolution of the DEM. As Figure 4.9 illustrates one of the tributaries of the Brazos is incorrectly delineated and this error is carried over to the coarse resolution stream network. Delineated direction of flow is shown with a red arrow in Figure 4.9 and correct flow direction is shown as a green arrow. Since the error in the DEM cannot be rectified, the correction is made manually in the coarse resolution stream network. The grid cell with the erroneous flow direction in the 16,090 m mesh is identified (BoxID = 2779) and flow direction and reach lengths are changed to correct values (see Table 4.5). The reach length was manually measured from exit point of the box until the user-defined threshold was reached and the next exit box (BoxID = 2720) was located. The flow direction was changed from 1 to 4. Reach and flow direction of BoxID = 2780 was also changed similarly.

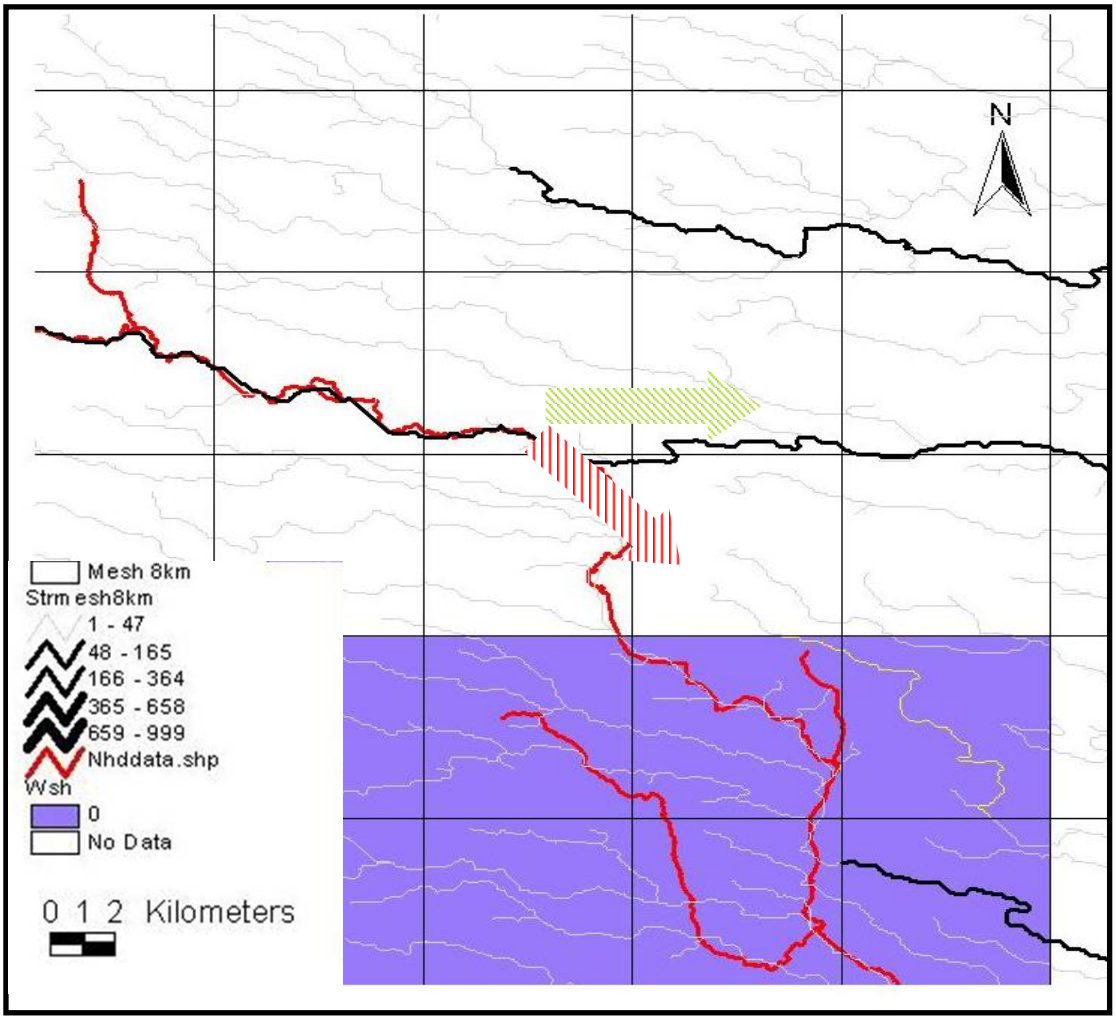

Figure 4.9. Error due to the incorrect delineation of the fine resolution stream network.

4.1.8.2 Errors due to NTM

NTM is a very accurate method of deriving coarse resolutions river network from fine resolution streams. However, there are some errors that are induced into the resulting network due to the complexity of the fine resolution stream network data. The following sections discuss these errors and the corrections done to improve the prediction of the watershed.

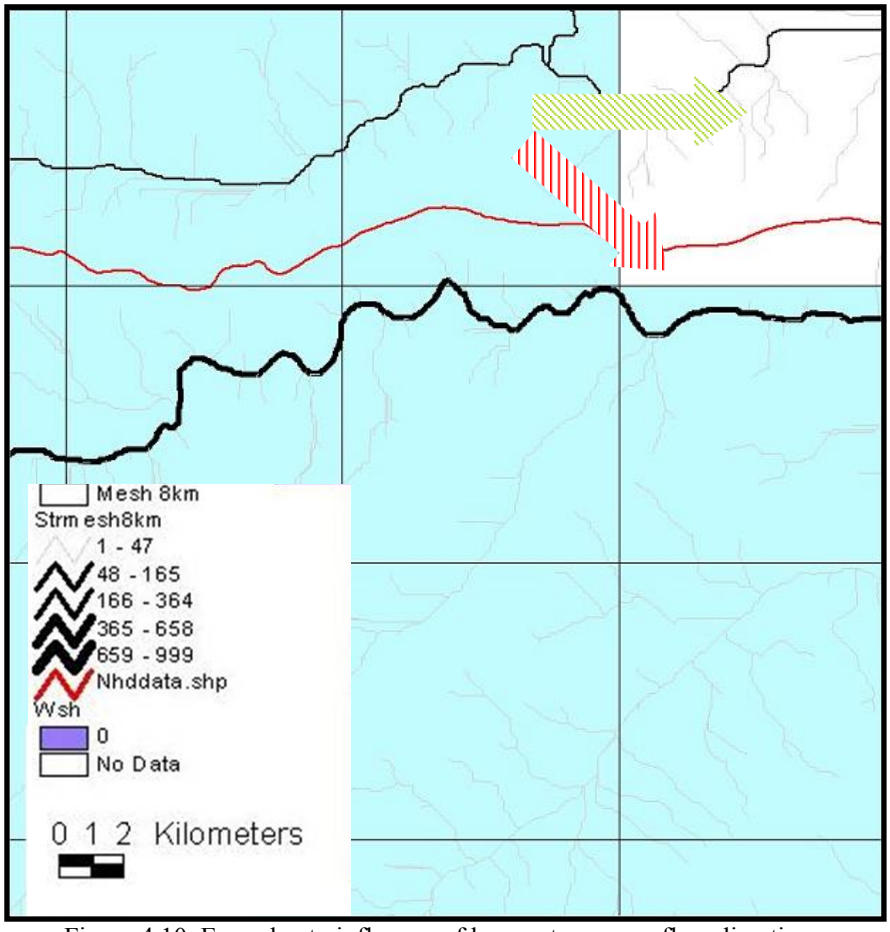

Figure 4.10. Error due to influence of larger streams on flow direction.

a) **Case 1 (Figure 4.10) Wrong flow direction due to influence of larger streams**

Figure 4.10 illustrates that, whenever a cell with a stream with a higher upstream length coexists with a stream with a shorter upstream length, NTM calculates the flow direction and reach using the longer stream. As in this case (Figure 4.10), the stream with the longer upstream flow length does not stay in the cell for a long time to be considered for calculation of flow direction and reach lengths and thus, leads to the error in flow direction determination (red arrow in the Figure 4.10). This

error was corrected by manually recalculating the stream length and flow direction (green arrow in Figure 4.10 on page 87) according to the logic behind the NTM algorithm with the stream that stays in the cell for the longest time.

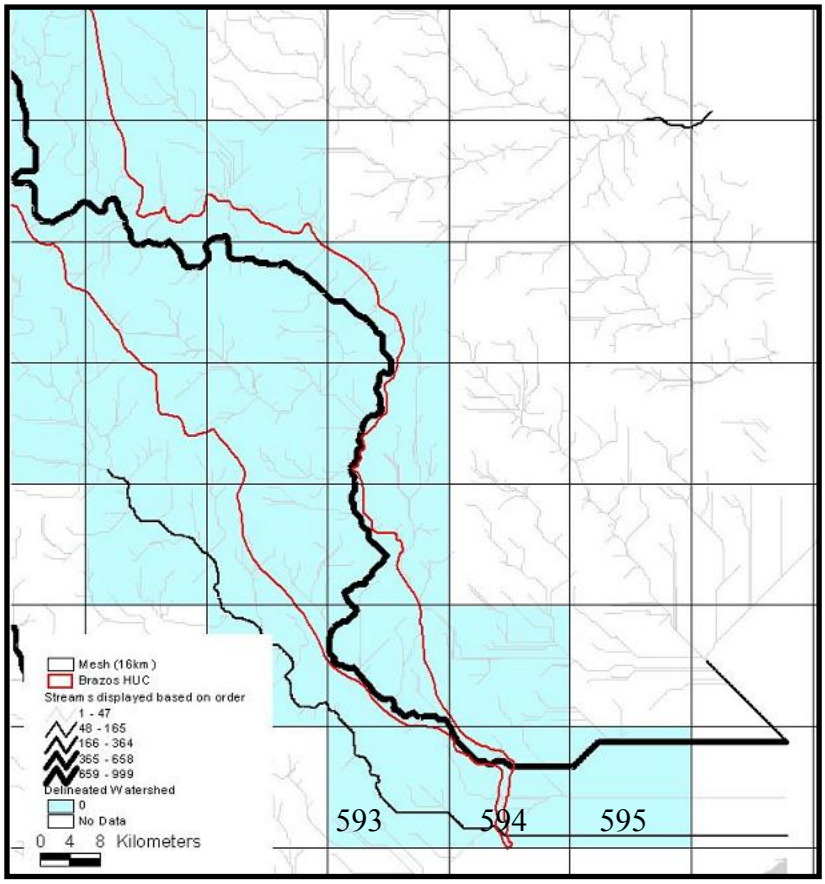

Figure 4.11. Error 2 at the outlet.

b) **Case 2 (Figure 4.11) Problem at the outlet**

This is a specific case related to this particular watershed. A stream with a higher upstream flow length swallows a watershed of a stream with a lower upstream flow length as they both enter the sea within the same cell (see Figure 4.11). This

problem was seen in all the watersheds except the 8, 045 m watershed. The correction to this error was done by manually removing the smaller watershed. The DSBoxID of the cell (BoxID = 593) was changed to zero (0) and its flow direction was set to zero (0).

Once all the errors were rectified (see Tables 4.6 to Table 4.9) the watersheds of the Brazos at four (4) resolutions (5 miles, 10 miles, 20 miles, and 40 miles) were re-delineated (see Figures 4.12 to 4.15) using the steps described earlier. The areas of the delineated watersheds were compared to the observed area of 118,215 km^2 (see Table 4.10). The delineated area of the Brazos and the observed area should be close because incorrect areas will result in misrepresentation of the runoff volumes. This is also a test for the NTM as irrespective of the shape of the watershed or the side to corner ratio the reach lengths should be predicted correctly.

Table 4.6. Changes made to the 16 km watershed cells to correct errors.

BoxID	DSBoxID	New DSBoxID	FDBoxID	New FDBoxID	Reach (m)	New Reach (m)
593	594	0	1	0	17483.8	0
2838	2839	2779	1	2	18655.07	19889.53
2779	2780	2720	1	2	18524.5	29422.41
2780	2720	2781	4	1	7250.25	18425
2550	2491	2551	2	1	40539.703	18494.0
1604	1544	1545	4	2	7075.95	26869.86
2720	2781	2660	128	4	23217.131	21373.0

Table 4.7. Changes made to the 16km watershed cells to correct errors.

BoxID	DSBoxID	New DSBoxID	FDBoxID	New FDBoxID	Reach (m)	New Reach (m)
11315	11316	11196	1	2	11573.19	18766.76
11077	11198	10958	128	2	17371.89	18061.21
10138	10139	10359	1	128	282.168	11063.4
10018	10139	10019	128	1	8748.02	11131.67
3346	3225	3467	8	128	11246.2	11776.44
3106	3105	2986	16	4	9816.923	8148.72
3225	3226	3105	1	4	1075.263	12441.92

Table 4.8. Changes made to the 32km watershed cells to correct errors.

BoxID	DSBoxID	New DSBoxiD	FDBoxID	New FDBoxID	Reach (m)	New Reach (m)
670	671	0	1	2	7608.16	39902.8
645	616	646	2	1	68482.86	37394.2
147	148	0	1	0	30026.6	0
178	148	0	4	1	2720	0

Table 4.9. Changes made to the 64 km watershed cells to correct errors.

BoxID	DSBoxID	New DSBoxiD	FDBoxID	New FDBoxID	Reach (m)	New Reach (m)
170	171	156	1	2	86448.51	96408
159	144	175	4	128	144444.07	236398.03
145	130	146	4	1	220779.10	111561.04
131	116	132	4	1	112261.40	109063.12

59	44	45	4	2	102309.38	153144.36

Table 4.10. Comparison of delineated areas of the Brazos River Basin.

Resolution	Delineated Area (km^2)	Observed Area (km^2)	No. of cells in watershed	Error (%)
8km	118,117.7	118,228.3	1825	-0.08
16km	118,570.7	118,228.3	458	+0.3
32km	120,124.1	118,228.3	116	+1.6
64km	120,124.1	118,228.3	29	+1.6

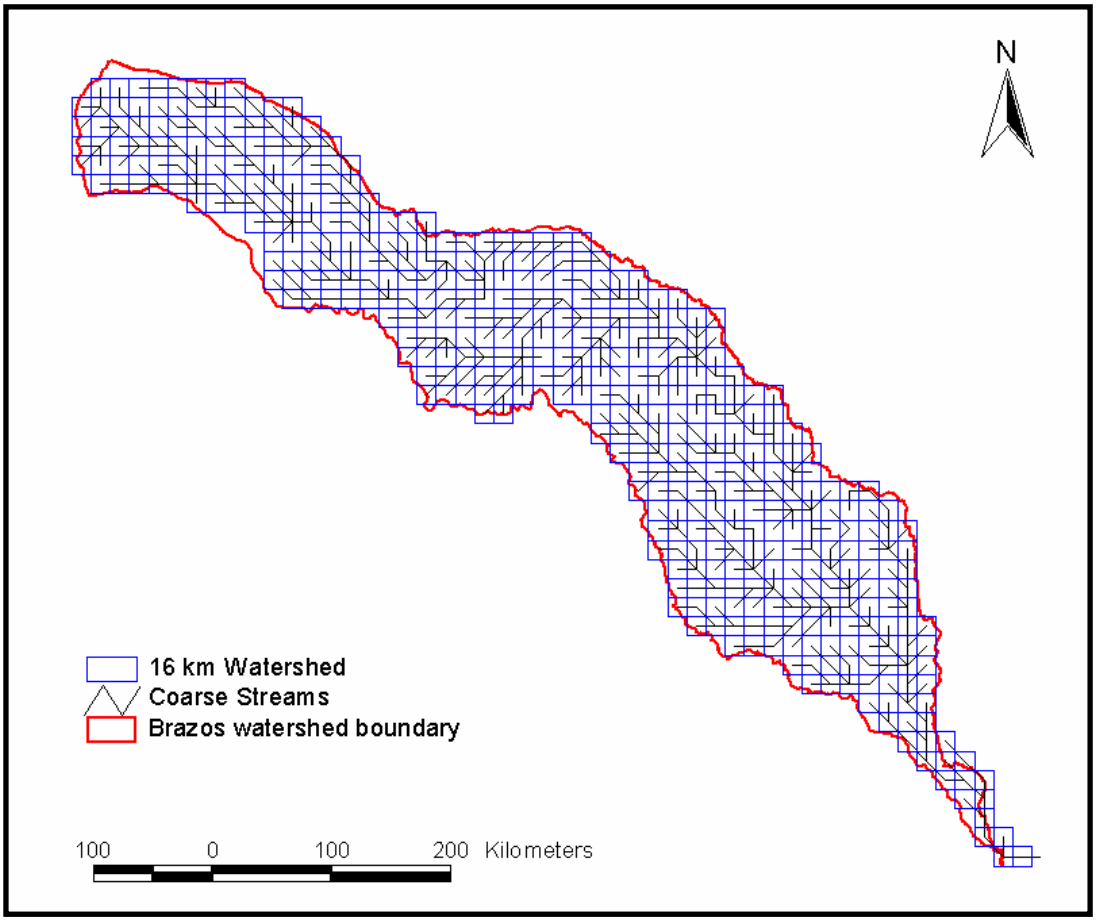

Figure 4.12. Brazos River watershed delineated with the cell size of 16,090 m.

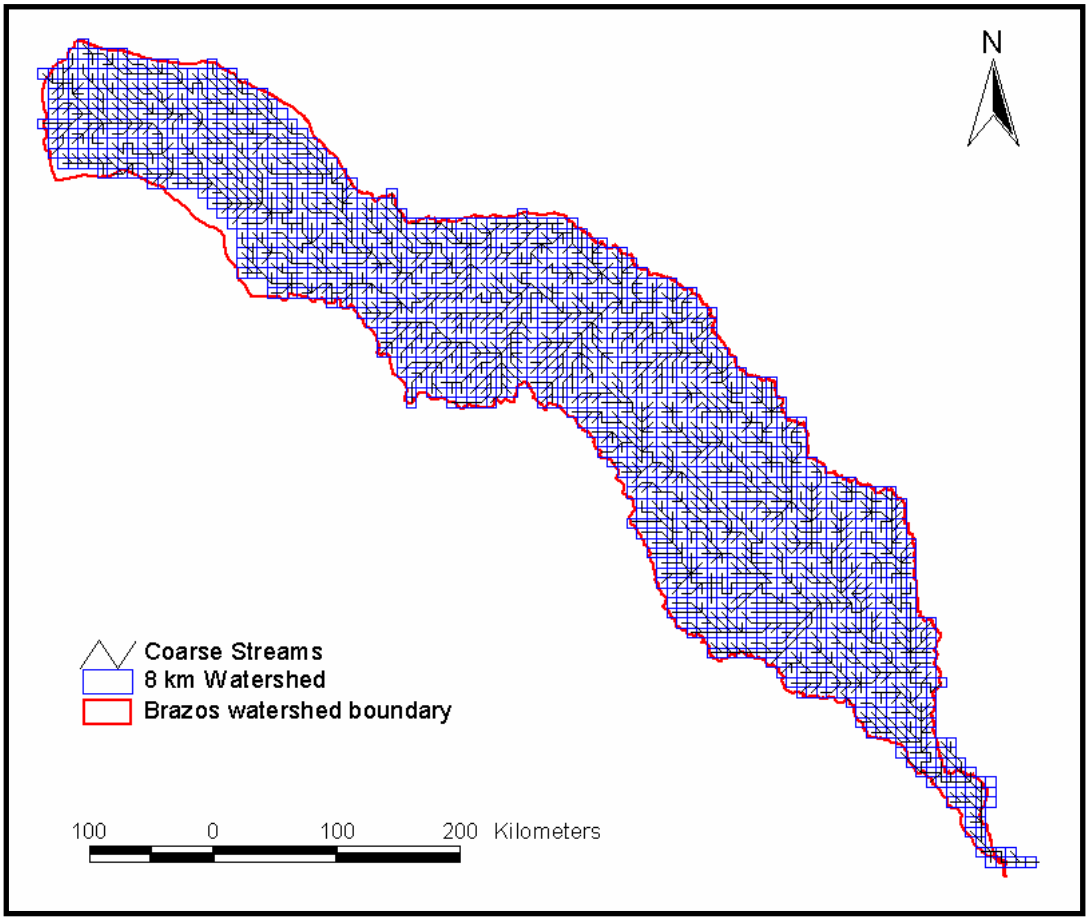

Figure 4.13. Brazos River watershed delineated with the cell size of 8,045 m.

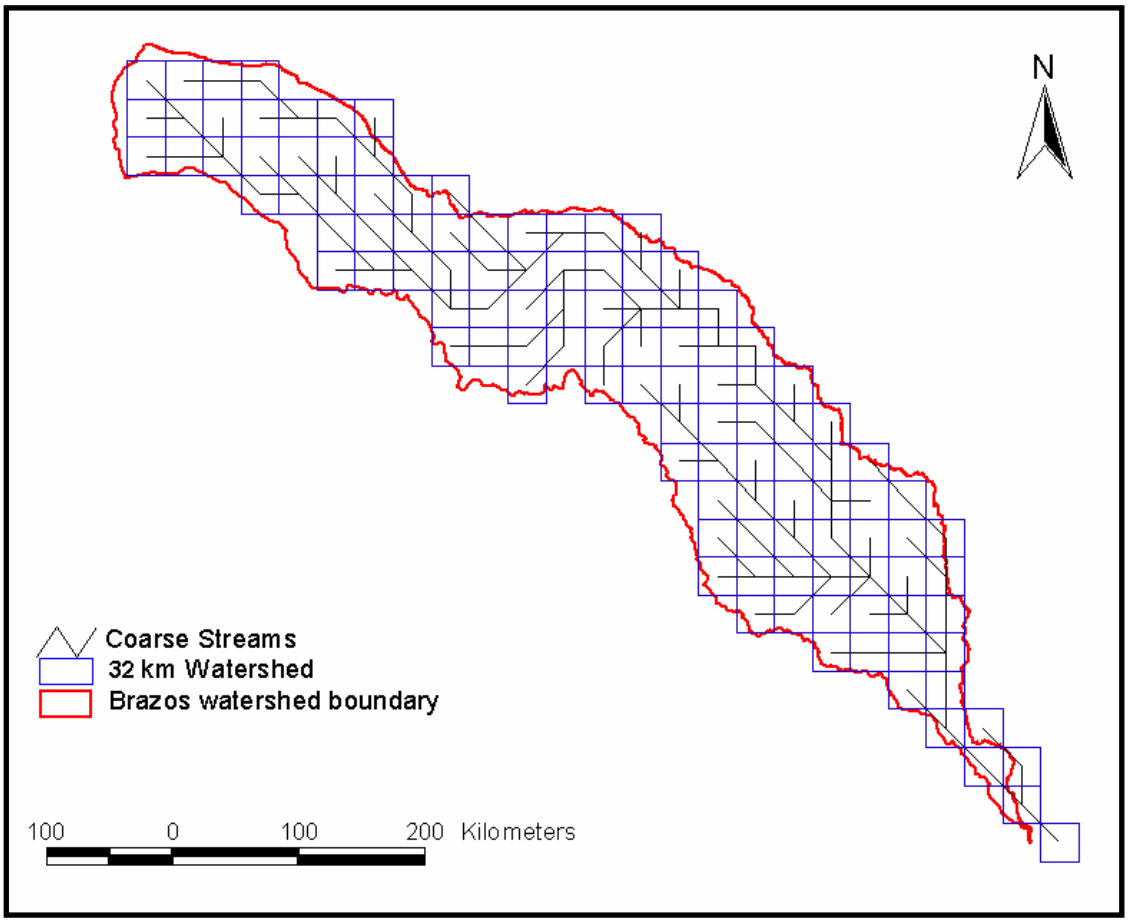

Figure 4.14. Brazos River watershed delineated with the cell size of 32,180 m.

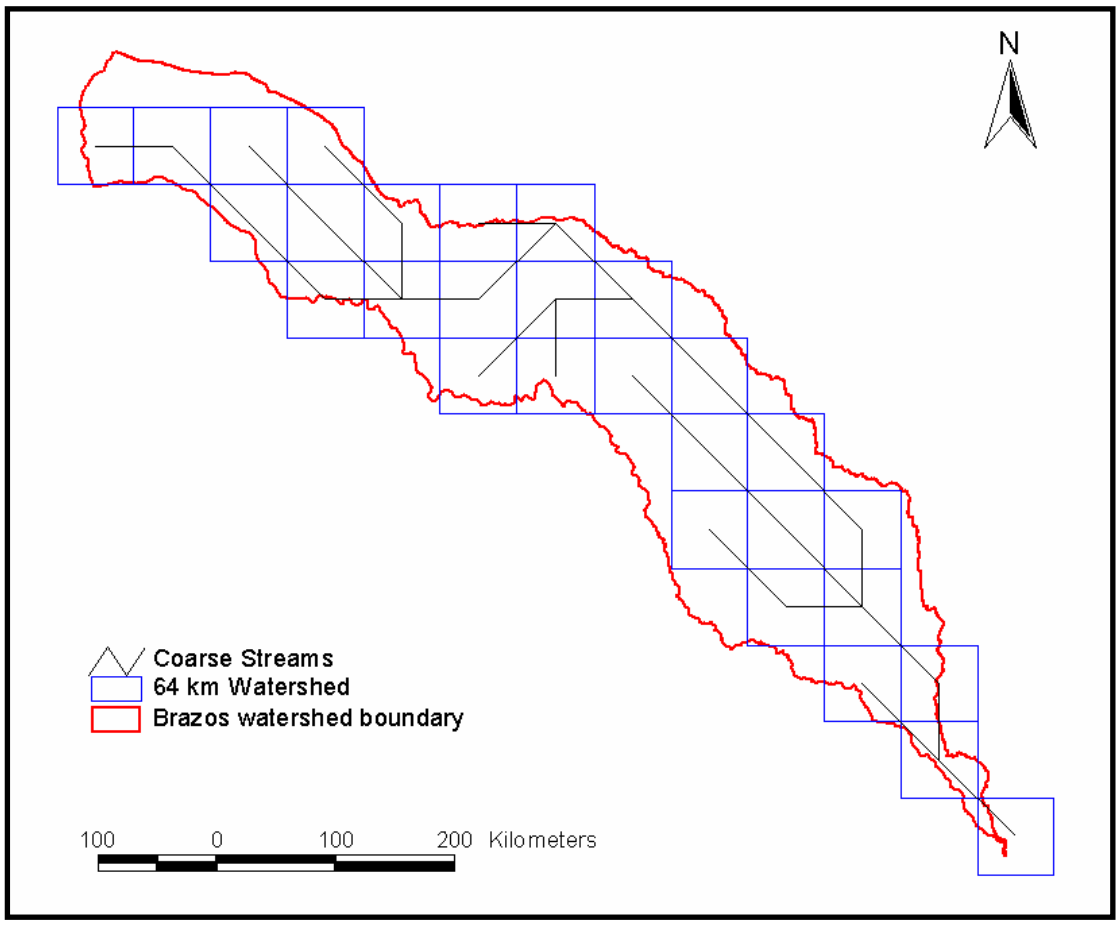

Figure 4.15. Brazos River watershed delineated with the cell size of 64,360 m.

4.1.9 Application of the cell-to-cell stream flow routing model

The cell-to-cell stream flow routing algorithm was applied to the Brazos river basin with the network data of four delineated watersheds (8,045 m, 16,090 m, 32,180m and 64,360 m). Table 4.12 lists the stream and overland velocity and dispersion used for the application of the cell-to-cell stream flow routing model. The stream velocities were fixed at 1m/s and stream coefficient of dispersion was fixed at 250m/s for all cells in the four resolutions. Overland flow velocities and dispersion coefficients are

dependent on the cell resolution. The coarser the resolution, the greater is the value for the two parameters. The overland flow velocities were initially calculated manually using sample case (Figure 4.16). These values were considered as starting points for the simulations and were changed accordingly in the subsequent simulations to achieve same mean and standard deviation for all the hydrographs. With an example case (Figure 4.16) of one 64 km cell, four 32km cells, sixteen 16 km cells, and sixty four 8km cell the computation of overland flow velocity is explained.

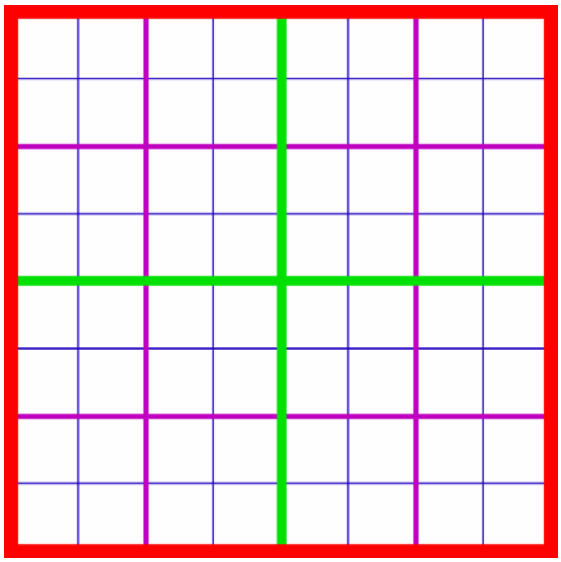

Figure 4.16. Calculation of overland flow velocity.

The red outline in Figure 4.16 is the 64 km cell the green outline is the 32 km cell, the purple outline is the 16 km cell and the blue outline is the 8 km cell. The value of overland stream flow velocity for 8 km watershed was taken as 0.025 m/s. The following method was used to compute the first approximation of the overland stream flow velocities of the 16 km, 32 km and the 64 km watersheds.

Considering one 16 km cell and four 8 km cells the calculation of first guess of the overland flow velocity is explained beneath.

One 16 km watershed cell has four 8 km cells. Assuming that each cell has a probability of flowing 41% the sides and 59% though the corners we have,

$$\left(\frac{16\times\sqrt{2}}{2}\times\frac{1}{v}\times\frac{59}{100}+\frac{16}{2}\times\frac{1}{v}\times\frac{41}{100}\right)=\frac{1}{4}\left(\frac{41}{100}\times\left(4\times\frac{8}{2}\right)\times\frac{1}{0.025}+\frac{59}{100}\times\left(4\times\frac{8\times\sqrt{2}}{2}\right)\times\frac{1}{0.025}+\Sigma reach_i\times\frac{1}{Vs}\right)$$

……(4.1)

Where, v is the overland flow velocity for the 16 km cell and $reach_i$ is the reach of each 8 km cell, Vs is the stream flow velocity, which in this case is equal to 1 m/s.

This equation is based on the principle that runoff is applied at the center of each cell and the average flow time from the center of the 16 km cell is equal to the average flow time of the four 8 km cells. In the case of a 16 km cell the water moves from the center of the cell to the edge of the corner of the cell as overland flow, while as for the 8 km cells the water first moves from the center of each cell to the edge or the corner as overland flow and then from the cell exit node to the outlet of the 16 km cell with stream flow velocity. Thus, for the 8 km cells we have to consider both stream flow velocity and overland flow velocity. The only unknown, the overland flow velocity (v) of the 16 km cell can be found out solving the equation. Both cases of flow either though the side or the corner has been considered to occur for the 16 km cell. Average of the two is considered as the starting point for the simulations.

The two overland flow parameters (velocity and coefficient of dispersion) of the watershed with the cell size of 8 km were kept as a reference and for the other resolutions these values were changed until the hydrographs had the same mean and

standard deviation (Table 4.12). The user time step chosen for the simulations was 6 hours (21600 seconds). In absence of real time runoff data for the Brazos River basin, a uniform runoff depth of 0.0001 mm was applied to all the cells in all the four delineated watersheds. The order of runoff depth was chosen to match the order of average flow at the outlet of the Brazos River basin.

Table 4.11. Flow parameters for the Brazos River Basin.

Flow parameters	**8km**	**16km**	**32km**	**64km**
Stream Velocity (m/sec)	1	1	1	1
Overland flow velocity (m/sec)	0.024	0.048	0.1	0.193
Coefficient of Dispersion for stream flow (m^2/sec)	250	250	250	250
Coefficient of Dispersion for overland flow (m^2/sec)	2	10	25	250

Table 4.12. Statistical parameters for the delineated watersheds.

Statistical parameters	**8,045 m**	**16,090 m**	**32,180 m**	**64,360 m**
Mean (days)	13.42	13.41	13.40	13.38
Standard deviation (days)	5.60	5.60	5.73	5.35

4.1.10 Effect of the cascade of tanks

The cell to cell stream flow routing model approximates a single cell in the watershed as a cascade of tanks (linear reservoirs). To demonstrate the impact of the cascade of tanks on the flow characteristics at the outlet, the flow at the outlet was computed using a stream network with each cell represented as a linear reservoir and not as a cascade of linear reservoirs. In physical meaning, the cascade of tanks in each cell was replaced by a single tank. All the four resolutions were tested with the same parameters given in Table 4.12. The results (see Figures 4.17 to 4.20) clearly show that the cascade produces much more variation in flow as compared to a single tank per cell. All flow variations in the hydrograph with one tank per cell are effectively overshadowed. Physically, this shows that dispersion is an important parameter. Also from the results of the four resolutions, it can be noted that as a the cell resolution increases the flow hydrograph with a cascade of tanks shows much more noise as compared to the hydrographs of smaller cell sizes. This shows that as the cell size increases the time for overland flow to reach the outlet compared to smaller cells increases and this leads to more noise. The average number of tanks in each cell is given in Table 4.13.

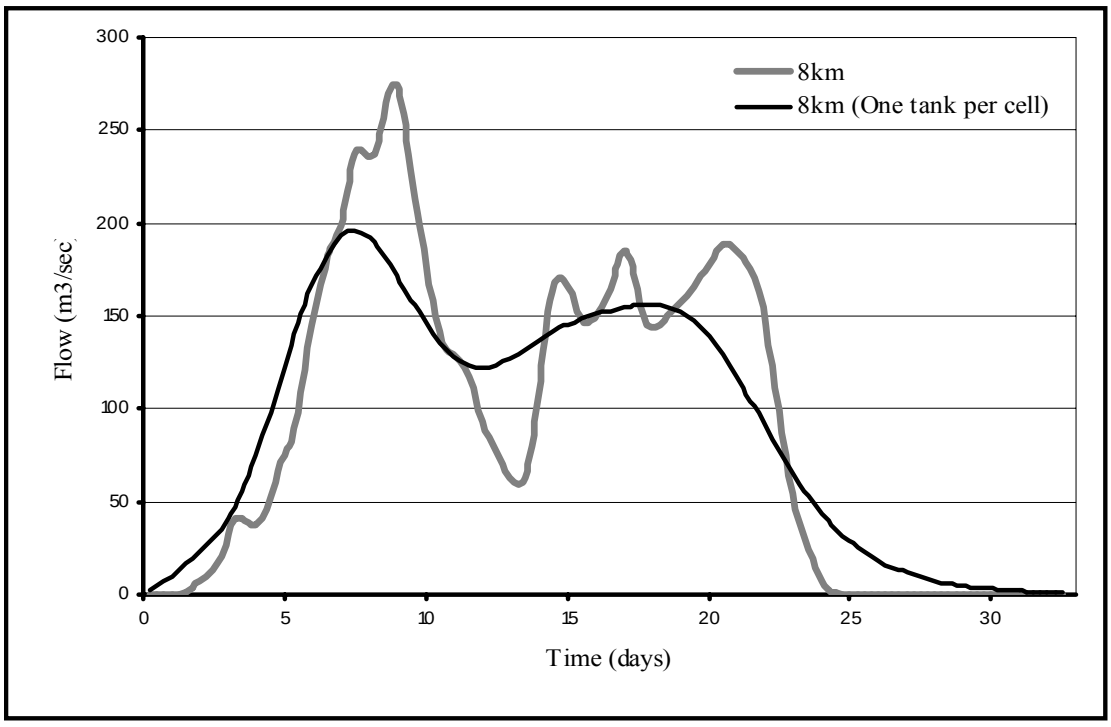

Figure 4.17. Flow at outlet with multiple tanks per cell vs. one tank per cell for 8km resolution.

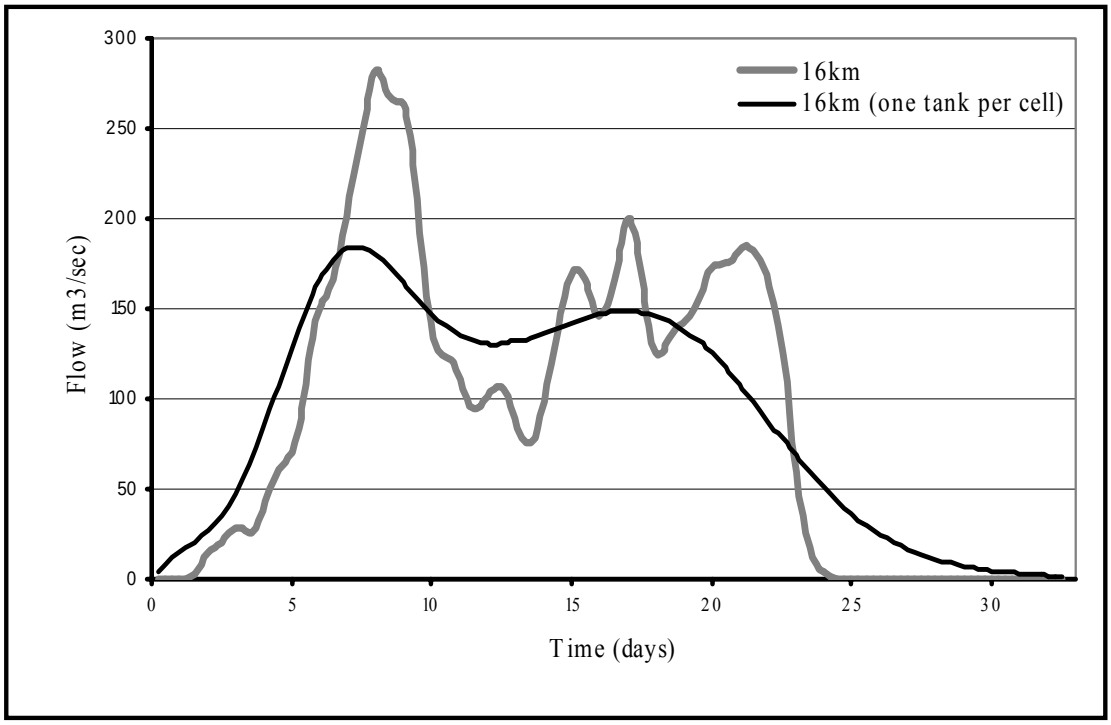

Figure 4.18. Flow at outlet with multiple tanks per cell vs. one tank per cell for 16km resolution.

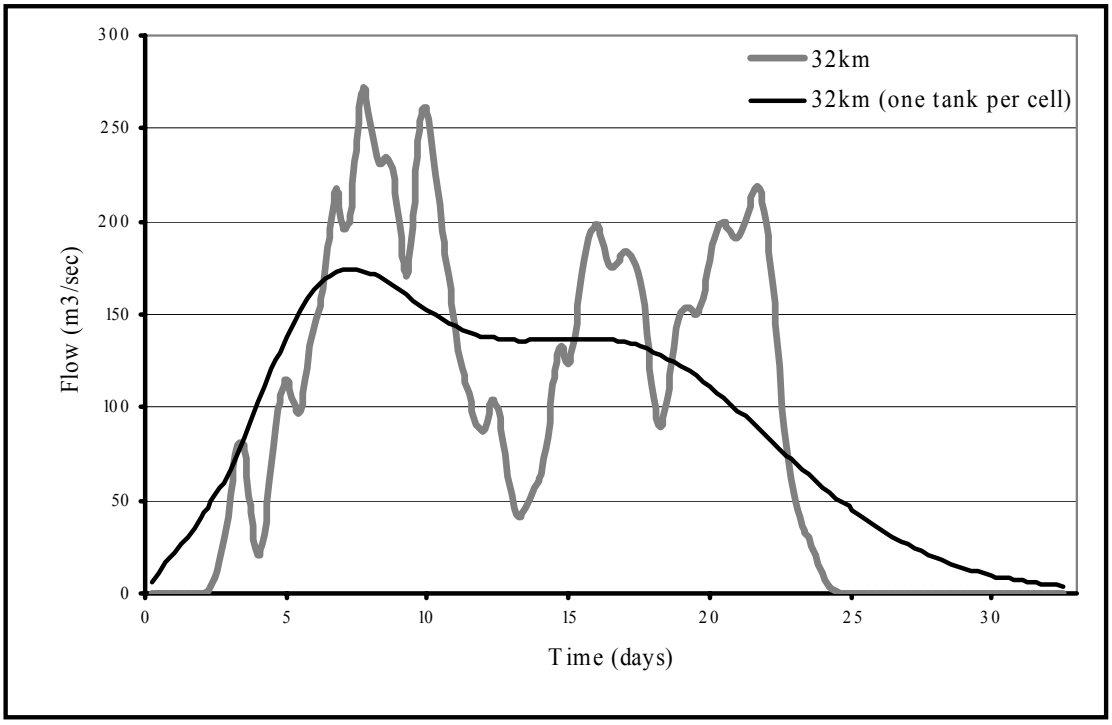

Figure 4.19. Flow at outlet with multiple tanks per cell vs. one tank per cell for 32km resolution.

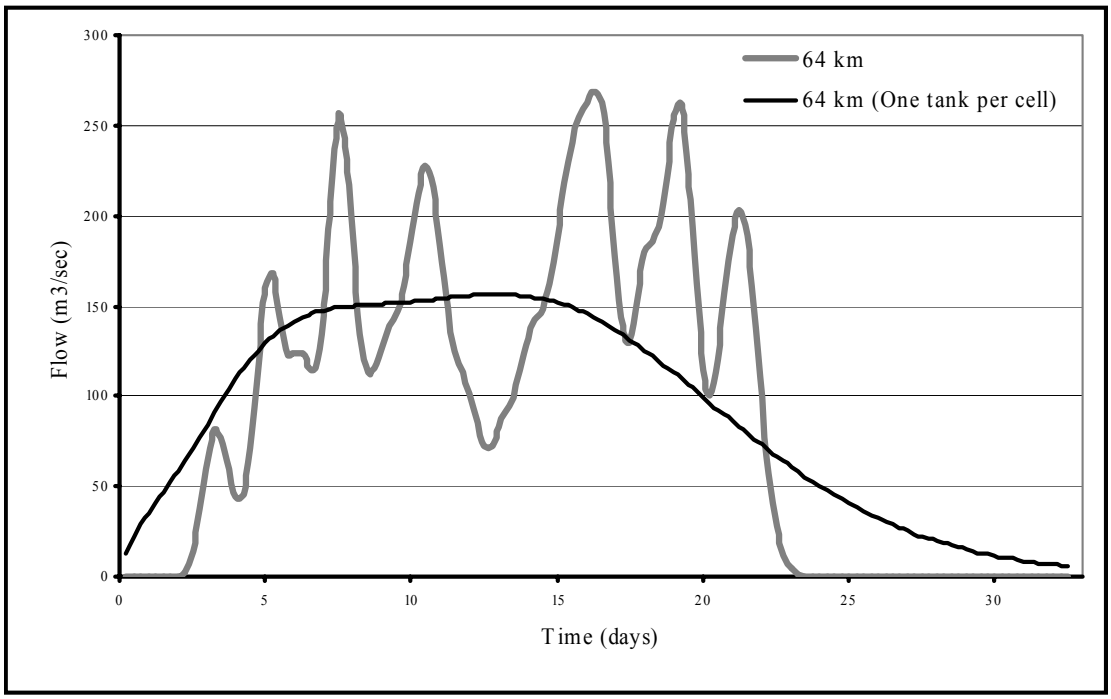

Figure 4.20. Flow at outlet with multiple tanks per cell vs. one tank per cell for 64km resolution.

Table 4.13. Range of the tanks for each cell in the four resolution watersheds.

Resolution	**8,045 m**	**16, 090 m**	**32,180 m**	**64,360m**
No. of Cells	1825	458	116	29
Average No of tanks per cell	24	51	109	245

4.1.11 Effect of change of resolution on the model output

To determine effect of cell resolution the model output of all the 10mile (16.090km), 20 mile (32.180km), and the 40 mile (64.360km) was compared to the model output of the 5 mile (8.045km). Figure 4.21 is the flow hydrograph when the time step of display of flow values is 6 hours for all the four resolutions. In Figure 4.22, hydrograph for 8 km is displayed at a time step of 6 hours, hydrograph for 16 km is displayed at a time step of 12 hours, hydrograph for 32 km is displayed at a time step of 24 hours, and hydrograph for 64 km is displayed at a time step of 48 hours.

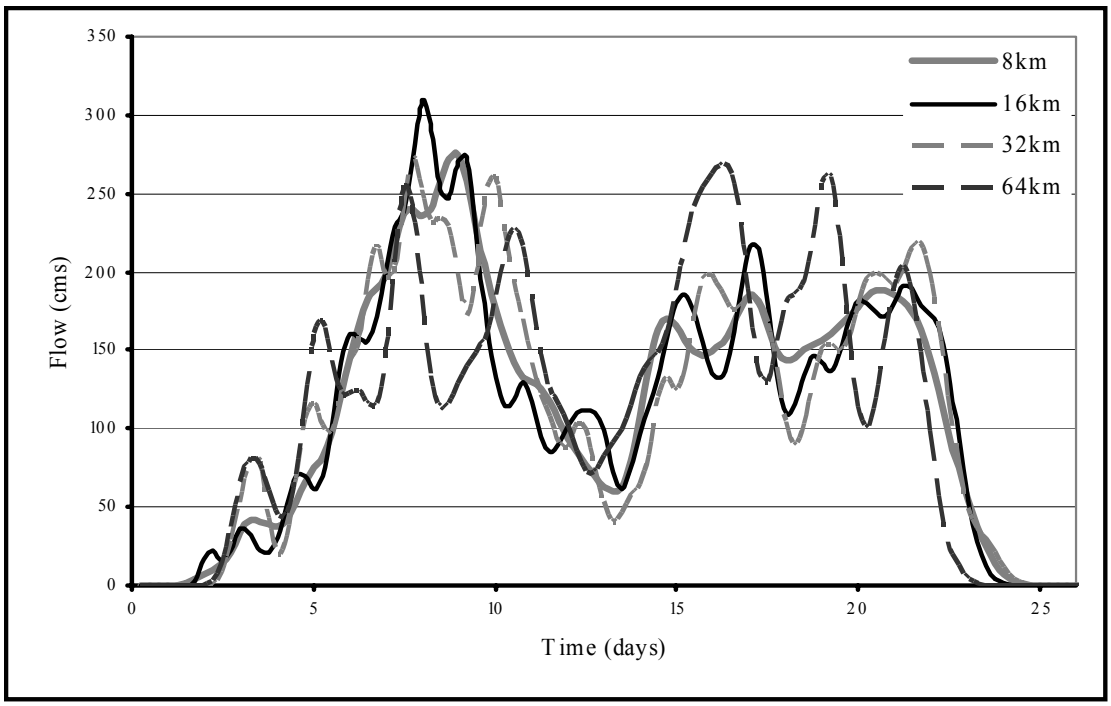

Figure 4.21. Comparison of flow from 8km, 16km, 32km and 64km resolutions.

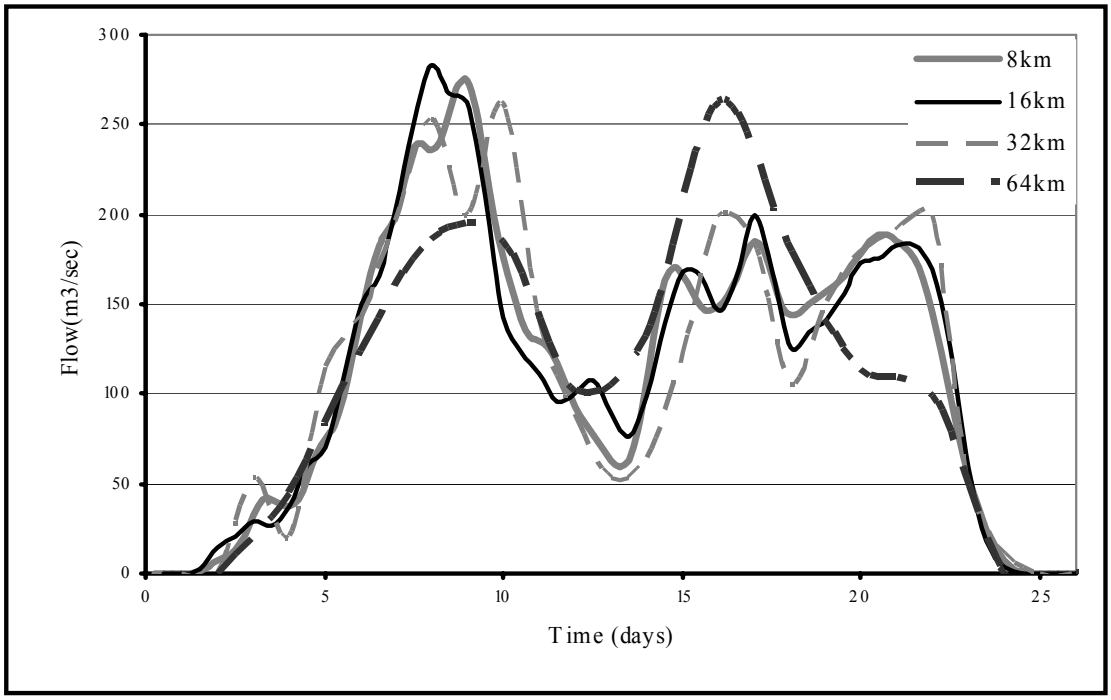

Figure 4.22. Comparison of flow from 8km, 16km, 32km and 64km resolutions with different time steps.

It is clear from the results that the four hydrographs do not match well. The 64, 360 m watershed is the worst fit. One of the reasons for this is misrepresentation of watershed area. Even though the difference between the observed area and the delineated area in the coarse resolution watershed is negligible, this is due to cancellation of errors. The watershed encompasses areas outside the observed watershed at some places and loses out on areas at other places (see Figure 4.23 on page 105). It is evident from the results, that as the cell size increases it leads to more noise in the watershed. This is because of the longer time it takes for the overland flow to reach the cell outlet in bigger cells. As a result, water comes out of the cell in bigger packets with very less dispersion leading to more noise as compared to the smaller cells, where water is geographically distributed leading to a smoother hydrograph. As a result, Figure 4.22 shows that when the hydrographs are shown at different time steps, it results in smoother hydrographs for 16,090 m and 32,180 m watersheds. With a greater time step the time allowed for the overland flow to reach the cell outlet is more. The 64,360 m watershed hydrograph is grossly misrepresented.

4.1.12 Effect of location of runoff on the model output

The Brazos river basin was distributed in four regions (Figure 4.23 and Table 4.14) namely lower Brazos, upper Brazos and the middle Brazos was divided into 2 parts. Model runs were carried out for all the four resolutions with runoff in only one of the four regions at a time. The aim of this exercise was to examine the impact of location of the runoff as well as identification of the source of errors in the earlier hydrographs (see Figures 4.21 and 4.22). The results clearly suggest that the

hydrographs for the 8,045 m and 16,090 m resolution watershed match closely. As compared to them, the 32, 180 m and 64,360 m resolution watersheds show much more noise and do not match well with the other two hydrographs.

Table 4.14. Areas of the four regions for the Brazos River basin.

Area	**8,045m**	**16,090m**	**32,180m**	**64,360m**
Lower Brazos (km^2)	9,837.74	9,837.74	12,426.62	16,568.83
Middle Brazos (part 1) (km^2)	47,635.40	47,635.40	47,635.40	37,279.88
Middle Brazos (part 2) (km^2)	25,500.47	24,853.25	24,853.25	28,995.46
Upper Brazos (km^2)	35,144.05	36,244.33	35,208.78	37,279.8

The reasons for the anomalies between the 8,045 m and the 64,360 m hydrographs can be identified by looking at the four regions individually in both watersheds (Figure 4.23).

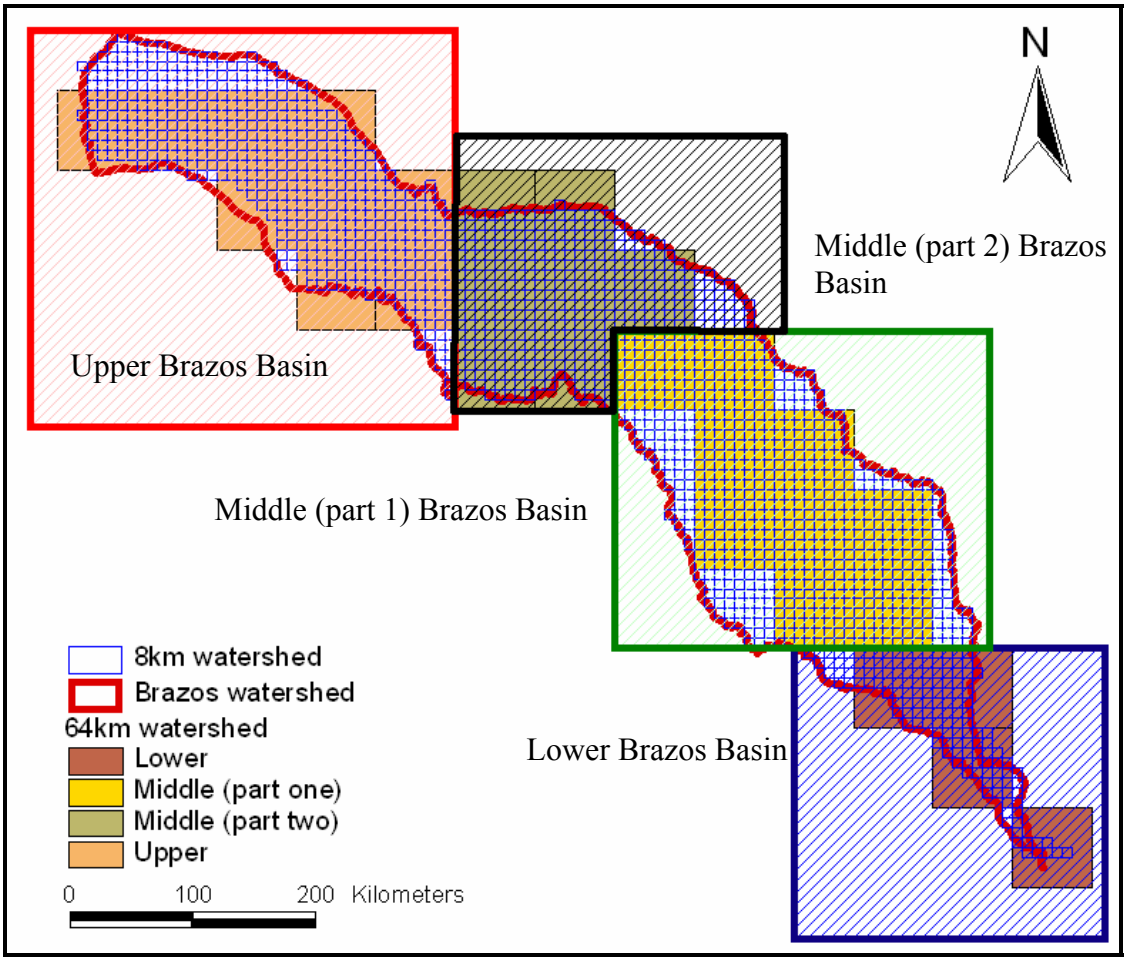

Figure. 4.23. Division of the Brazos River Basin into four regions.

a) Lower Brazos

The 8,045 m watershed matches pretty well with the observed watershed (Figure 4.23). The 64,360 m watershed due to a larger cell size encompasses areas outside the observed watershed. This leads to an error in the runoff volumes, clearly seen in the hydrograph (Figure 4.24). Also the hydrograph shows much more noise as compared to the 8,045 m watershed. The 32,180 m watershed hydrograph also shows much more noise as compared to the 8,045 m and 16, 090 m watershed hydrographs.

Also, due to more area the flow volume is incorrectly predicted in the case of 32,180 m watershed as compared to the 8,045 m and 16,090 m watersheds.

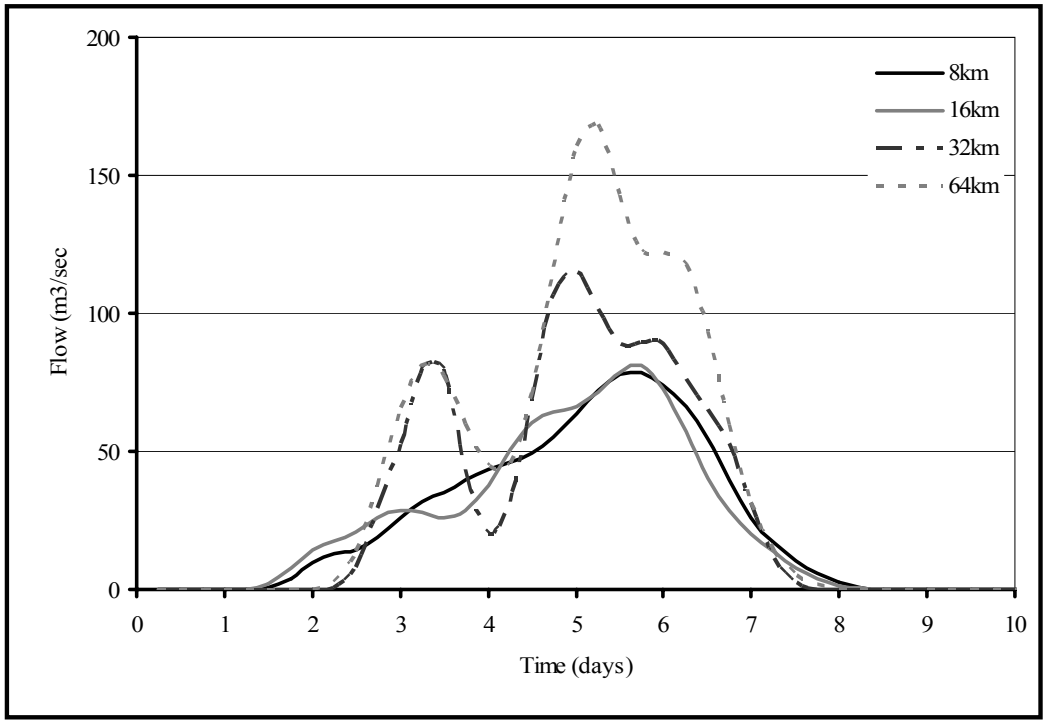

Figure 4.24. Comparison of flow for lower Brazos River.

b) The middle (part 1) Brazos River Basin

The 64,360 m watershed due to a larger cell size loses areas inside the observed watershed. This leads to an error in the runoff volumes, clearly seen in the hydrograph (Figure 4.25). The hydrograph of this watershed shows much more noise as compared to the other hydrographs. The 8,045 m watershed hydrograph matches closely with the 16,090 m watershed.

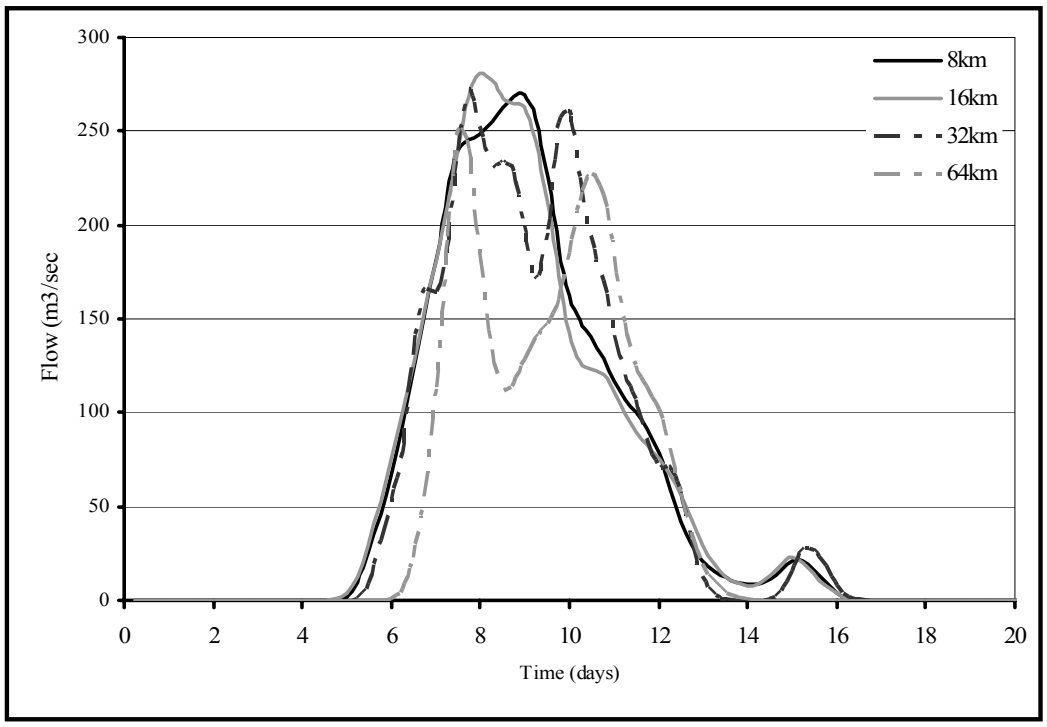

Figure 4.25. Comparison of flow for middle (part 1) Brazos River.

c) The middle (part 2) Brazos River Basin

The 64,360 m watershed does not taken into account part of the watershed as a result the area is less than the other watershed as a result runoff volume is less, clearly seen in the hydrograph (Figure 4.26).

d) The upper Brazos River Basin

In the 64,360 m resolution watershed, due to a larger cell size encompasses areas outside the observed watershed in some cases and loses out areas at other places. This leads to an error in the runoff volumes, clearly seen in the hydrograph (Figure 4.27).

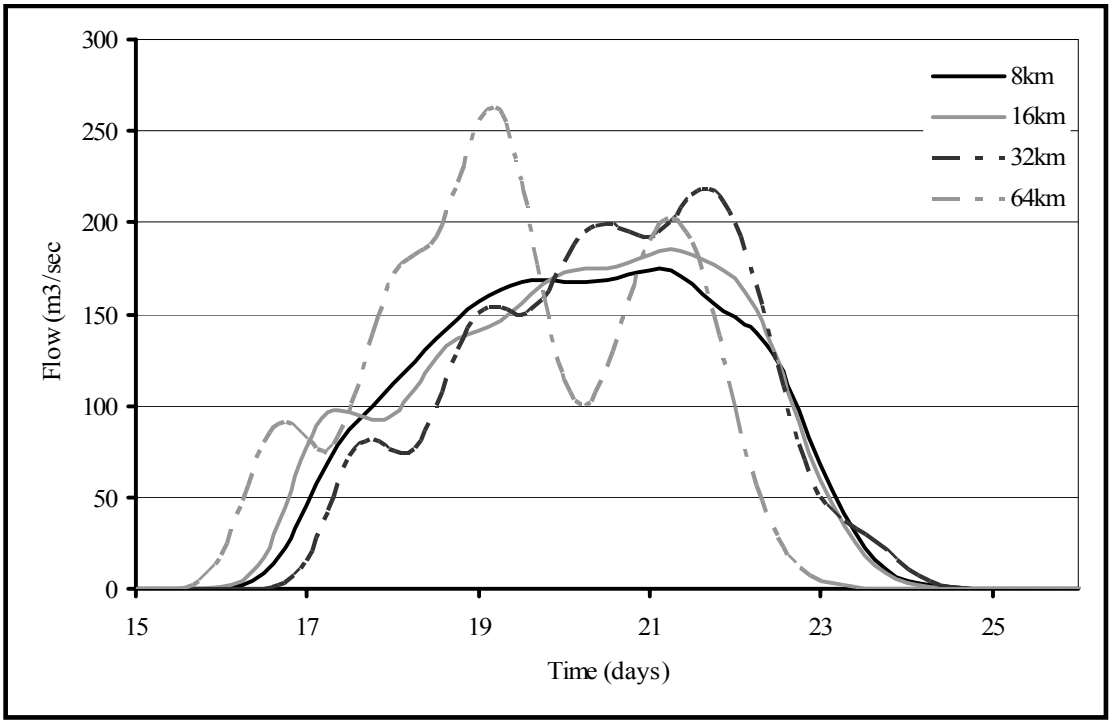

Figure 4.26. Comparison of flow for middle (part 2) Brazos River.

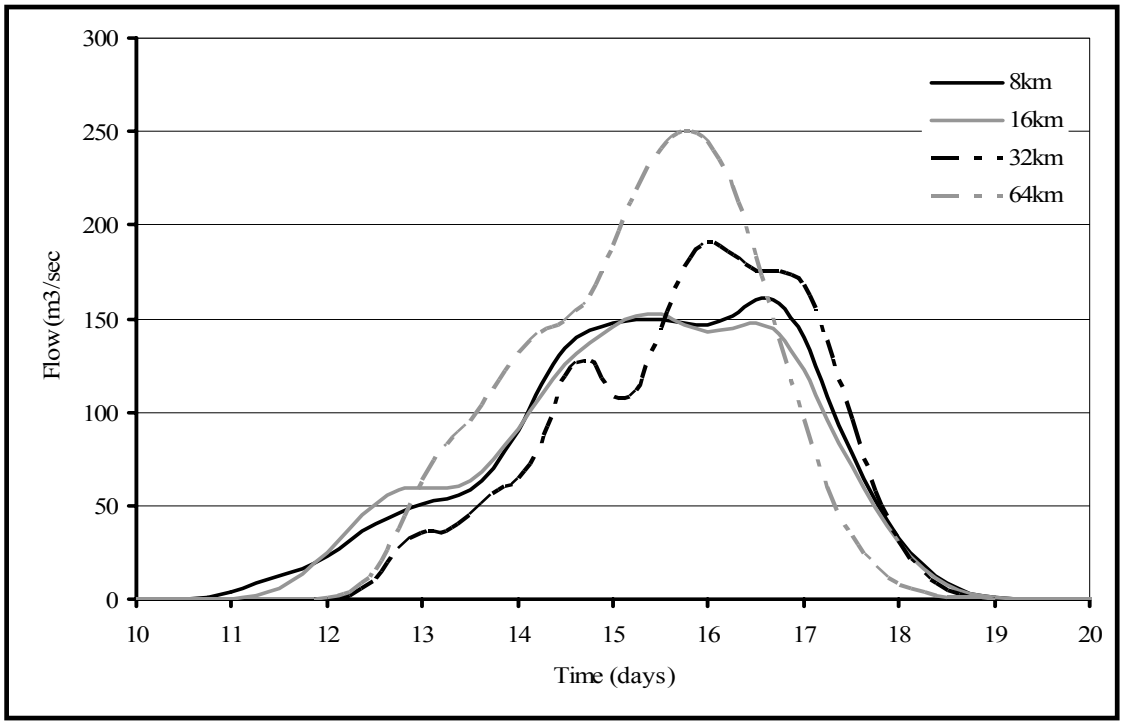

Figure 4.27. Comparison of flow for upper Brazos River.

4.2 Case study: Waller Creek, Austin

The lack of runoff depth data for the Brazos river basin did not given an opportunity for calibration and validation of model parameters with observed flows. The 12 sq. km Waller Creek watershed (Figure 4.28) within Austin city limits was used for the calibration and validation of the parameters in the cell-to-cell stream flow routing model. Runoff depth data and stream flow data used for the application of the routing algorithm is documented by Olivera et al. (1996). The runoff data for calibration analysis is available from October 14th, 1994, at 7:45 p.m. to October 17th , 1994, at 6:45 p.m. at a time step of fifteen (15) minutes representing two hundred eight four (284) time intervals.

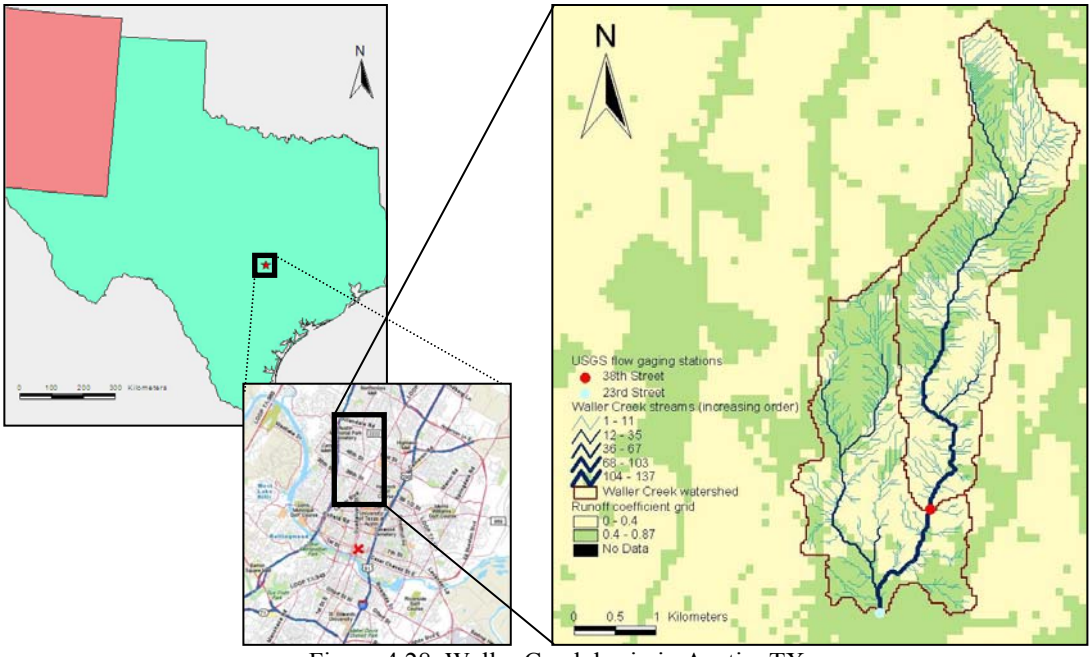

Figure 4.28. Waller Creek basin in Austin, TX.

A small time-step is chosen because this is a small watershed and water reaches the outlet in a matter of few hours. 15-minute flow records are available for the 23rd Street and 38th Street USGS gauging stations (Olivera et al, 1996). For the application of the cell-to-cell stream flow routing model three resolutions (cell size of 250m 500m and 1000m) are considered. The stream network used is the same as the one described in Olivera and Maidment (1999). It was delineated from a 30m DEM. Figure 4.29 shows the coarse resolution mesh and the fine resolution stream network displayed with respect to "stream rank".

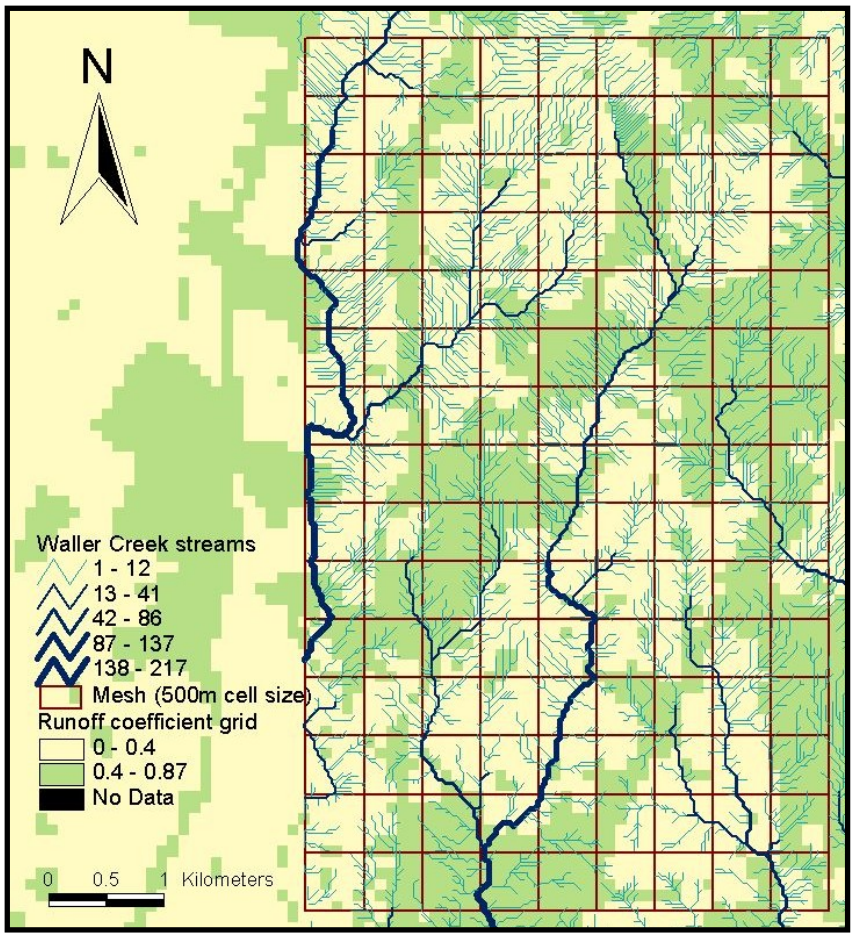

Figure 4.29. Mesh of cell size 500m and stream network of the Waller Creek.

4.2.1 Watershed delineation

Analysis of the Waller Creek was done with three (3) watersheds delineated with a similar methodology as followed with the delineation of the watersheds of the Brazos River basin. The watersheds were delineated at resolutions of cell sizes 250m, 500m, and 1000m (see Figures 4.30 to 4.32) for the purpose of application of the cell-to-cell stream flow routing algorithm. Figure 4.31 shows the watershed delineated for Waller Creek for a cell resolution 500 m. There are 49 cells of 250,000 sq. m representing the watershed. The total area with this cell resolution is 12,250,000 sq. m, representing an error of 1.6% from the documented area of 12,052,000 sq m. The 250m resolution (Figure 4.31) delineated watershed has 189 cells with a total area of 11,812,000 sq m. and the 1000m resolution watershed (Figure 4.32) with 13 cells has a total area of 13,000,000 sq. m. The error in areas represented by the 250m and the 1000m resolutions is equal to 2.03% and 7.2% when compared to the actual area of 12,052,000 sq m.

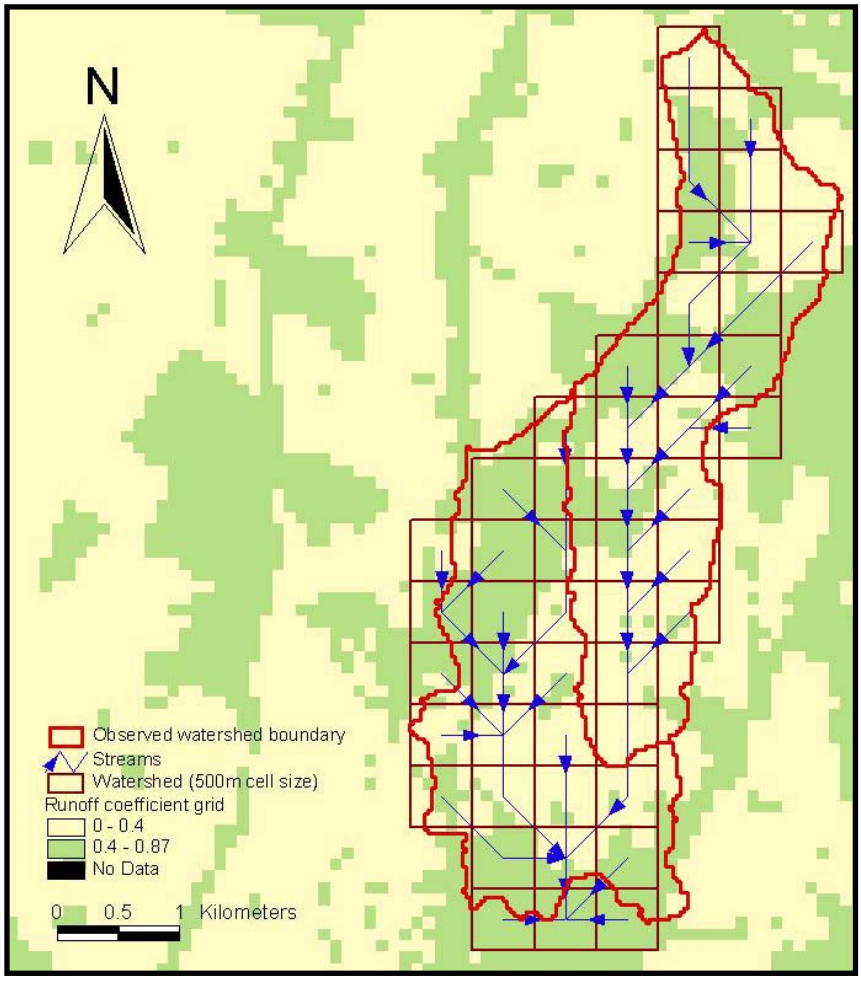

Figure 4.30. Waller Creek watershed delineated at the cell resolution of 500m.

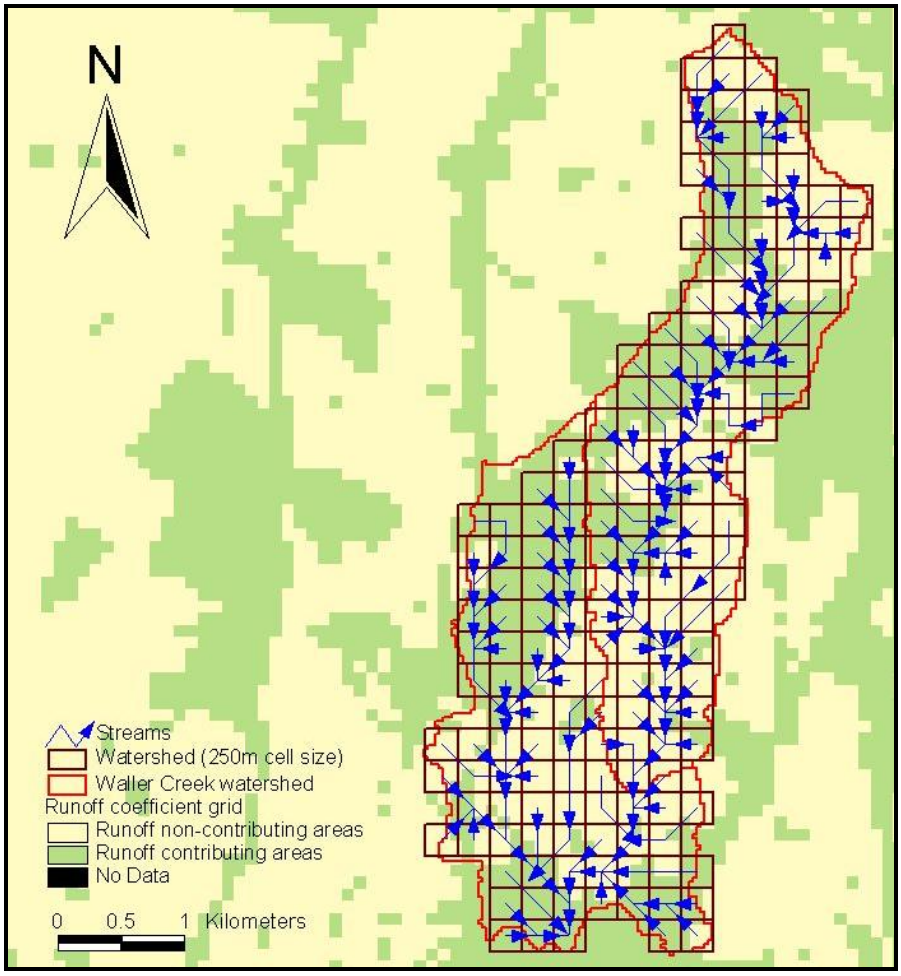

Figure 4.31. Waller Creek watershed delineated at the cell resolution of 250m.

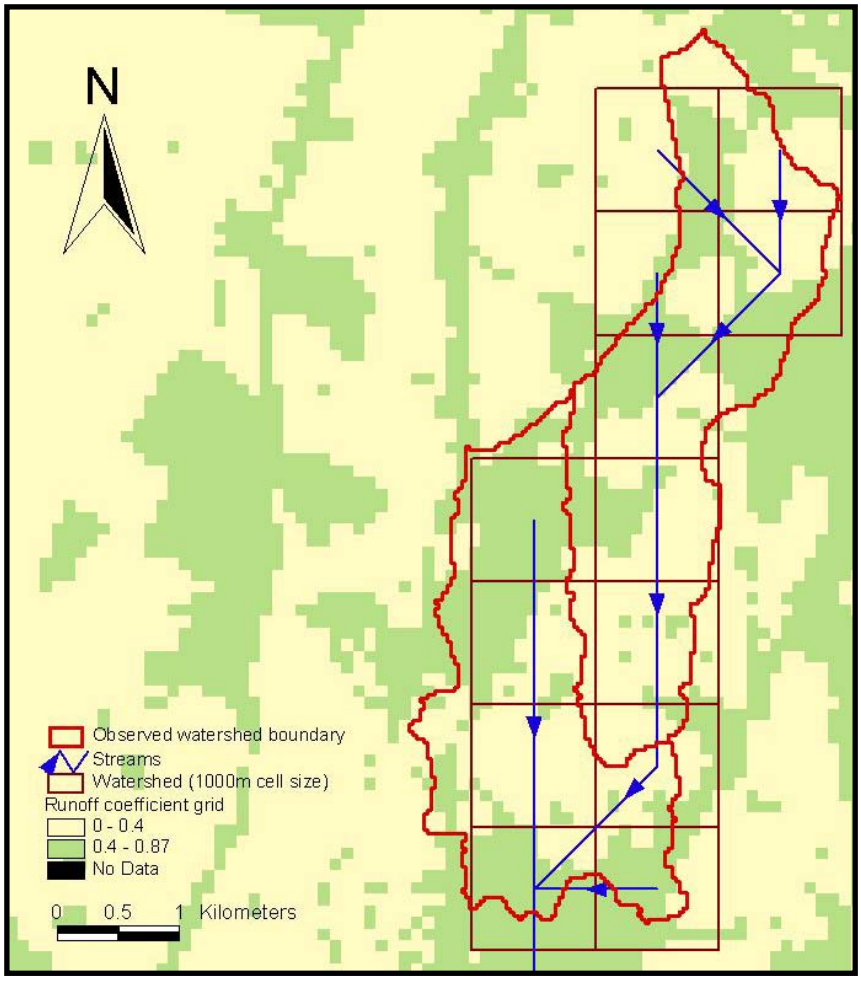

Figure 4.32. Waller Creek watershed delineated at the cell resolution of 1000m.

4.2.2 Distribution of runoff to each cell in the watershed

The runoff depth data for the Waller Creek watershed (Olivera et al., 1996) ranges from October 14th, 1994, at 7:45 p.m. to October 17th , 1994, at 6:45 p.m. The runoff data was distributed over the watershed in each cell using runoff coefficients. The runoff coefficient is a dimensionless number that is defined as the ratio of the peak discharge to the rainfall intensity multiplied by the drainage area (Olivera et al., 1996). The method of calculation of the runoff coefficients is described in detail in Olivera et al (1996). They have calculated the runoff coefficients for the Austin area.

It is available in a grid format of cell size 30m. This grid was used for distribution of runoff over the entire watershed. Figure 4.33 presents the runoff coefficient map of the Waller Creek watershed. It can be noted that just upstream of the 38th Street station there is an area that generates little water runoff (runoff coefficient values less than 0.4); while just upstream of 23rd Street the area, yielding much more runoff. This shows that area above 38th Street is less developed as compared to the area above 23rd Street.

4.2.2.1 Computation of runoff for each cell

Each cell of the watershed was associated with a time series of runoff depth values that is to be routed to the outlet at 23rd Street. Olivera et al. (1996) have documented the runoff values for this watershed. These values were used for this calibration of the two parameters of the watershed, respectively velocity and coefficient of dispersion.

In the discussion below, the method of computation of runoff for the watershed with the cell size 500 m is described. The cell size of the runoff coefficients grid is 30 m. However, the size of the cell in the watershed is 500m, so an average of runoff coefficient values within each cell was used for runoff prediction. All the cells of the runoff coefficients grid that fell within a cell of the watershed were considered to compute an average value of runoff coefficient for that cell. The calculated average runoff coefficients were reduced by a value of 0.4 as suggested by Olivera et al. (1996) to account for infiltration. Cells that had values of 0.4 or less were given a value of zero (0). From the physical viewpoint, this means that all cells with a runoff

coefficient less than or equal to 0.4 generate no runoff. The areas where the value of runoff coefficient is assumed to be zero (0) are shown in Figure 4.29 through Figure 4.33 as non -contributing areas. For cells with values greater that zero (0) the runoff time series for each contributing cell was calculated from the available data (Olivera et al. 1996), using the following relationship,

$$R_{celli,t} = R_t \times \frac{CROC_i}{CROC_{avg}} \quad \text{.....(4.2)}$$

Where,

$R_{cell(i,\ t)}$ is the runoff at cell i and at time t, R_t is the runoff at time t, $CROC_i$ is the runoff coefficient of the cell i and $CROC_{avg}$ is the average runoff coefficient over the watershed.

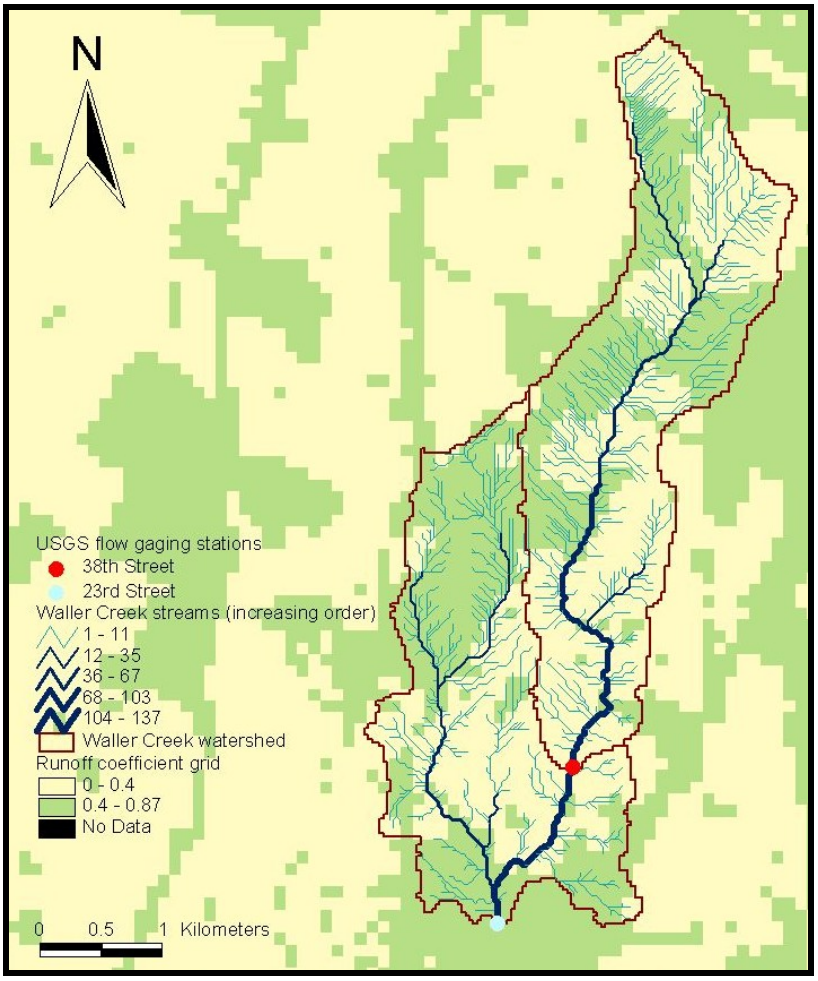

Figure 4.33. Waller Creek watershed along with the runoff coefficients grid and the USGS gaging stations.

4.2.3 Application of the cell-to-cell stream flow routing model

The flow with the available runoff data and the coarse resolution network data is calculated at 23rd Street and 38th Street. The model parameters were first calibrated at 23rd Street from October 14th, 1994 at 7:45pm to October 16th, 1994 at 3:45am and then validated at 23rd Street from October 16th, 1994 at 3:45 am to October 17th, 1994 at 6:45pm. The model was then validated at 38th Street for the

whole time period of October 14th, 1994 at 8:45pm to October 17th, 1994 at 6:45pm. The user defined time step was chose as 15 minutes.

4.2.3.1 Calibration at 23rd Street

The runoff values obtained for the watershed at a cell size of 500 m in section 4.2.2 were used as the input to the cell-to-cell stream flow routing model. The time step of 15 minutes was used, which is consistent with the time step of available runoff. The calibration of the model was done from 23rd Street from October 14th, 1994 at 7:45pm to October 16th, 1994 at 3:45am. Initially, values of stream velocity and stream coefficient of dispersion were assumed to be the same for all cells. This assumption did not produce a good fit with the observed flow at 23rd Street. Hence, different values of velocity and coefficient of dispersion in streams was assumed for contributing (urban) areas and non-contributing (non-urban) areas. The values of overland flow velocity and coefficient of dispersion were kept constant for all cells irrespective of the location of the cells (refer Table 4.14 for further details).

Calibration of the model was based on fine-tuning the flow velocity, the overland flow velocity, the channel dispersion coefficient and the overland flow dispersion coefficient. A near perfect fit (Figure 4.34) was achieved while calibrating the model using the stream and overland flow velocities and stream and overland flow coefficient of dispersion given in Table 4.15.

Table 4.15. Stream and overland velocity and dispersion values for 500 m resolution.

Stream and overland flow parameters	**Values**
Stream Velocity (m/sec)	
a. Developed areas	1.24
b. Undeveloped areas	0.09
Overland flow velocity (m/sec)	0.06
Coefficient of Dispersion for stream flow (m^2/sec)	
a) Developed areas	100
b) Underdeveloped areas	25
Coefficient of Dispersion for overland flow (m^2/sec)	2.5

The assumption behind the choice of different stream and overland flow velocities and dispersion coefficients is that in developed areas there is very little resistance to the flow of water as a result the velocity is higher. Most of the draining area in the 23rd Street watershed is highly developed as compared to the 38th Street sub watershed. This also explains the observation that the flow at 38th Street is only 39% of the flow at 23rd Street, instead of 53% as the ratio of the areas, and that the flow peaks first at 23rd Street and 30 minutes later at 38th Street.

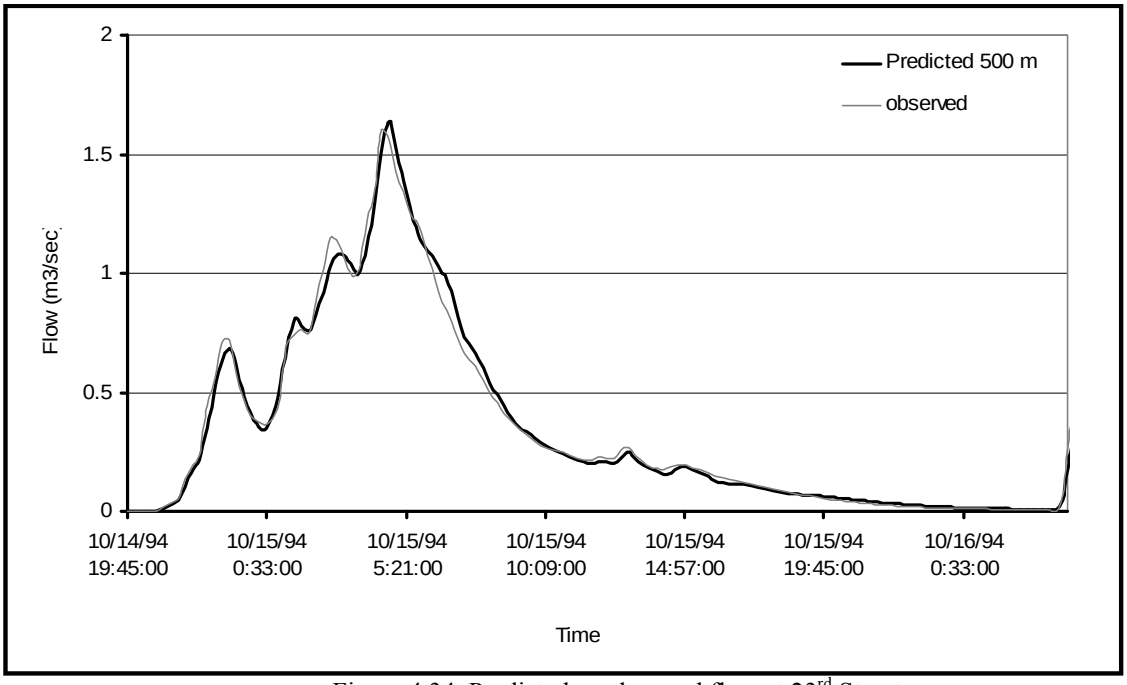

Figure 4.34. Predicted vs observed flow at 23rd Street.

4.2.3.2 Validation at 23rd Street

Once the routing model was calibrated for 23rd Street, the model parameters were frozen and it was validated for the flow at 23rd Street from October 16th, 1994 at 3:45 am to October 17th, 1994 at 6:45 pm and the fit achieved is within acceptable limits (see Figure 4.35).

4.2.3.3 Validation at 38th Street

The validation of the routing model parameters at 23rd Street was followed by validation of the model parameters at 38th Street from October 14th, 1994 at 7:45 pm to October 17th, 1994 at 6:45 pm with the same parameter used in calibration and the fit achieved is within acceptable limits (see Figure 4.36).

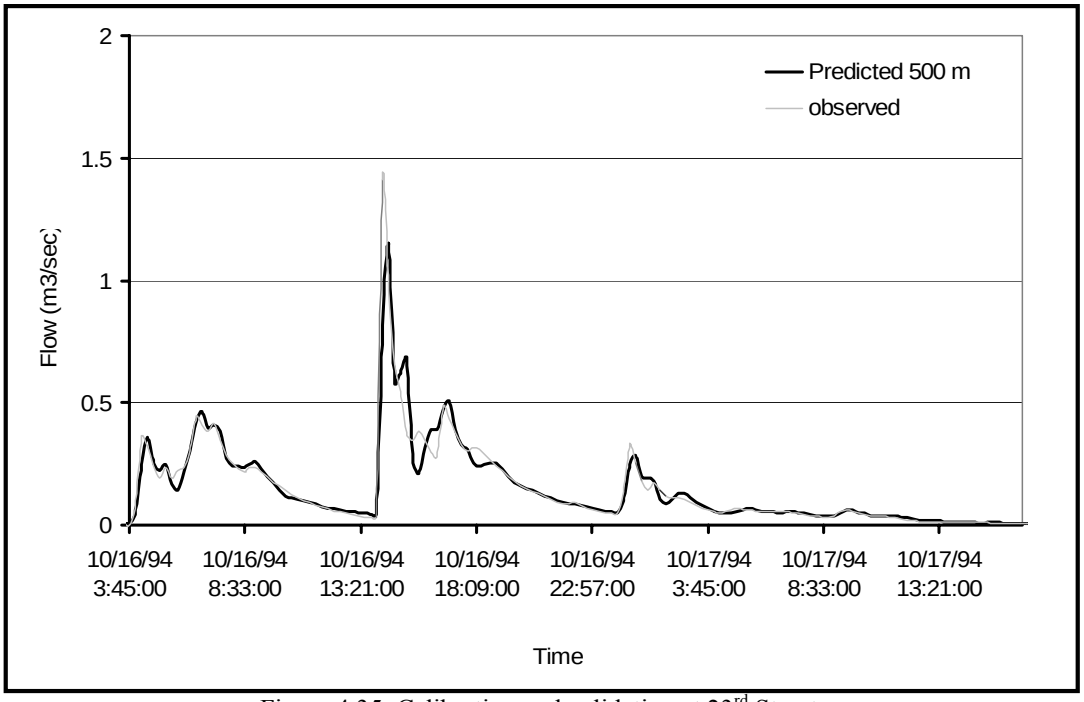

Figure 4.35. Calibration and validation at 23rd Street.

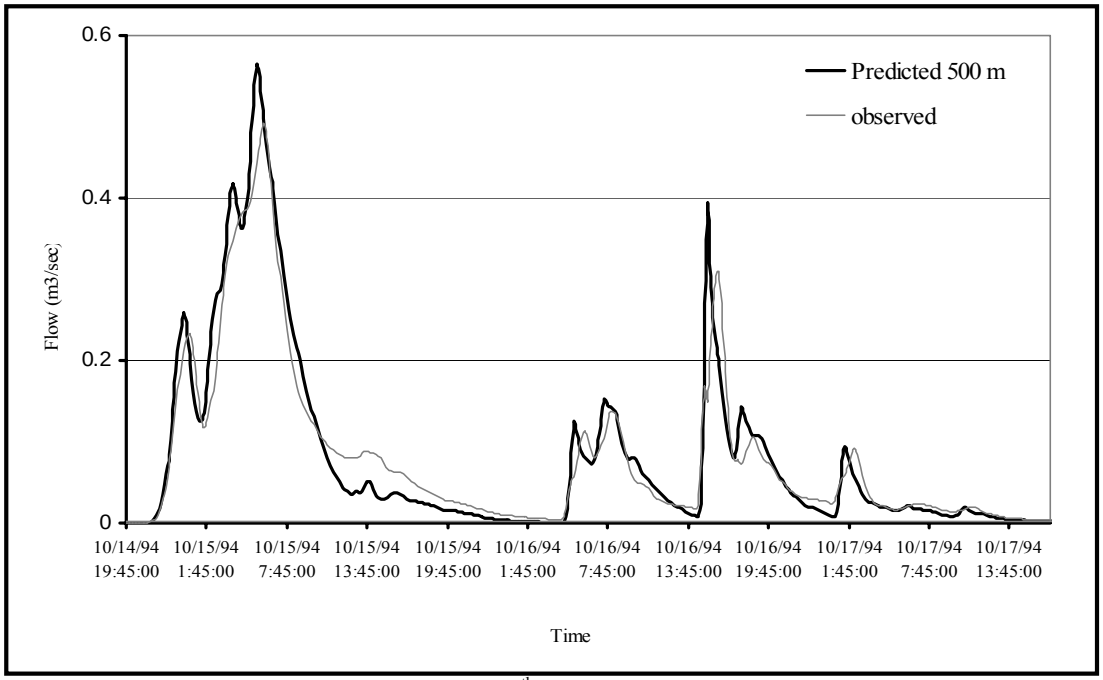

Figure 4.36. Validation at 38th Street at the resolution of 500 m.

4.2.4 Resolution dependency of model parameters

The cell-to-cell stream flow routing model is a resolution independent routing model. The model parameters once calibrated need not be changed once the resolution changes. To show the parameter independence of the model when the cell size changes the cell-to-cell stream flow routing model was applied to the watersheds of resolutions 250 m and 1000 m (see hydrographs in Figure 4.37). These watersheds were delineated in a similar fashion as the 500 m cell size watershed (see Figure 4.31 and Figure 4.32). Table 4.16 gives a comparison of the number of cells and tanks per cells for all the three resolutions.

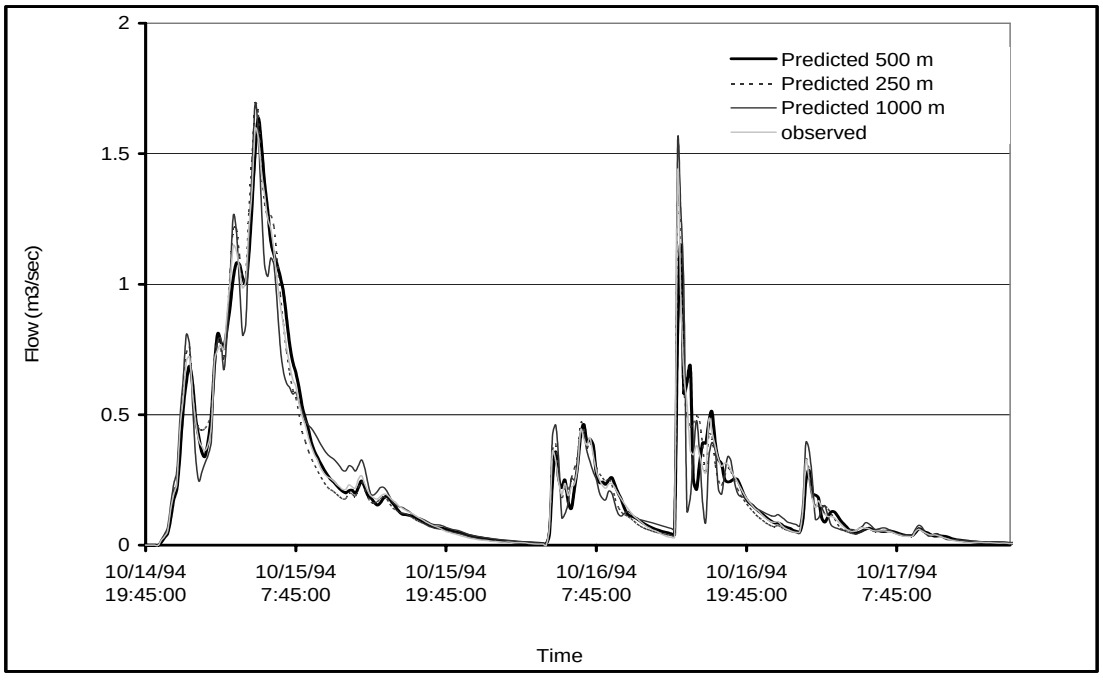

Figure 4.37 Comparison of flows at cell resolution of 250 m, 500 m, and 1000 m with observed flows.

The runoff for each cell of the two watersheds was computed using the methodology explained in section 4.2.2. The cell-to-cell stream flow routing algorithm was applied to both the watersheds with a time step of 15 minutes from October 14th, 1994 at 7:45 p.m. to October 17th, 1994 at 6:45 p.m. (Figure 4.29). The stream flow and overland flow parameters used were the same as given in Table 4.14. The predicted discharges of 250m resolution matches pretty well with the 500m resolution predictions. However, this is not the case with the 1000 m watershed. This can be due to averaging of the parameters over a number 500 m cells to get the parameters for the 1000 m cell. Some cells in the in 1000 m resolution watershed incorporated both contributing areas and non-contributing areas. This might have led a non-representative velocity and dispersion coefficient leading to a not near perfect match of the hydrographs.

Table 4.16. Number of tanks in each cell for the three different resolutions.

Resolution	**250 m**	**500 m**	**1000 m**
Area (sq. meters)	11,812,000	12,250,000	13,000,000
No. of cells	189	49	13
No. of tanks	364	161	90

4.2.5 Effect of number of tanks in a cascade

To study the impact of the number of tanks in a cell, the cell to cell stream flow routing algorithm was applied to the Waller creek at a cell resolution of 500m. In

one case, the model was run with just one tank per cell and in the other case; the model was run with a very high number of tanks per cell. This is nothing but pure translation as explained by Singh (1988). A high number of tanks per cell was achieved by choosing a very high dispersion coefficient and since the number of tanks in a cell is inversely dependent on the dispersion, less dispersion means more tanks. The number of the tanks per cell ranged from 350-450 for the cell size 500 m.

4.2.5.1 Effect of one tank per cell

The flow hydrograph (Figure 4.38) produced by the routing model with just one tank per cell produced the same result as the model with multiple tanks per cell leading to a conclusion that with a small cell size is no difference in the hydrographs produced in the two cases. The reason for this is that is that number of tanks in smaller cells is much less (~3-5) as a result they happen to be governed by dispersion only and do not show any change in behavior with a cascade of tanks. This behavior changes when the cell size increases, as is seen in the case of Brazos river basin, where with a cell size of 8,045m we see a substantial difference in the hydrographs when the number of tanks per cell is changed for a cascade to a single tank.

4.2.5.2 Effect of infinite number of tanks (pure translation)

Figure 4.38 shows that nearly infinite number of tanks per cell leads to more noise in the hydrograph, which is comparable to pure translation.

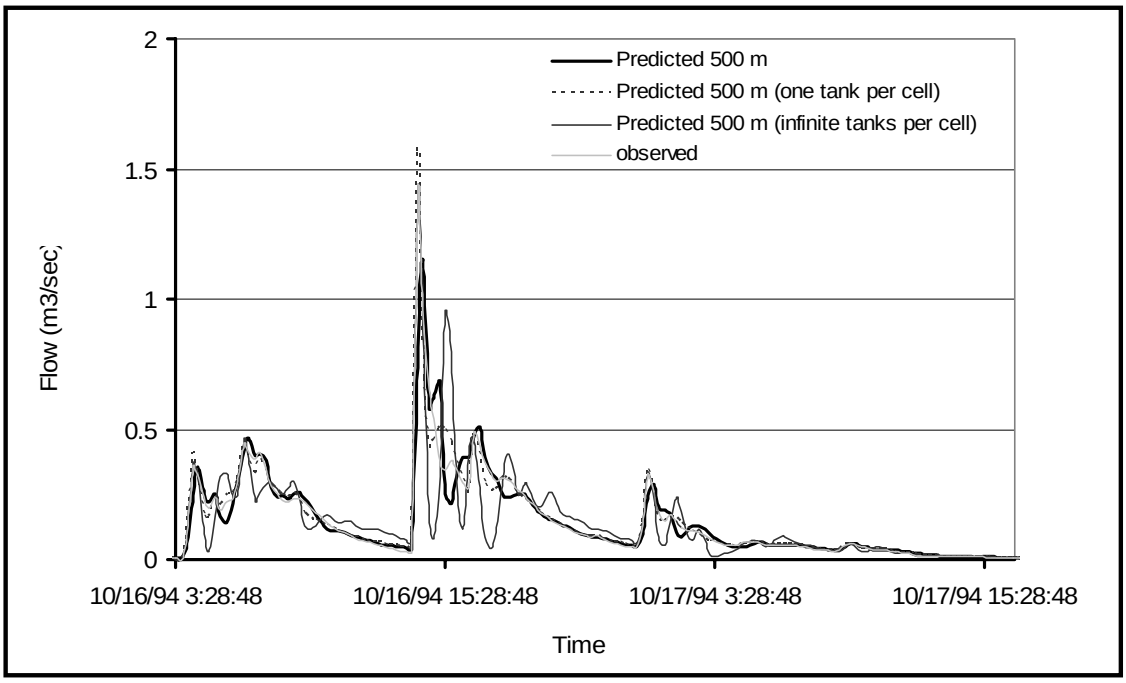

Figure 4.38. Impact of the number of tanks in a cell of a watershed.

5. CONCLUSIONS

The purpose of this study was to develop a cell-based stream flow routing model. This model takes advantages of the advances made in the field of Geographical Information Systems (GIS) in the field of water resources engineering and coarse resolution networks.

The cell-to-cell stream flow routing model is a two-parameter routing model. It uses a coarse resolution stream network to route the excess rainfall or the runoff from each cell to the outlet of the watershed. A watershed is divided into a number of equal cells, which are approximated as a cascade of linear reservoirs. Routing is done in two phases. The first phase is the overland flow in which a cascade of linear reservoirs or tanks is used to transfer the given runoff depth from the center of a cell to the corner or the side of the cell depending on the flow direction of the given cell. The number of tanks in the cascade is dependent on the overland flow velocity and the overland flow coefficient of dispersion. The second phase is the stream flow routing, where a cascade of tanks is used to route the runoff from the exit box of the cell to the outlet of the watershed across the watershed over the coarse resolution stream network. The number of tanks in the cascade is dependent on the stream flow velocity and the stream flow coefficient of dispersion. The tanks in the cascade are linear reservoirs as the outflow from each tank varies linearly to the storage.

A program was developed in Visual Basic to implement the model. The program takes as input the network data and the runoff data. The program first delays the runoff depth in each cell using the cascade of tanks for overland flow and then

uses that runoff depth as input to the routing algorithm, which uses the coarse resolution stream network to track the water downstream and to calculate the flow at the outlet of each cell. The program operates at a model time step, which is governed by the courant condition. The program output consists of four files including the flow and storage output data files.

The cell-to-cell stream flow routing model was applied to the Brazos River basin. The 90 m DEM of the Brazos river basin was used to delineate a fine resolution stream network. This fine resolution stream network was intersected with four coarse resolution meshes to generate four coarse resolution stream networks of 8,045 m, 16,090 m, 32,180 m and 64,360 m cell sizes. A uniform runoff of 0.0001 mm was applied to all the cells in the watershed, which was routed to the outlet of the watershed at a user time step of 6 hours. Results of the Brazos river basin clearly indicate that more than one cell is required to capture all the flow variations in the hydrograph. Results of the 8,045 m and the 16,090 m resolution watersheds match closely, however, as the resolution increases the noise in the hydrograph also increases. This is attributed to the fact that as the cell size increases, the time of overland flow in a cell also increases. As a result, flow occurs in large chunks leading to more noise. This noise becomes evident in the 32, 180 m resolution hydrograph. In the hydrographs displayed with different time steps the 8,045 m, 16,090 m resolution watershed match well and 32, 180 m resolution watershed the hydrograph shows much less noise. The 64, 360 m hydrograph does not match at all with the rest of the hydrographs. This is attributed to the fact that even thought the error in total watershed

area is negligible it is misrepresented, leading to error in the peak and flow volumes. This error is clearly isolated in the hydrographs when runoff is applied to sub watersheds of the Brazos River basin.

To calibrate the model parameters, the cell-to-cell stream flow routing model was applied to Waller Creek, Austin. Runoff data and stream flow data is documented by Olivera et al. (1996) from October 14th, 1994 at 8:45pm to October 17th, 1994 at 6:45pm. The fine resolution data used was the same as developed by Olivera et al. (1996). Coarse resolution stream networks were created for three resolutions (250m, 500m, and 1000 m). The flow with the available runoff data and the coarse resolution network data is calculated at 23rd Street and 38th Street. The model parameters were first calibrated at 23rd Street from October 14th, 1994 at 7:45pm to October 16th, 1994 at 3:45am and then validated at 23rd Street from October 16th, 1994 at 3:45 am to October 17th, 1994 at 6:45pm with the 500 m resolution watershed. The model was then validated at 38th Street for the whole time period of October 14th, 1994 at 8:45pm to October 17th, 1994 at 6:45pm. The user defined time step was chose as 15 minutes. The calibrated model parameters were used for the validation of the model at the 250m and the 1000m resolutions. Hydrographs of the 250 m watershed and the 1000 m resolution watershed closely match with the 500 m resolution watershed hydrograph. However, the effect of the cascade of tanks in not evident with this watershed. Hydrographs for one tank per cell and the cascade do not show any difference. One of the reasons for this is that Waller Creek watershed is a very small watershed that is driven solely by dispersion.

Like most models, the cell-to-cell stream flow routing model has its share of limitations. The model is resolution independent for stream flow routing only and not overland flow routing. The overland flow parameters are resolution dependent and they change as the cell size changes. With smaller cells, the effect of the cascade of tanks in a cell over a cell with a single linear reservoir is unclear. The time of computation is high for larger watersheds like the Brazos river basin, especially with smaller cell sizes. The program accepts input data in only one format, any other formats lead to errors. Runoff input is acceptable only in depth and no other format.

This cell-to-cell stream flow routing tool is a stand alone program and it requires input as comma delimited text files. Future work on this model will concentrate in incorporating this model into ArcGIS, so that data can be easily fed into the model without the hassles of exporting text files from the GIS interface. This model can also be coupled to a general circulation model (GCM) from which it can derive its runoff. Also, a distributed method to treat runoff and overland flow can help in improving the model flow prediction.

LITERATURE CITED

Arora, V. K., 2001. Streamflow Simulations for Continental-Scale River Basins in a Global Atmospheric General Circulation Model. Advances in Water Resources 24(7):775-791.

Arora, V. K., and G. J. Boer, 2001. Effect of Simulated Climate Change on the Hydrology of Major River Basins. Journal of Geophysical Research 106(D4):3335-3348.

Arora, V. K., and G. J. Boer, 1999. A Variable Velocity Flow Routing Algorithm for GCMs. Journal of Geophysical Research 104(D24):30965-30979.

Arora, V. K., F. H. S. Chiew, and R. B. Grayson, 1999. A River Flow Routing Scheme for General Circulation Models. Journal of Geophysical Research 104(14):14,347-14,357.

Arora, V. K., F. Seglenienks, N. Kouwen, and E. Soulis, 2001. Scaling Aspects of River Flow Routing. Hydrological Processes 15:461-477.

Chow V. T, D. R. Maidment., and L. W. Mays, 1998. Applied Hydrology. McGraw-Hill, New York, New York.

Coe, M. T., 2000. Modeling Terrestrial Hydrological Systems at the Continental Scale: Testing the Accuracy of an Atmospheric GCM. Journal of Climate 13(4):686-704.

Coe, M. T., 1998. A Linked Global Model of Terrestrial Hydrologic Processes: Simulation of Modern Rivers, Lakes and Wetlands. Journal of Geophysical Research 103(D8):8885-8899.

Coe, M. T., 1997. Simulating Continental Surface Waters: An Application to Holocene Northern Africa. Journal of Climate 10:1680-1689.

Coe, M. T., M .H. Costa, A. Botta, and C. Birkett, 2002. Long-Term Simulations of Discharge and Floods in the Amazon Basin. Journal of Geophysical Research 107(D20): 8044, doi: 10.1029/2001JD000740.

Costa, M. H., C. H. C. Oliveira, R. G. Andrade, T. R. Bustamante, F. A. Silva, and M. T. Coe, 2002. A Macroscale Hydrological Data Set of River Flow Routing Parameters for the Amazon Basin. Journal of Geophysical Research 107 (D20): 8039, doi: 10.1029/2000JD000309.

Costa, M. H., J. A. Foley, 1997. Water Balance of The Amazon Basin: Dependence on Vegetation Cover and Canopy Conductance. Journal of Geophysical Research 102(D20):23973-23989.

Downer, C. W., F. L. Ogden, W. D. Martin, and, R. S. Harmon, 2002. Theory, Development, and Applicability of the Surface Water Hydrologic Model CASC2D. Hydrological Processes 16:255-275.

Ducharne, A., C. Golaz, E. Leblois, K. Laval, J. Polcher, E. Ledoux, and G. de Marsily, 2003. Development of a High Resolution Runoff Routing Model, Calibration and Application to Assess Runoff From the LMD GSM. Journal of Hydrology 280:207-228.

ESRI (Environmental Systems Research Institute), 1992. Cell-Based Modeling with Grid 6.1: Supplement – Hydrologic and Distance Modeling Tools. ESRI Inc., Redlands, California.

Fekete, B. M., C. J. Vörösmarty, and R. B. Lammers, 2001. Scaling Gridded River Networks for Macroscale Hydrology: Development, Analysis, and Control of Error. Water Resources Research 37(7):1955-1967.

Graham, S. T., J. S. Famiglietti, and D. R. Maidment, 1999. Five-minute, 1/2º, and 1º Data Sets of Continental Watersheds and River Networks for Use in Regional and Global Hydrologic and Climate System Modeling Studies. Water Resources Research 35(2):583-587.

Gutowski, W. J., C. J. Vörösmarty, M. Person, Z. Otles, B. M. Fekete, and J. York, 2002. A Coupled Land-Atmosphere Simulation Program (CLASP): Calibration and Validation. Journal of Geophysical Research-Atmospheres 107 (D16): 4283 doi: 10.1029/2001JD000392.

Hagemann, S., and L. D. Gates, 2001. Validation of the Hydrological Cycle of ECMWF and NCEP Reanalysis Using the MPI Hydrological Discharge Model. Journal of Geophysical Research 106 (D2):1503-1510.

Hagemann, S., and L. Dumenil, 1999. Application of a Global Discharge Model to Atmospheric Model Simulations in the BALTEX Region. Nordic Hydrology 30(3):209-230.

Hagemann, S., and L. Dumenil, 1998. A Parameterization of the Lateral Water Flow for Global Scale. Climate Dynamics 14:17-31.

Hansen, J., G. Russell, D. Rind, P. Stone, A. Lacis, S. Lebedeff, R. Ruedy, and L. Travis, 1983. Efficient Three Dimensional Models for Climate Studies: Models I and II. Monthly Weather Review 111(4):609-662.

Jayawardena, A. W., and S. P. P. Mahanama, 2002. Meso-Scale Hydrological Modeling: Application to Mekong and Chao Phraya Basins. Journal of Hydrologic Engineering 7(1):12-26.

Jingyong, Z., D. Wenjie, F. U. Congbin, W.U. Lingyun, X. Zhe, M. A. Jun, and Z. Kejia, 2003. Streamflow Simulations for the Yellow River Basins Using RIEMS and LRM. Advances in Atmospheric Sciences 20(3):415-424.

Julien, P. Y., B. Saghafian, and F. L. Ogden, 1995. Raster-Based Hydrological Modeling of Spatially Varied Surface Runoff. Water Resources Bulletin (31)3:523-536.

Kalnay, E., M. Kanamitsu, R. Kistler, W. Collins, D. Deaven, L. Gandin, M. Iredell, S. Saha, G. White, J. Woollen, Y. Zhu, M. Chelliah, W. Ebisuzaki, W. Higgins, J. Janowiak, K. C. Mo, C. Ropelewski, J. Wang, A. Leetmaa, R. Reynolds, R. Jenne, and D. Joseph, 1996. The NCEP/NCAR 40-Year Reanalysis Project. Bulletin of the American Meteorological Society 77(3):437-471.

Kondo, J., 1993. A New Bucket Model for Predicting Water Content in the Surface Soil Layer. Journal of the Japan Society of Hydrology and Water Resources 6:344-349.

Kucharik C. J., J. A. Foley, C. Delire, V. A. Fisher, M. T. Coe, J. D. Lenters, C Young- Molling, N. Ramankutty, J. M. Norman, and S. T. Gower, 2000. Testing the Performance of a Dynamic Global Ecosystem Model: Water

Balance, Carbon Balance, and Vegetation Structure. Global Biogeochemical Cycles 14(3):795-825.

Ledoux, E., 1980. Modélisation Intégrée des Écoulements de Surface et des Ecoulments Souterrains sur un Bassin Hydrologique. Thése de Docteur-Ingénieur, Ecole Nationale Superiéure des Minés De Paris et Universite Paris 6, Paris, France.

Liang X., D. P. Lettenmaier, E. F. Wood, 1999. One-Dimensional Statistical Dynamic Representation of Subgrid Spatial Variability of Precipitation in the Two-Layer Variable Infiltration Capacity Model. Journal of Geophysical Research 101(D16):21403-21422.

Liang X., D. P. Lettenmaier, E. F. Wood, and S. J. Burges, 1994. A Simple Hydrologically Based Model of Land-Surface Water and Energy Fluxes for General-Circulation Models. Journal of Geophysical Research-Atmospheres 99(D7):14415-14428.

Liston, G. E., Y. C. Sud, and E. F. Wood, 1994. Evaluating GCM Land Surface Hydrology Parameterization by Computing River Discharges Using a Runoff Routing Model. Journal of Applied Meteorology 33:394-405.

Lohmann D., E. Raschke, B. Nijssen and D. P. Lettenmaier, 1998a. Regional Scale Hydrology: I. Formulation of the VIC-2L Model Coupled to a Routing Model. Hydrological Sciences 43(1):131-142.

Lohmann D., E. Raschke, B. Nijssen and D. P. Lettenmaier, 1998b. Regional Scale Hydrology: II. Application of the VIC-2L Model to the Weser River, Germany. Hydrological Sciences 43(1):143-158.

Lohmann, D., R. Nolte-Holube, and E. Raschke, 1996. A Large Scale Horizontal Routing Model to Be Coupled to Land Surface Parameterization Schemes. Tellus 48A:708-721.

Lucas-Picher, P., V. K. Arora, D. Caya, and R. Laprise, 2003. Implementation of a Large-Scale Variable Velocity Flow Routing Algorithm in the Canadian Regional Climate Model (CRCM). Atmosphere-Ocean 41(2):139-153.

Ma, X. Y., Y. Fukushima, T. Hiyama, T. Hashimoto, and T. Ohata, 2000. A Macro-Scale Hydrological Analysis of the Lena River Basin. Hydrological Processes 14:639-651.

Marengo, J. A., J. R. Miller, G. L. Russell, C. E. Rosenzweig, and F. Abramopoulos, 1994. Calculations of River-Runoff in the GISS GCM - Impact of a New Land-Surface Parameterization and Runoff Routing Model on the Hydrology of the Amazon River. Climate Dynamics 10(6-7):349-361.

Miller, J., G. Russel, and G. Caliri, 1994. Continental Scale River Flow in Climate Models. Journal of Climate 7:914-928.

Naden, P., P. Broadhurst, N. Tauveron, and A. Walker, 1999. River Routing at the Continental Scale: Use of Globally-Available Data and an apriori Method of Parameter Estimation. Hydrology and Earth System Sciences 3(1):109-124.

Nijssen, B., G. M. O'Donnell, and D. P. Lettenmaier, 2001. Predicting the Discharge of Global Rivers. Journal of Climate 14(15):3307-3323.

Nijssen, B., D.P. Lettenmaier, X. Liang, S.W. Wetzel, and E.F. Wood, 1997. Streamflow Simulation for Continental-scale River Basins. Water Resources Research 33(4):711-724.

O'Donnell, G., B. Nijssen, and D.P. Lettenmaier, 1999. Simple Algorithm for Generating Streamflow Networks for Grid-based, Macroscale Hydrological Models. Hydrological Processes 13:1269-1275.

Ogden, F. L., 2004. A Brief Description of the Hydrologic Model CASC2D. *Available at* http://www.engr.uconn.edu/~ogden/casc2d/casc2_desc.htm. *Accessed on* January 10, 2004.

Oki T., 1997. Validating the Runoff from LSP-SVAT Models Using a Global River Routing Network by One Degree Mesh. In: Proceedings of 13th Conference on Hydrology, American Meteorological Society 319-322.

Oki T. and Sud Y.C., 1998. Design of Total Runoff Integrating Pathways (TRIP) – A Global Scale Runoff Routing. Earth Interactions 2(2-001), 40pp.

Oki, T., T. Nishimura, and P. Dirmeyer, 1999. Assessment of Annual Runoff From Land Surface Models Using Total Runoff Integrating Pathways (TRIP). Journal of the Meteorological Society of Japan 77(1B):235-255.

Oki T., S. Kanae, and K. Musiake, 1996. River routing in the global water cycle. GEWEX News 6:4-5.

Olivera, F., 1996. Spatially Distributed Modeling of Storm Runoff and Non-point Source Pollution Using Geographical Information Systems. Doctoral Dissertation, Department of Civil Engineering, University of Texas at Austin.

Olivera, F., and R. Raina, 2003. Development of Large Scale Gridded River Networks from Vector Stream Data. Journal of the American Water Resources Association 39(5):1235-1248.

Olivera, F., and D. Maidment, 1999. Geograhical Information Systems (GIS) Based Spatially Distributed Model for Runoff Routing. Water Resources Research 35(4):1155-1164.

Olivera, F., M. S. Lear, J. S. Famiglietti, and K. Asante, 2002. Extracting Low-Resolution River Networks from High-Resolution Digital Elevation Models. Water Resources Research 38(11):1231, doi: 101029/2001WR000726.

Olivera, F., J. Famigletti, and K. Asante, 2000. Global-scale Flow Routing Using a Source to Sink Algorithm. Water Resources Research 36(8):2197-2207.

Olivera, F., J. Famigletti, and M. Branstetter, 1999. Resolution Dependency of Cell-to-Cell Runoff Routing Models. EOS, Transactions American Geophysical Union 80(17):S153.

Ponce, V. M., R. Li, and, D. B. Simmons, 1978. Applicability of Kinematic and Diffusions Models. Journal of the Hydraulic Division, ASCE 104(HY3):353-360.

Renssen, H., and J. M. Knoop, 2000. A Global River Routing Network for Use in Hydrological Modeling. Journal of Hydrology 230(3-4):230-243.

Roeckner, E., 1992. Simulation of the Present Day Climate with the ECHAM Model: Impact of Model Physics and Resolution. Report 93, Max-Plank Institute for Meteorology, Hamburg, Germany.

Sausen, R., S. Schubert, and L. Dumenil, 1994. A Model of River Runoff for Use in Coupled Atmosphere-Ocean Models. Journal of Hydrology 155:337-352.

Singh, V. P., 2002. Is Hydrology Kinematic? Hydrologic Processes 16:667–716

Singh, V. P., 1988. Hydrologic Systems. Prentice Hall, New York, New York.

United States Army Corps of Engineers (USCOE) - Hydrologic Engineering Center, 2004. HEC-HMS, Hydrologic Modeling Software. *Available at* http://www.hec.usace.army.mil/software/hec-hms/hechms-hechms.html. *Accessed on* January 10, 2004

United States Department of Agriculture (USDA), 2004. KINEROS2: A Kinematic Runoff and Erosion Model. *Available at* http://www.tucson.ars.ag.gov/ kineros/. *Accessed on* January 10, 2004.

United States Geological Study (USGS), 2004a. USGS Geographic Data Download. *Available at* http://edcsgs9.cr.usgs.gov/glis/hyper/guide/1_dgr_demfig/index1 m.html. *Accessed on* January 10, 2004.

Vörösmarty, C. J., and B. Moore III. Modeling Basin-scale, 1991. Hydrology in Support of Physical Climate and Global Biogeochemical Studies: An Example Using the Zambezi River. Surveys in Geophysics 12(1-3):271-311.

Vörösmarty, C. J., B. Moore III, A. Grace, M. Gildea, J. Melillo, B. Peterson, E. Rasteller, and P. Steudler, 1989. Continental-Scale Model of Water Balance

and Fluvial Transport: An Application to South America. Global Biogeochemical Cycles 3:241-265.

VITA

Rajeev Raina

ADDRESS

Department of Civil Engineering
Texas A & M University
College Station, TX 77843
Cell: (979) 571 6035

EDUCATION

- Master of Science in Civil Engineering.
  (September 2001 – May 2004)
  Texas A&M University
  GPA: 3.89
  Research Interest: Environmental and Water Resources Engineering
- Bachelor of Engineering in Civil Engineering
  (1997-2001)
  Veermata Jijabai Technological Institute, Mumbai University, India.
  GPA: 3.68

EXPERIENCE

- **Texas A&M University, College Station, Texas (Dec. 2001 – Oct. 2003)**
  Graduate Research Assistant
    - Environmental credit trading program for the lake Lewisville, Texas